

Protective Design • Mandatory Center of Expertise  
Technical Report 92-2

## Facility And Component Explosive Damage Assessment Program

**(FACEDAP)**

Theory Manual

Version 1.2

**SwRI** Project No. **06-5145-001**  
Contract No. DACA 45-91-D-0019

Prepared for:

Department of the **Army**  
Corps of Engineers, Omaha District  
CEMRO-ED-ST  
215 N. 17th **Street**  
**Omaha**, Nebraska 68102-4978

Modified May 1994

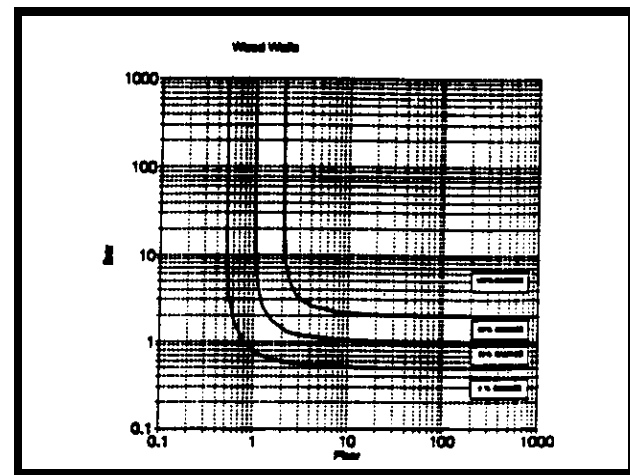
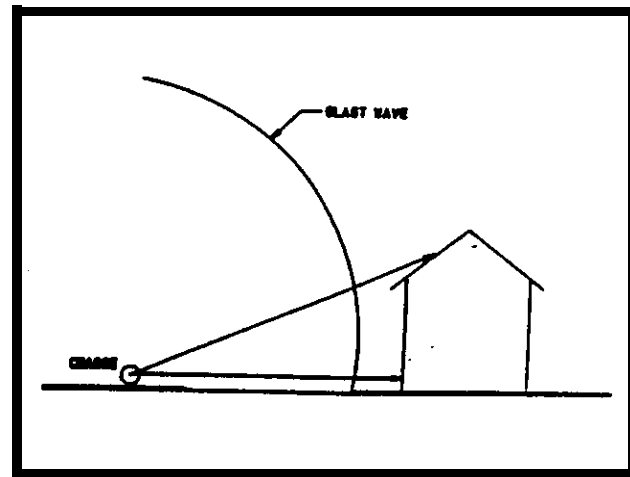
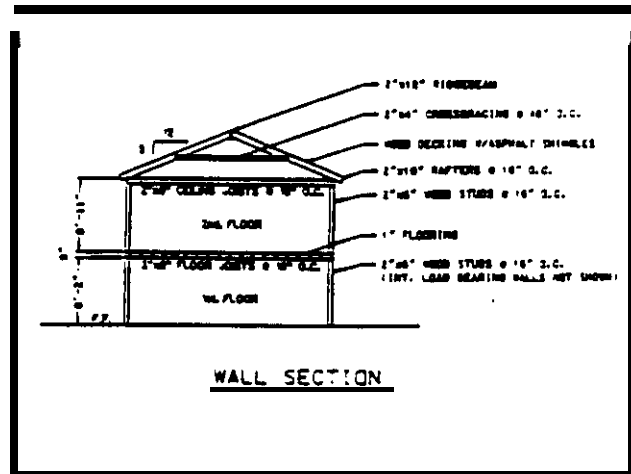


# Table of Contents

	<b>Page</b>
List of Figures .....	<b>ix</b>
<b>List</b> of Tables .....	<b>ix</b>
1.0 INTRODUCTION .....	1
1.1 Overview of FACEDAP Program .....	2
2.0 HARDWARE REQUIREMENTS .....	4
3.0 INSTALLATION INSTRUCTIONS .....	5
4.0 <b>REQUIRED FILES</b> .....	7
5.0 <b>INPUT AND OUTPUT FILES</b> .....	7
6.0 INPUT/OUTPUT SCREENS <b>IN</b> FACEDAP .....	9
6.1 Vertical Menu .....	10
6.2 Pull Down Menu .....	11
6.3 Multi Row and Column Menu .....	11
6.4 Form-Style Screens .....	12
6.5 Spreadsheet-Style Screens .....	15
7.0 FACEDAP DRIVER PROGRAM .....	18
7.1 <b>File Option</b> .....	19
7.2 <b>Overview of Preprocess Option</b> .....	19
7.3 overview of Analysis option .....	20
7.4 <b>Overview of Postprocess</b> Option .....	20
7.5 Utilities Option .....	21
8.0 PREPROCESSOR .....	21
<b>8.0.1</b> Selecting Single Component or Building <b>Type</b> of Analysis .....	21.1
8.0.2 Preprocessor Input for Single Component <b>Analysis</b> .....	21.2

## Table of Contents (Continued)

		<b>Page</b>
8.0.2.1	Main Single Component Preprocessor Menu .....	21.2
8.0.2.2	Problem Title .....	21.3
8.0.2.3	Load Definition .....	21.4
8.0.2.4	Component Properties .....	21.5
8.0.2.5	Component Selection .....	21.5
8.0.2.6	Save, Retrieve, Clear, Print <b>and</b> Return options .....	21.6
8.1	Preparation of Input into the <b>Preprocessor</b> .....	22
8.1.1	Types of Structural Components Which can <b>be</b> Analyzed .....	22
8.1.2	<b>Preparation</b> of Component Property Input .....	23
8.1.3	Preparation of Component Geometry Input .....	23
8.1.4	Preparation of Building Geometry and Charge Location Input .....	24
8.1.5	<b>Summary</b> of Problem Preparation .....	24
8.1.6	Maximum Limits on Input Building Component Data ....	25
8.2	Main Preprocessor Menu .....	26
8.3	Problem Title .....	28
8.4	<b>Load</b> Definition .....	28
8.5	<b>Component Properties</b> .....	29
8.5.1	Selecting Component Types for Component <b>Property</b> Input .....	<b>30</b>
8.5.2	<b>Description</b> of Required Component <b>Property</b> Input for Each Component Type .....	32
8.5.2.1	Component <b>Property</b> Input for <b>Reinforced Concrete Beam</b> .....	35

## List of Figures (Continued)

<b>Figure</b>		<b>Page</b>
15	Comparison of Damage Data from Blast Loaded Steel <b>Frames</b> to P-i <b>Diagram</b> for Steel Frames .....	95
16	Compression Membrane Response .....	97
17	Comparison of Damage Data from Blast Loaded Unreinforced One-Way Masonry Walls with Arching to the P-i Diagram for This Component . . . . .	99
18	Comparison of Damage Data from Blast Loaded Unreinforced Two-Way Masonry Walls with Arching to the P-i Diagram for This Component . . . . .	<b>100</b>
19	Comparison of Damage Data <b>from</b> Blast <b>Loaded</b> Reinforced <b>Concrete</b> Two-Way <b>Masonry</b> Slabs with <b>Arching</b> to <b>the</b> P-i Diagram for This Component .....	101

## List of Tables

<b>Table</b>		<b>Page</b>
1	<b>Structural</b> Components Considered in the FACEDAP Program . . . . .	15
2	<b>Quantitative</b> Criteria Defining Damage Levels for Each Component Type . . . . .	17
3	Rules Used in FACEDAP Program <b>to</b> Calculate Component Dependencies . . . . .	103
4	Lit Showing the “Dependency Type” of Each Component . . . . .	104
<b>5</b>	Correlation Between Component Damage and Assumed Replacement . . . . .	107

## List of P-i Diagrams

<b>P-i Diagram</b>	<b>Page</b>
Reinforced Concrete Beam .....	19
One-Way Reinforced Concrete Slabs .....	21
Two-Way Reinforced Concrete Slabs .....	23
Reinforced Concrete Exterior Columns .....	25
Reinforced Concrete Interior <b>Columns</b> .....	27
Reinforced Concrete <b>Frames</b> .....	29
Reinforced Concrete <b>Prestressed</b> Beams .....	31
Steel Beams .....	33
Metal <b>Stud</b> Walls .....	35
Steel Open Web Joists .....	37
Steel Corrugated Decking .....	3 9
Steel Exterior Columns .....	41
Steel <b>Interior Columns</b> .....	43
<b>Steel Frames</b> .....	45
<b>Masonry One-Way Unreinforced Walls</b> .....	47
<b>Masonry</b> Two-Way Unreinforced Walls .....	49
<b>Masonry One-Way Reinforced Walls</b> .....	51
<b>Masonry Two-Way Reinforced Walls</b> .....	53
<b>Masonry</b> Pilasters .....	55
<b>Wood</b> walls .....	57
Wood Roofs .....	59
Wood Beams .....	61
<b>Wood Exterior</b> Columns .....	63
Wood Interior <b>Columns</b> .....	65

## 1.0 INTRODUCTION

This manual discusses the development of the blast damage assessment method used in the FACEDAP computer program to calculate blast damage to individual structural components, or to an entire building, from an external explosive threat. The FACEDAP program is intended to be a tool for quickly determining the approximate structural damage to conventional buildings and building components caused by a given external explosive threat (e.g., no gas pressure loads are considered). Non-structural components, such as windows and doors, are not currently considered by the program. This manual is intended as a reference to users of the FACEDAP program. Therefore, it is intended to supplement the FACEDAP User's Manual<sup>[1]</sup>, and the FACEDAP Programmer's Manual<sup>[2]</sup>. In one form or another, the basic blast damage assessment methodology incorporated in the FACEDAP program has been used in a number of previous projects<sup>'''</sup> and in previous computer programs<sup>[5,6]</sup> over the last five years. However, its gradual development, and the assumptions upon which it is based, have not been discussed and summarized in a single document. This has been due, in large part, to the incremental development of the current methodology. Therefore, this theory manual is also intended to provide a summary of the development of the blast damage calculation method currently in the FACEDAP program and to assess the strong points and weak points of this methodology for its use as a relatively quick, approximate means of determining blast damage to conventional buildings and structural building components.

The methodology in the FACEDAP program is based on a graphical procedure which compares the dynamic response characteristics of structural components (i.e. mass, stiffness and strength of the components) to calculated blast load characteristics (i.e. peak shock pressure and impulse) and, based on the comparison, defines four different levels (0%, 30%, 60%, and 100% damage) of blast induced damage. The dynamic response and blast load characteristics are used to calculate two non-dimensional parameters that define a point on a graph, known as a pressure-impulse diagram, which is divided into regions corresponding to each of the four damage levels. This procedure is intended to predict damage without the built-in conservatism that is usually present in design procedures. The four damage levels listed above have been correlated with the levels of protection used by the U.S. Army Corps of Engineers as follows<sup>[4]</sup>: 1) the 0% damage level is similar to the High Level of Protection; 2) the 30% damage level is similar to the Medium Level of Protection; 3) the 60% damage level is similar to the Low Level of Protection; and 4) the 100% damage level is similar to Collapse.

Building vulnerability is based on the calculated damage level of each component in the building. The percentage of building damage is calculated by "weighting" each calculated component damage level with a weighting factor, summing the weighted damage of all building components, and then dividing this sum by the value corresponding to total failure of all building components and converting this ratio to a percentage. Cascading failure, where failure of a supporting component causes failure of all supported components, is considered in the summation algorithm. Building repairability and reusability are also considered in similar summation processes. Finally, the building level of protection is assumed equal to the lowest level of protection calculated for any of the building components. The component damage and building vulnerability calculation procedures are discussed in more detail in the following chapters.

Because of assumptions used in the methodology and because of limited validation, there are several recommended limitations on the use of the blast damage assessment methodology which is in the FACEDAP program. The FACEDAP program should not be used for final design or for any case where high accuracy is required. This caution is necessary because the pressure-impulse diagrams, which predict building component blast damage for the twenty-four different structural components considered in the methodology, are based on limited data in some cases, and on simple dynamic structural response theory and a number of assumptions in other cases. Neither the pressure-impulse diagrams, nor the summation procedure used to get percentage of building damage, have been fully validated yet to determine the bounds on their accuracy. The explosive charge should be at a scaled standoff between  $3.0 \text{ ft/lb}^{1/3}$  and  $100 \text{ ft/lb}^{1/3}$  away from the building and located near the ground surface so that assumptions used in the methodology related to the blast load on each building component will be applicable.

Some conservatism can be built into the calculated building damage if conservative strength properties are input for building components. However, the pressure-impulse diagrams **only** predict damage to components during **flexural** or buckling mode response and do not consider any damage due to shear failure. Although the available test data has not shown that conventionally designed components tend to fail in shear under blast loads that are applied at scaled standoffs greater than  $3.0 \text{ ft/lb}^{1/3}$ , no thorough study has been made of how this limitation **affects** the FACEDAP program.

## 2.0 HISTORY OF THE DEVELOPMENT OF THE BLAST DAMAGE ASSESSMENT PROCEDURE USED IN THE FACEDAP PROGRAM

The blast damage assessment procedure in the FACEDAP **program** is an extension of work performed by Southwest Research Institute (**SwRI**) during a number of previous projects. **The** development of this procedure was initiated by **SwRI** in 1987 during a project for the Naval **Civil** Engineering Laboratory (**NCEL**) in Port **Hueneme, California**<sup>[3]</sup>. During this **project**, the **basic** two-step procedure discussed above was developed as a hand calculation procedure to **determine** building blast damage. Pressure-impulse diagrams which predicted blast damage to twenty-three different components commonly used in construction were **developed** based on available test **data**, basic structural dynamics theory, and a number of **assumptions**. Procedures to calculate overall building damage, based on **the** summation of calculated damage to all building components, were also developed. Building damage was **characterized** in terms of the percentage of building damage, a repairability factor, and a **building reusability** percentage. Twelve common **buildings, considered** typical of conventional buildings on U.S. Naval bases, were “designed” by **SwRI**, and the blast damage assessment methodology was exercised for given explosive threats to these buildings. Curves for each common building which related the explosive threat to the calculated percent building damage, **repairability** factor, and **building reusability** factor were **plotted**. These curves could then be used to quickly assess blast damage to any **building** which could be categorized as similar to one of the twelve common buildings.

**Following this initial development effort, the U.S. Army Corp of Engineers, Omaha District** funded work that used the basic **procedure developed** for NCEL, but considered component blast **damage in terms of specific categories used by the Army**<sup>[4]</sup>. **It was determined that the Army's** damage categories, or levels of **protection**, could be equivalent to the existing damage categories used in the initial development for NCEL. **During** the work funded by **the Army**, the **pressure-impulse** diagrams used for calculating blast damage to masonry and reinforced concrete components **were** modified. **These** diagrams were largely based on available test data. The same data used in **the initial** project for NCEL was used again, but **this** time data from tests **where arching**, or compression membrane response, **occurred** was separated **from tests** where such **response** did not occur. For some component types, two separate pressure-impulse diagrams were developed one applicable for components in buildings **where arching** could be expected, and one applicable where no arching was expected. In general, the **pressure-impulse diagrams** for all masonry and reinforced concrete components were **modified** so that they predicted more damage than before. **a factor of two or more times as much damage in many cases. A pressure-impulse diagram to** predict the blast damage to **prestressed** concrete beams and one-way slabs was also developed. In

addition, the pressure-impulse diagrams used to predict blast damage for most steel components **was** simplified from the two-step procedure developed for NCEL into a one-step process. **The** previous method involved determining both the ductility ratio and the ratio of **midspan** deflection to span **length** of a steel component, and then basing **the** component damage on the more severe of **these** two ratios compared to given criteria. The simplified procedure bases all calculated damage on **the** ductility ratio. After these modifications were made to the pressure-impulse diagrams, the two-step procedure to determine building damage parameters developed for NCEL was used to calculate the level of protection for **the** twelve common buildings and also for a thirteenth building constructed with **prestressed** concrete components.

During the effort for the **Corp** of Engineers and during a period after this work, NCEL funded **SwRI** to develop a computer program, named BDAMAEXE, which incorporated the blast damage assessment procedure as it **was modified** for the Corp of **Engineers**<sup>[5]</sup>. Then, engineers at NCEL incorporated BDAMAEXE into the **BDAM** program, which has a preprocessor and postprocessor to facilitate user input and **output**<sup>[6]</sup>. NCEL also **funded SwRI** to validate the blast damage **assessment** methodology incorporated into the **BDAM code** against some building blast damage data **from** World War **II**<sup>[7]</sup>. Unfortunately, very little information was available on the **size** of the damaged building components and therefore many **assumptions** had to be made. The "validation" of **the** code **therefore depended** very heavily on what **particular assumptions** were made;

The most current effort related to the blast damage assessment procedure has resulted in this theory manual and **the** FACEDAP computes program. The FACBDAP **computer** program incorporates the BDAMAEXE program, with **modifications** made to the equations from the pressure-impulse diagrams for steel and wood components described in the next paragraph, in a user friendly computer program. This program has a more sophisticated **preprocessor** and postprocessor than the **BDAM code**, which greatly reduces the **amount** of user effort required to input the properties and geometry of each **structural** component **in** a given building and allows more inspection of calculated component damage levels and calculated blast loads on building components. The FACEDAP program is discussed in detail in Reference 1.

Several **modifications** to **the** originally developed pressure-impulse diagrams have also been made **during** this project. These **modifications** were made because of observed inconsistencies **in the pressure-impulse diagrams for different component types, where damage calculated for wood and steel components was much less than that for apparently stronger reinforced masonry and concrete components.** Limited data from steel **beams** responding in tensile membrane response had been broadly assumed applicable for other steel components, such as metal stud walls, corrugated steel decking, and open web steel joists, during the original development **of** the pressure-impulse **diagrams** for these componenta. The pressure-impulse diagrams for these steel components were reformulated during this project baaed on more conservative assumptions which are discussed in this **manual**. The pressure-impulse diagrams for wood components have also been reformulated based on a more conservative **interpretation** of the data originally used to develop the **curves**. The methodology used to calculate blastdamage to frames has also been modified Damage to open web steel joists has been simplified to the extent that prediction of blast damage due to web buckling has been eliminated and damage from flexmal response is predicted more conservatively. Many of the pressure-impulse diagrams developed **in** the original work for NCEL have been modified in subsequent work so as to predict more damage than they originally did. These

addition, the pressure-impulse diagrams used to predict blast damage for most steel components was **simplified** from the two-step procedure developed for NCEL into a one-step process. The previous method involved determining both the ductility ratio and the ratio of **midspan** deflection to span length of a **steel component, and then basing the component damage on the more severe of** these two ratios **compared to given criteria**. The simplified procedure bases all calculated damage on the ductility ratio. **After these** modifications were made to the pressure-impulse diagrams, the two-step procedure to **determine** building damage parameters developed **for NCEL was used** to calculate the level of **protection for** the twelve common **buildings** and also **for a thirteenth building** constructed with **prestressed concrete components**.

During the effort for **the Corp** of Engineers and **during a period** after this work, NCEL funded **SwRI** to **develop a computer program, named BDAMA.EXE, which** incorporated the blast damage assessment procedure **as it was** modified for the **Corp of Engineers**<sup>[5]</sup>. Then, engineers at NCEL incorporated **BDAMA.EXE** into the **BDAM** program, **which** has a preprocessor and postprocessor to facilitate user input **and output**<sup>[6]</sup>. NCEL also funded **SwRI** to validate the blast damage assessment methodology **incorporated into the BDAM code** against some building blast damage data from World War **II**<sup>[7]</sup>. Unfortunately, **very little information** was available on the size of the damaged building components and **therefore many assumptions had to be made**. The "validation" of the code therefore **depended very heavily on what particular assumptions were made**.

The most current effort related to **the blast damage assessment** procedure has **resulted in** this theory manual and the **FACEDAP computer program**. The **FACEDAP** computer program incorporates the **BDAMA.EXE** program, **with modifications** made to the equations from the pressure-impulse diagrams for steel and wood components **described in the next paragraph, in a** user friendly computer program. This **program has a more sophisticated preprocessor and** postprocessor than the **BDAM** code, which **greatly reduces** the amount of user effort required to input the properties and geometry of each **structural component** in a given building and allows more inspection of calculated component **damage levels and** calculated blast loads on building components. The **FACEDAP** program **is discussed in detail in Reference 1**.

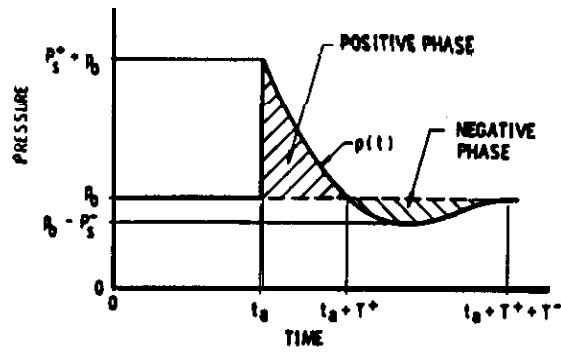
Several modifications to the **originally developed** pressure-impulse diagrams have also been made during this project. **These modifications were made** because of observed inconsistencies in the pressure-impulse diagrams **for different component types**, where damage calculated for wood and steel components was much **less** than that for **apparently** stronger reinforced masonry and concrete components. Limited **data from** steel beams **responding** in tensile membrane response had been broadly **assumed applicable** for other steel components, such as metal stud walls, corrugated steel **decking, and open web steel joists, during the** original development of the pressure-impulse **diagrams for** these components. The pressure-impulse diagrams for these steel components were **reformulated during this project based on more conservative assumptions which** are discussed in this manual. The pressure-impulse diagrams for wood components have also been reformulated based on a more conservative interpretation of the **data originally** used to develop the curves. The methodology used to calculate blast damage to frames **has also** been modified. Damage to open web steel joists **has been simplified to the extent that prediction of blast damage due to web** buckling has been eliminated and damage from **flexural** response is predicted more conservatively. Many of the pressure-impulse diagrams developed in the original work for NCEL have been modified in subsequent work so as to predict more damage than they originally did. These

modifications, which have been made possible by continuing funding, are based on more careful analysis of assumptions and the available test data. The development and assumptions used to develop the current pressure-impulse diagram for each of the twenty-four component types considered in the **FACEDAP** blast damage assessment procedure are explained in Section 4 of this manual.

A methodology has also been developed to predict blast damage from internal blast loading. None of this methodology is incorporated into the FACEDAP program, which is only intended for use in predicting building damage from exterior blast as described above. This information is included in this section, however, for completeness. The methodology described in Reference 8 is a two-step procedure to determine damage to a one-room building which is similar in concept to that described above for externally loaded buildings. However, an approximate energy balance is used to determine component damage rather than pressure-impulse diagrams. The applied energy (i.e., the work energy and kinetic energy) is **first** calculated based on the assumptions that the blast load from the **shock** wave in the building is a purely impulsive loading and the blast load from the quasistatic pressure buildup is an immediately applied load with a long duration compared to the natural period of the building components. The work energy and kinetic energy terms calculated with these simplifying assumptions are then modified by reduction factors based on some single-degree-of-freedom dynamic analyses of typical building components which considered the actual calculated durations of shock and quasistatic blast load and the natural periods of the building components. The calculated strain energy absorbed by the building components in the energy balance is increased relative to theoretical values by a factor which is based on comparisons between damage calculated with a theoretical analysis and that calculated using the original pressure-impulse diagrams for various components.

### 3.0 CALCULATION OF BLAST LOADS

As mentioned in the first section, the calculation of building damage begins with **the** calculation of blast loads on each component of the input **building**. The blast pressure history is calculated based on the input equivalent TNT charge weight, the charge location relative to the building, and the assumption of a surface burst explosion. The pressure history is characterized in terms of the positive phase impulse and peak pressure. The impulse is **the** integral, or area, of **the** pressure under the pressure-time curve. This is **illustrated** in Figure 1. Only the positive portion of the blast pressure history shown in Figure 1 is considered in the blast damage assessment procedure. This simplification is discussed later in this section. The peak positive phase pressure and impulse are calculated for each building component using curve-fit equations to data from Reference 9, which are also those used in the recently updated version of **TM5-1300** "Structures to Resist the Effects of Accidental **Explosions**"<sup>(10)</sup>. The curve-fit equations are high-order polynomial curve-fits which are a function of the scaled standoff (the standoff between **the** charge and building component divided by the cube root of the charge weight) and the charge weight. The standoff is calculated as the straight line distance from the charge to the geometric center of the component. Either fully reflected or incident (**free-field**) blast pressures on each component are calculated according to logic which is based on the angle of incidence between the direction of blast wave propagation and the outward normal from the component surface. This angle is illustrated in Figure 2.



Ideal Blast Wave

$$i_S^+ = \int_{t_a}^{t_a + T^+} [p(t) - p_0] dt$$

and

$$i_S^- = \int_{t_a + T^+}^{t_a + T^+ + T^-} [p_0 - p(t)] dt$$

$P_s^+$  = peak positive phase **overpressure**

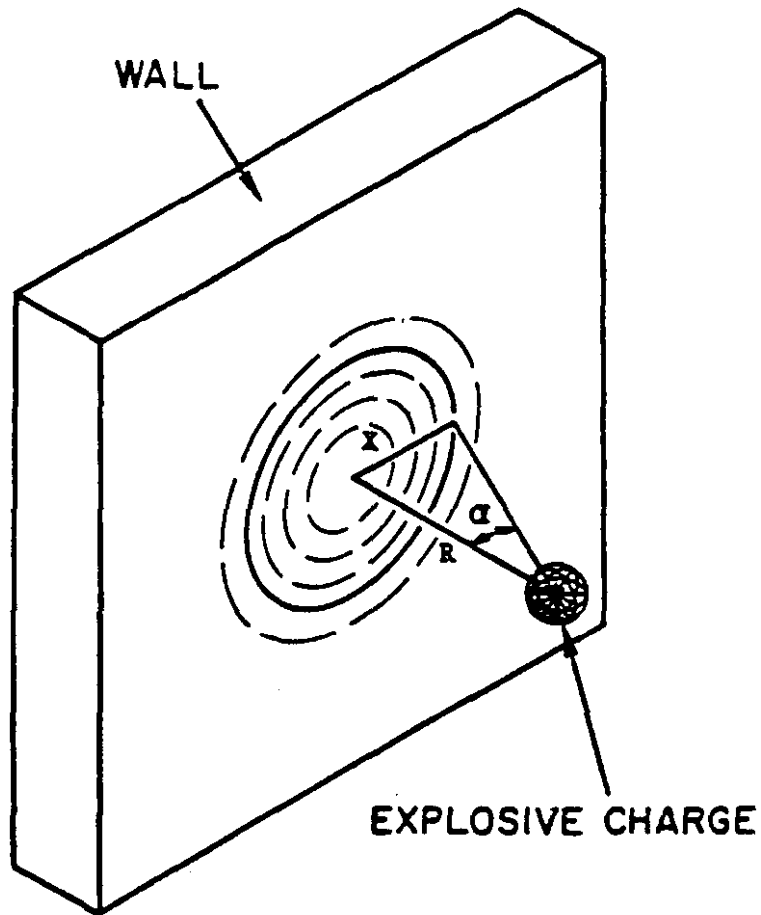
$P_s^-$  = peak negative phase **overpressure**

$i_t^+$  = positive **phase** impulse

$i_t^-$  = negative phase impulse

$P_0$  = ambient pressure

Figure 1. Ideal Blast Wave Shape and Definition of Blast Wave Parameters



- where
- R = **shortest** distance from center of explosive charge to wall (length of normal vector)
  - X = distance from closest projected point on the wall from the charge to the point on the wall at which loading will be determined
  - a = angle of incidence which is the **angle** between normal vector and direct vector between charge and point on the wall **will be** determined

**Figure 2. Angle of Incidence of Point on Wall Relative to Explosive Charge**

The previous summary describes the simplified method used in the blast damage assessment procedure in the FACEDAP program to calculate blast loads on each building component. According to the current state of knowledge, there are a number of factors which generally affect the blast load on structural components which are not included in this procedure. If these factors do not cause more than a 15% to 30% error in the calculated blast loads, then it is appropriate to ignore them since the blast damage **assessment** methodology does not calculate structural blast damage very precisely and is intended to be a relatively quick procedure to determine the approximate amount of blast damage. As the error exceeds this amount, it may begin controlling the overall accuracy of the methodology. Therefore, it is important to look at the variables not **considered in this procedure and assess the effect of their exclusion or simplification on the calculated** blast loads for typical conditions. The next paragraphs describe major variables which are not included and give a discussion on how each simplification **affects** the accuracy of the calculated blast loads. A more thorough discussion of each of these variables can be found in Chapter 2 of Reference 10.

### THE MACH STEM HEIGHT

The blast loads are always calculated assuming a hemispherical surface burst of the explosive. This assumption is always conservative and it is realistic if the “triple point”, which defines the height of the Mach stem off the ground, is greater than the building height. For most expected uses of this procedure, the scaled height of burst (the charge height off the ground divided by the cube root of the charge weight) will be less than  $1.0 \text{ ft/lb}^{1/3}$  and the scaled standoff will be greater than  $3.0 \text{ ft/lb}^{1/3}$ . For these cases, the triple point is usually greater than the height of a one or two story building and the assumption of a surface burst is therefore a realistic one. Section 2-13.2 of Reference 10 gives more explanation which is pertinent to this assumption.

### THE ANGLE OF INCIDENCE

When a building surface partially blocks the propagation of a shock wave, it reflects the leading portion of the shock wave back into the trailing portion of the wave. This causes a buildup of temperature and density in the air immediately in front of the surface which, in turn, causes the pressure acting on the surface to almost instantaneously **rise** to a value at least twice as large as the free-field pressure. The intensity of the pressure build up, or rise to **its** “reflected” magnitude, depends on several parameters including the scaled standoff and the angle of incidence between the reflecting surface and the direction of shock wave propagation. The angle of incidence of a point on a surface is the angle between the outward normal and the direct vector from the explosive charge to the point. This is illustrated in Figure 2. The point of interest is always at the center of the component and the blast load at the center is used as a uniform load over the entire component. For a given scaled standoff, the pressure measured on a large rigid surface and an angle of incidence equal to **zero** degrees is the fully reflected pressure at that scaled standoff. For a given scaled standoff, the pressure measured at a point on a surface which has an angle of incidence of 90 degrees (i.e., it is parallel to the direction of blast wave propagation and does not reflect the shock wave at all), is the incident, or free **field** pressure at the given scaled standoff. Since the impulse is the integral of the pressure history, the impulse applied to a surface is also increased from its free field value if the angle of incidence is less than 90 degrees.

According to the simplified procedure, the blast pressure on the building components can be either the **fully** reflected or the incident pressure corresponding to the **calculated** scaled standoff, depending on the angle of incidence. **If the** angle of incidence is less than 45 degrees, fully reflected peak pressure and impulse are calculated. Otherwise, the incident peak pressure and impulse are calculated. In reality, the peak pressure transitions from fully reflected to fully incident as the angle of incidence changes from **zero** degrees to **90** degrees as a function of the incident pressure. Figure 3 (**from** Reference 1) shows this relationship with a series of calculated curves. The fully reflected peak pressure corresponding to each side-on pressure shown is the product of the side-on pressure and the reflection factor shown on the vertical axis of the **figure**. The recommended minimum scaled standoff is  $3.0 \text{ ft/lb}^{1/3}$ . This implies that only curves corresponding to peak incident, or side-on pressures less than 150 psi are applicable. Figure 3 shows that, for the applicable side-on pressure levels, the peak blast pressure **remains** close to **its full reflected value** for angles of incidence less than 45 degrees. Therefore, the simplification that the blast pressure is constant at its full reflected value in this range of incident angles is a good simplifying approximation. On the other hand, the pressures at angles of incidence greater than 45 degrees are always greater than the incident, or free-field, pressure level that is assumed. This is particularly true for pressures near 150 psi, and therefore scaled standoffs near  $3.0 \text{ ft/lb}^{1/3}$ , and at angles of incidence between 45 and 60 degrees. The reflection factor for impulse is also a function of angle of incidence, but it is a smoother relationship than that shown in Figure 3. Impulse on components with angles of incidence between **zero** and 45 degrees are predicted well with the simplified blast load calculation method (usually within 20% and on the conservative side), but impulse on components with angles of incidence greater than 45 degrees are underestimated, although to a lesser extent than the peak pressure. Impulse is underestimated by factors from 2.5 to 1.5 for angles of incidence between 45 degrees and 70 degrees. In summary, **the** simplified consideration of the relationship between angle of incidence and reflection of the blast wave is quite accurate for components with a center point at either small angles of incidence (less than 45 degrees) or large angles of incidence (near 90 degrees or greater than 90 degrees). However, it underestimates the peak pressure and impulse on components with angles of incidence between 45 degrees and approximately 70 degrees by factors between two and five. For many buildings at larger standoffs from the charge, most of the components on walls subjected to reflected pressures will be at angles of incidence less than 45 degrees because the radius of wall area which is at an angle of incidence less than a given value  $\alpha$  in Figure 2 increases with the distance **R**, or the standoff.

#### CLEARING TIME OF RELIEF WAVES **OFF** BUILDING FREE EDGES

The angle of incidence affects the **magnitude** of the reflected pressure on a component. The clearing time of the relief waves off building free edges affects the **duration** of the reflected pressure, and therefore affects the impulse. The duration of the reflected shock pressure on a surface, and thus the **magnitude** of the impulse, is dependent on the distance from the component to the nearest free edge of the structure. This is true because when the blast wave first begins to propagate past the free edges of a surface, relief waves are formed at these edges which propagate toward the center of the surface and, as they propagate, relieve the density and pressure buildup along the reflecting surface. After the relief waves **have** cleared through an area of the surface, the reflection factor shown in Figure 3 is no longer relevant and the pressure is **equal** to the free field value. **If**

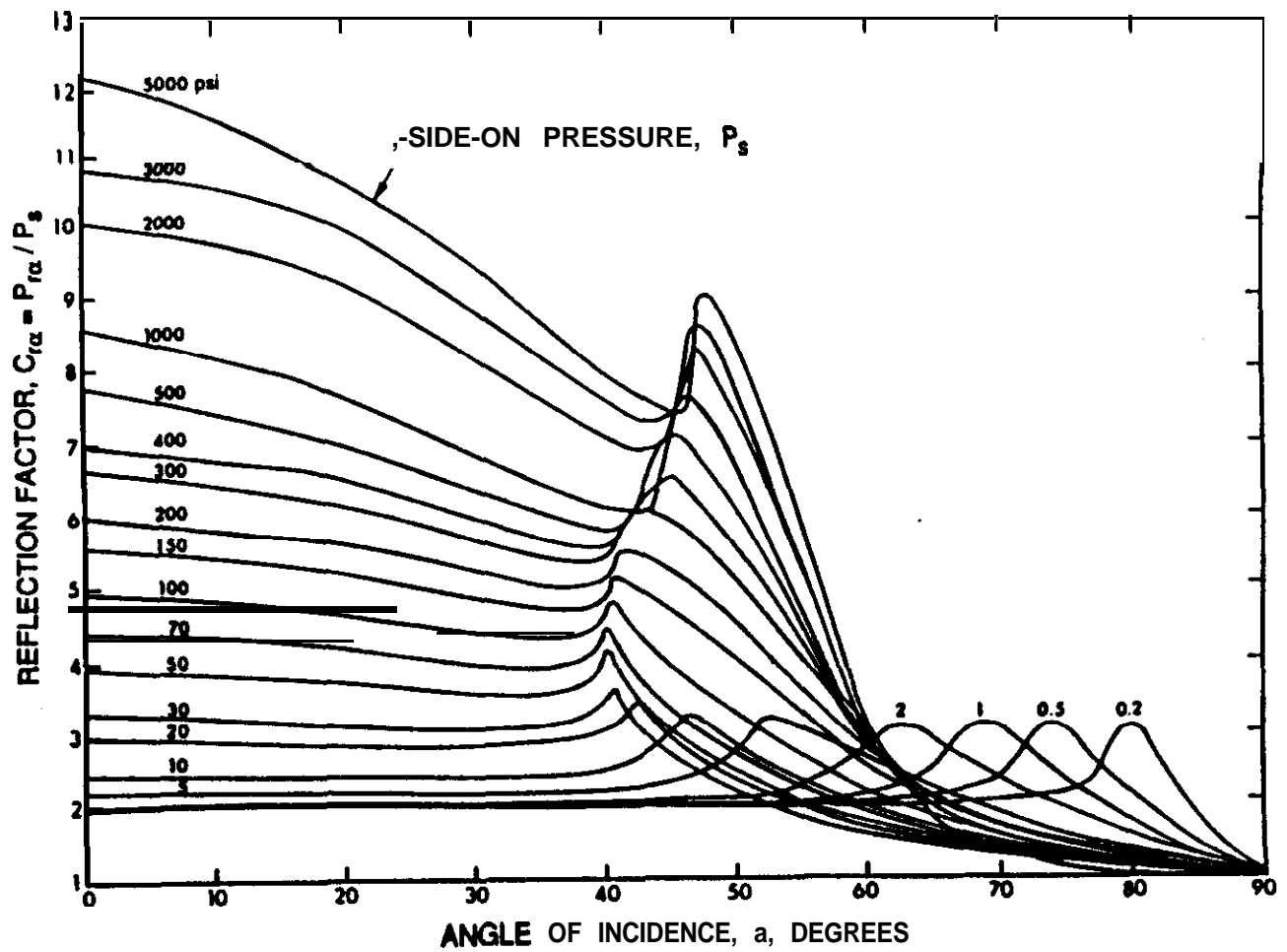


Figure 3. Reflected **Pressure** Coefficients versus Angle of Incidence for a Plane **Shock** Wave (Reference 10)

the time required for the relief wave to reach a point of interest on the surface is greater than the positive duration of the blast pressure, then no reduction in the reflected pressure occurs. The simplified blast load calculation procedure assumes that **there is** never any reduction in the reflected pressure due to the presence of relief waves. Therefore, it assumes that the bulk of the impulse is always applied to a reflecting surface prior to the arrival of relief waves. As Figure 1 shows, most of the impulse is applied early within the duration due to the shape of the blast pressure history.

The approach taken by the **simplified** blast load calculation procedure is always conservative and for most cases it is relatively accurate. For scaled standoffs between 3.0  $\text{ft/lb}^{1/3}$  and 10  $\text{ft/lb}^{1/3}$ , the total positive phase duration, in milliseconds, is approximately twice the scaled charge weight (the cube root of the charge weight). This can be **verified** by inspecting Figure 2-15 in Reference 10. For a typical **building** in this range of scaled standoffs, the clearing time required to relieve the reflected pressure on the **wall** is approximately 18 ms using the approximate empirical formula below taken from Chapter 8 of Reference 11.

$$t_c = 3S/U \quad (3.1)$$

$t_c$  = clearingtime  
 $S$  = height of wall (or **one-half wall** width if this is less than height) • a value of 12 ft was used in above estimate  
 $U$  = shock front velocity • a value of 2 **ft/ms** was used for above estimate (see Figure 2-15 in Reference 10)

We will assume that almost **all** of the impulse **occurs** within the **first** half of the pressure history here. Based on the discussion above, at least one half of the positive phase duration, and thus most of the impulse, **will** occur within the clearing time (before the relief waves relieve the reflected pressure) when the charge weight is less than  $18^3 = 6000$  lb. This implies that, for charge weights less than 6000 lbs and scaled standoffs between 3.0  $\text{ft/lb}^{1/3}$  and 10  $\text{ft/lb}^{1/3}$ , the arrival of the relief wave will be too late to significantly affect the impulse. It is thought that these charge weight and scaled standoff ranges include the **bulk** of the situations which **will** probably be considered. Therefore, the assumption in the simplified blast load calculation procedure that relief waves do not affect **impulse** on reflecting surfaces is a reasonable assumption that does not significantly reduce the accuracy of the blast load calculations for most expected uses of the code.

## DRAG PRESSURES

The effect of the drag phase of the blast load is not considered by the simplified blast load calculation procedure. Drag loads are caused by the “wind” that occurs as the shock wave accelerates **air** particles which interact **with** the structure. Just as with a typical wind gust, the load on the structure front **wall** which blocks the wind is increased and the load on the roof and other walls is decreased due to a suction effect. In Reference 10, drag pressures are equal to the product of the dynamic blast pressure and a drag factor ( $q_d \times C_d$ ). The drag pressures only add to the incident shock pressure because the reflected pressure includes the effects of both the shock wave and the pressure of the accelerated air particles **which** are stopped by the surface. For the front wall, which blocks the accelerated air particles, the drag factor is equal to 1.0. However, most of the components on this surface are subject to reflected pressures and therefore no additional drag force is required.

The blast load on those components on this wall at an angle of incidence greater than 45 degrees is already underestimated since no reflection is assumed, as discussed previously, so ignoring the drag force on these components is secondary. The drag factor on all other building walls and roof (which are loaded by an incident pressure history) is negative, since the accelerated air particles cause a suction pressure on these surfaces as they flow by. Ignoring the drag forces on these surfaces is conservative. Moreover, the product of  $(q_u \times C_d)$  is almost always less than 20% of the peak incident pressure so that the reduction in loading that is being ignored is not substantial. This can be verified by inspecting the ratio of the dynamic pressure to incident pressure, which is always less than 1.0, in Figure 2-3 of Reference 10 and the negative drag factors recommended in Section 2.15.3.3 in Reference 10. In summary, the approach to ignore the effect of the drag phase is a good simplifying assumption for the expected uses of this code.

## RATIO OF SHOCK WAVELENGTH TO COMPONENT SPAN

Components which lie along the direction of shock wave propagation are loaded gradually by the shock. When the center of the component is loaded with the peak incident shock pressure, no load is (yet) applied to the far edge of the component away from the charge, and the near edge of the component is loaded with a reduced pressure that is dependent on the ratio of the wavelength to the component length. For structural analysis and design purposes, the transit time of the shock wave across the component span is not considered explicitly. Instead, the pressure is assumed constant along the span and is calculated based on the scaled standoff to the center of the span. This is the approach taken by the simplified blast load calculation procedure. However, the peak pressure calculated with this scaled standoff is often multiplied by a reduction factor to account for the fact that the actual average pressure which acts on the span is always less than the calculated peak pressure. If this more accurate approach is taken, the duration is also multiplied by an increase factor to account for the fact that the total time over which some part of the component is loaded by the blast is increased. If the wavelength is long compared to the span, then most of the span is subjected to the same pressure at any given moment, and both the reduction factor on the pressure and the increase factor on the duration approach 1.0. Thus, the increase and reduction factors are a function of the ratio of the blast wavelength to the component span.

The magnitude of the increase on the duration and the reduction factor on the peak pressure can be estimated for the range of expected uses. In Figure 2-15 of Reference 10, the scaled blast wavelength varies from  $0.5 \text{ ft/lb}^{1/3}$  to  $2.0 \text{ ft/lb}^{1/3}$  for scaled standoffs between  $3.0 \text{ ft/lb}^{1/3}$  and  $10 \text{ ft/lb}^{1/3}$ . An "average" scaled wavelength of  $1.0 \text{ ft/lb}^{1/3}$  will be used here. Assuming a span length of 20 ft, the average wavelength is less than the span when the charge weight is less than 8000 lbs. This is equivalent to saying that the span length **will** typically be greater than the blast wavelength. Figure 2-196 in Reference 10 shows that, when the span is greater than the blast wavelength, a significant reduction factor is recommended for the equivalent peak pressure (a reduction factor between 2 and 4). Figure 2-198 indicates that, for this same case, the effective duration increases by a factor between 1.5 and 3. This latter statement is based on the curves in Figure 2-198 for 16 and 32 psi incident pressure and a comparison of the scaled durations in Figure 2-198 to the scaled durations at the same pressures (16 and 32 psi) in the free field shown in Figure 2-15. The reduced **equivalent** peak pressure and increased effective duration work together to keep the impulse approximately the same as that predicted by simply assuming the blast load constant over the span

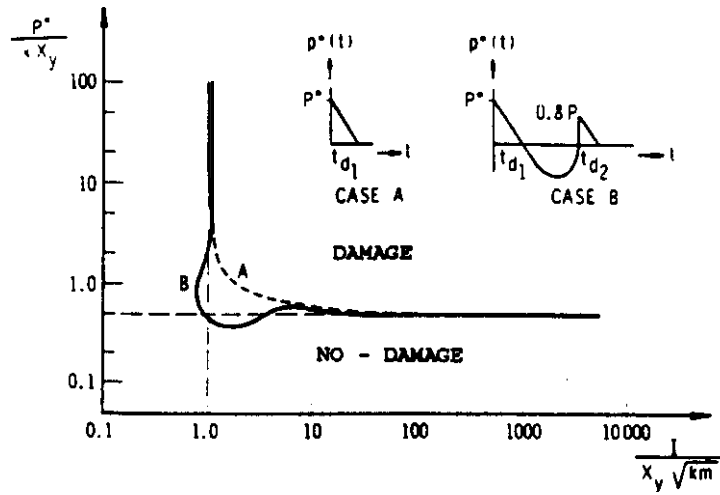
and equal to the value calculated using the scaled standoff to the center of the span. As mentioned previously, this is the assumption made in the simplified blast load calculation method in the FACEDAP code. However, this method **will** overestimate the equivalent peak pressure by a significant margin. Therefore, the **simplified** method will reduce the accuracy of damage calculated to components which are sensitive to the peak pressure by overestimating the peak pressure but will not affect the accuracy of damage calculated for impulse sensitive components. Pressure sensitive components are those which have a natural period at least three times the blast wave duration. The beams, or **girts** along sidewalls, and roof beams and roof slabs typically have spans parallel to the direction of the blast wave propagation.

#### EFFECT OF THE NEGATIVE PHASE OF THE BLAST PRESSURE HISTORY

The simplified blast load calculation method does not calculate the negative phase blast pressures and therefore assumes that these pressures do not significantly affect component damage. **In** general, the negative phase can be “in-phase” with the component response so that it occurs during rebound and causes damage or failure during rebound. If the negative phase pressures are significant compared to the positive phase pressure, then the additional damage occurring during rebound for a case of m-phase negative phase loading can be significant. Figure 4 from Reference 12 illustrates how the inclusion of the negative phase loading can influence a damage curve on a P-i diagram. The approximate ratio of negative phase pressure to positive phase pressure is relatively small (less than 20%) except when the peak positive phase incident pressure is less than 2 psi. **This can be verified by comparing Figures 2-15 and 2-16 in Reference 10 using the theoretically predicted peak negative phase pressures in Figure 2-16.** These figures also show that the negative phase duration is typically much longer than the positive phase duration. **Therefore the damage contributed** by the negative phase pressure can be significant compared to that caused by positive phase loading when the component strength is on the order of 2 psi and when the response of these components is in-phase with the arrival of the negative phase blast. According to calculations in the appendix of Reference 7, where response properties (such as the ultimate resistance and natural period) of a large number of components in twelve “typical” **unstrengthened** buildings were calculated, this includes a surprising number of components. These components include open web joists, cold formed steel beam sections, wood components, unreinforced masonry components, and even some lightly reinforced concrete components. Prediction of negative phase pressure and impulse is plagued by the fact that there are relatively few measurements of this phase of the blast pressure history as evidenced by the fact that the blast curves in Reference 10 rely on theory rather than on empiricism, as is the case for the positive phase blast.

#### UNIFORMITY OF **THE** SPATIAL **PRESSURE** DISTRIBUTION

The structural analysis procedures in the simplified blast load calculation method assume a **spatially** uniform pressure distribution on the component. This is the same assumption used **in** Reference 10 **for blast resistant** structural design and in many other **simplified** analyses of structural response to blast load. The restriction that this methodology be used for **scaled** standoffs at least equal to 3.0 **ft/lb<sup>1/3</sup>** ensures that the actual pressure distribution on components will be uniform for practical purposes. This restriction is also intended to ensure that the code is not used to predict



$P^*$  = peak pressure

$I$  = impulse

$K, X_y, m$  = structural parameters

Figure 4. Effect of Negative Phase Blast Pressure on Structural Dam-age

damage for situations where local damage mechanisms, such as local breach or shear failure, can cause significant amounts of component damage. The component blast damage prediction methods only consider damage which occurs during **flexural** response or column buckling.

## SUMMARY

In summary, the method used in the FACEDAP blast damage assessment procedure for calculating the positive phase blast pressure and impulse is **generally** conservative although it is nonconservative for some components on building walls where reflected blast pressures occur. The calculated peak pressure and impulse are **unconservative** for components which are subjected to reflected blast pressures and are oriented at angles of incidence between 45 degrees and 70 degrees **with respect to the direction of blast wave propagation because only free field pressures are calculated** on these surfaces. The nonconservatism in the simplified blast load calculation procedure for this case is a factor between two and **five** for the peak pressure and a factor between 1.5 and 2.5 for the impulse compared to more accurate methods in Reference 10. The peak blast pressure can be **overconservatively calculated (conservative by a factor between 2 and 4) on components in sidewalls** and roofs with spans parallel to the direction of shock wave propagation in the **simplified** procedure because it does not consider the reduction in effective peak pressure that occurs when the **shock** wavelength is less than the span length. For most other cases, the **simplified** method calculating positive phase blast loads gives results which are close to those which would be calculated using the more accurate methods in Reference 10. An important unknown is the amount of **nonconservatism** inherent in the fact that the simplified procedure ignores the effect of the negative phase blast pressure on the damage of light building components (building components with an **ultimate resistance less than 2 psi**). As a final note, where the component damage prediction methods are based on data from explosively loaded buildings (and, to a lesser degree, explosively loaded components) rather than on theoretical methods, some of the variables affecting blast loads are considered implicitly in the damage data.

## 4.0 PREDICTION OF COMPONENT DAMAGE

As mentioned in the introduction, the component damage assessment procedure is based on available data and basic structural dynamic theory. The theoretical development is based on an idealization of the building components as single-degree-of-freedom (**SDOF**) systems responding in flexure or buckling to linearly decaying blast loads. The exponentially decaying positive phase pressure history in Figure 1 is idealized as **a linearly decaying pressure history with the same impulse**. This **results** in a “pseudo” load duration which is shorter than **the** actual duration  $T^*$  shown in Figure 1. Using these idealizations, component response, or damage, is related to the component properties for a full range of possible blast loads with equations that are derived from basic structural dynamics theory. This is done using pressure-impulse diagrams, or P-i diagrams, which separate damage into four damage categories with “damage curves”, as discussed below. The graphical nature of P-i diagrams allows damage data to be directly plotted against the theoretically determined damage curves. In some cases, the data “validated” the theoretical curves in the sense that it shows that they predicted damage which fell in the same damage category, or damage level, predicted by the theoretically determined damage curves. In other cases, the theoretically generated damage **curves**.

were “shifted” to match the damage data. Generally this latter case occurred when the component was responding in some response mode other **than** the **flexural** mode assumed in the development of the theoretical damage **curves**.

An understanding of the development of the P-i diagrams is essential to an understanding of the building damage predicted by the FACEDAP program. Considerable explanation is provided in the following sections on both the theoretically developed damage curves and on the data used to validate or shift the curves. The P-i diagrams used to predict component damage for each of the twenty-four component types considered in this methodology are presented in the next section, and the development of each of these diagrams is explained in the following sections.

#### 4.1 Component P-i Diagrams

The following table lists the twenty-four component types **considered** in the FACEDAP program.

**Table 1. Structural Components Considered in the FACEDAP Program**

<b>Concrete Components</b>	<b>Steel Components</b>	<b>Masonry Components</b>	<b>Wood Components</b>
R/C Beams	Steel Beams	One-Way Unreinforced Masonry	Wood Stud Walls
R/C One-Way Slabs	Metal Stud Walls	Two-Way Unreinforced Masonry	Wood Roofs
R/C Two-Way Slabs	Open Web Steel Joists (bending response)	One-Way Reinforced Masonry	Wood Beams
R/C Exterior Column (bending response)	Corrugated Metal Deck	Two-Way Reinforced Masonry	Wood Exterior Columns
R/C Interior Column (buckling response)	Steel Exterior Columns (bending response)	Masonry Pilasters	Wood Interior Columns
R/C Frames (lateral frame sway)	Steel Interior Columns (buckling response)	-	-
Prestressed Beams	Steel Frames (lateral frame sway)	-	-

All component response is determined in terms of the four qualitative damage levels described below. These are not "official" descriptions; they are a synthesized combination of the qualitative descriptions found in References 3 and 4. The four damage levels have also been correlated with the levels of protection defined in Reference 13, which are used by the U.S. Army Corp of Engineers<sup>(4)</sup>. These correlations are included in the damage level descriptions.

- 0% Damage:** No appreciable damage; the component is reusable without repair. This damage level can be equated with a High Level of Protection.
- 30% Damage:** Moderate damage; the component is probably repairable and it has provided a medium, or generally adequate level of protection to personnel and equipment from the effects of the explosion. This damage level can be equated with a Medium Level of Protection.
- 60% Damage:** Severe damage; the component is not worth repairing, but it has not failed and it has provided at least some protection to personnel and equipment from the effects of the explosion. This damage level can be equated with a Low Level of Protection.
- 100% Damage:** The component is definitely beyond repair but it has not necessarily completely collapsed. It has undergone a deformation such that it cannot be counted on with high certainty to protect personnel and equipment from the effects of the explosion. This damage level can be equated with "collapse" as it is used in terms of a Level of Protection. However, components with 100% damage which is relatively near the borderline between 100% damage and 60% damage will most probably not be collapsed in terms of the general usage of this word.

These damage categories were selected in the original development of the blast damage assessment procedure based in part on the qualitative damage descriptions found in test data. They were also based in part on some consideration of component response criteria (i.e., ductility ratios and end support rotations) called out in design criteria for different protection levels in References 10 and 14. A qualitative description of damage definitions was selected as opposed to a more quantitative description of damage since it is more appropriate for expressing the component response calculated with the approximate damage assessment techniques in the methodology. However, in subsequent work the four damage categories were correlated with specific component response criteria for most of the twenty-four component types because it was judged that in spite of the approximate nature of the methodology, it was nonetheless better to provide some qualitative description of the four damage levels<sup>(4,7)</sup>.

AU component **response** is determined in terms of **the** four qualitative damage levels described below. The descriptions shown for each damage level are not "**official**" descriptions; they are a **synthesized** combination of the qualitative descriptions found **in References 3 and 4**. The four damage levels have also been **correlated** with the levels of **protection** defined **in Reference 13**, which are used by the U.S. Army Corps of Engineers<sup>[4]</sup>. These **correlations** are included in the damage level descriptions.

- 0% Damage: No appreciable damage; the component is reusable without repair. This damage level **can be equated with a High Level of Protection.**
- 30% Damage: Moderate damage; the component **is** probably repairable and it has provided a medium, or generally adequate level of **protection** to personnel and equipment from the effects of the explosion. This damage level can be equated with a **Medium Level of Protection.**
- 60% Damage: Seven damage: the component is not worth repairing, but it has not failed and it has provided at least some protection to personnel and equipment **from** the effects of the explosion. **This** damage level can be equated with a **Low Level of Protection.**
- 100% Damage: The component is **definitely** beyond repair but it has not necessarily completely collapsed. It **has** undergone a deformation such that it cannot be counted on with high certainty to protect personnel and equipment from the effects of the explosion. **This damage level is equated with "Collapse" as it is used in terms of a Level of Protection.** However, components with **100%** damage which is relatively near the borderline between 100% damage and 60% damage will most probably not be collapsed in terms of the general usage of this word.

These damage levels were selected in the **original** development of the blast damage **assessment** procedure based in part on the qualitative damage descriptions found in test data **They were** also based in **part** on some consideration of component response criteria (i.e., ductility ratios and end support rotations) called out in design criteria for different protection levels in References **10 and 14**. A qualitative description of damage definitions was selected as opposed to a more quantitative description of damage because it is more consistent with the approximate damage assessment techniques in the methodology. However, **in** subsequent work the four damage categories were **correlated** with specific component response criteria for most of the twenty-four component types because it was judged that **in** spite of the approximate nature of the methodology, it **was** nonetheless better to provide some **qualitative description** of the four damage levels<sup>[4,7]</sup>. These qualitative **descriptions** were modified slightly during the development of the **FACEDAP** program.

**Approximate correlations** between quantitative measures of component response (i.e.  $\mu$  and  $w/L$ ) and the four damage levels are shown in Table 2. **The** ductility ratio ( $\mu$ ) is equal to the ratio of the maximum deflection to the yield deflection at **midspan** and the deflection to span ratio ( $w/L$ ) is equal to the **ratio** of the maximum deflection to the span length. **The** ductility ratios corresponding to each damage level **in** Table 2 **are** based on ductility ratios measured in tests where the four damage levels were observed or **they** are assumed based on **engineering judgement** and criteria suggested **in** other references. As explained in Section 4.4, the P-i **diagrams** were developed so that they only correlate the component dynamic response and blast load characteristics to the **ductility** ratio of the component response. Therefore, the damage **levels** can only be directly expressed quantitatively in terms of corresponding **ductility** ratios. The **w/L** values in Table 2 were derived **from** the corresponding ductility ratios for each component damage level using an assumed "typical" yield deflection **value** as a function of **span** for each component type (i.e.,  $w/L = \mu(W)$ , where  $W = (\text{yield deflection}/L)$ ). For components with arching, **w/L** values from data were used to directly determine the **w/L** limits for each damage level.

Table 2. Quantitative Criteria **Defining Damage** Levels for Each Component Type

Component Type	Damage Criteria						Notes (see text for more discussion and see general notes)
	Lower Limit of 30% Damage		Lower Limit of 60% Damage		Lower Limit of 100% Damage		
	$\mu$	w/l	$\mu$	w/l	$\mu$	w/l	
Reinforced Concrete (R/C) Beam	1	.005	5	.022	20	.09	Ductility values assumed same as one-way R/C slab
R/C One-Way Slabs	1	.007	5	.034	20	.135	Ductility values validated w/data
R/C Two-Way Slabs without Arching	1	.015	5	.08	20	.31	Ductility values assumed same as one-way R/C slab
R/C Two-Way Slabs with Arching	1	.005	5	.013	20	.20	Ductility values determined from approx. theoretical approach, w/l values based directly on data
R/C Exterior Columns (bending)	1	.003	5	.014	20	.054	Ductility values assumed same as one-way R/C slab
R/C Interior Columns (buckling)	--	--	--	--	1	.002	Criteria apply only to impulsive response and are assumed
R/C Frames	1.3	.014	6	.066	12	.133	Ductility values validated w/some data, w/l values are ratio of max. frame sway to column height
Prestressed Beams	.5	.005	1	.01	2	.02	Ductility values are assumed
Steel Beams	2	.012	7	.04	15	.009	Ductility values are based on some data
Metal Stud Walls	2	.02	7	.07	15	.15	Ductility values are assumed same as steel beams
Open Web Steel Joists (based on flexural tensile stress in bottom chord)	1	.01	3.5	.035	6	.06	Ductility values are assumed
Corrugated Metal Deck	2	.012	7	.042	15	.09	Ductility values validated w/some data
Steel Exterior Columns (bending)	2	.009	7	.032	15	.068	Ductility values are assumed same as steel beams
Steel Interior Columns (buckling)	--	--	--	--	1	.0045	Ductility values apply only to impulsive response and are assumed
Steel Frames	1.3	.021	6	.10	12	.20	Ductility values validated w/some data, w/l values are ratio of max. frame sway to column height
One-Way Unreinforced Masonry (unarched)	--	--	--	--	1	.0005	Ductility values are assumed
One-Way Unreinforced Masonry (arched)	.25	.005	.5	.02	1.0	.04	Ductility values determined from data using approx. theoretical approach, w/l values based directly on data

**Table 2. Quantitative Criteria Defining Damage Levels for Each Component Type  
(Continued)**

Component Type	Damage Criteria						Notes (See text for more discussion and see general notes below)
	Lower Limit of 30% Damage		Lower Limit of 60% Damage		Lower Limit of 100% Damage		
	$\mu$	w/l	$\mu$	w/l	$\mu$	w/l	
Two-Way Unreinforced Masonry (fully arched)	.1	.005	.15	.02	.25	.04	Ductility values determined from data using approx. theoretical approach, w/l values based directly on data
One-Way Reinforced Masonry	1	.0016	5	.008	20	.032	Ductility values assumed same as one-way R/C slab
Two-Way Reinforced Masonry	1	.0016	5	.008	20	.032	Ductility values assumed same as two-way R/C slab
Masonry Pilasters	1	.0006	5	.003	20	.012	Ductility values assumed same as R/C beam
Wood Stud Walls	.5	.01	1	.021	2	.043	Ductility values based on data
Wood Roofs	.5	.01	1	.021	2	.043	Ductility values based on data
Wood Beams	.5	.008	1	.016	2	.032	Ductility values assumed same as wood walls/roof
wood Exterior Columns (bending)	.5	.01	1	.021	2	.043	Ductility values assumed same as wood walls/roof
Wood Interior Columns (buckling)	--	--	--	--	1	.021	Ductility values apply only to impulsive response and are assumed

**General Notes:**

1. All w/l values are derived from ductility values using an assumed ratio of yield deflection to span length for a "typical" component except where indicated otherwise.
2. All values in this table are intended to correlate as well as possible to damage observed in test data and therefore will not always correlate with design criteria
3. The lower limits of 30%, 60%, and 100% damage referred to in this table correspond directly to the upper bounds of High, Medium, and Low Levels of Protection, respectively, as discussed in Section 4.1.

The following pages show the P-i diagrams for each of the twenty-four component types which are used in the FACEDAP program to predict component damage. The equations for the  $\bar{p}$  and  $\bar{i}$  terms on each axis of the P-i diagrams are shown below the diagram. Each of the parameters in these equations is explained in table format on the page preceding the P-i diagram. Also, each of the parameters related to material or cross sectional properties of the component is illustrated in an example below the table. The  $\bar{p}$  and  $\bar{i}$  terms are always dimensionless. Therefore, the parameters used in the equations to calculate  $\bar{p}$  and  $\bar{i}$  must always be converted into a consistent set of units (i.e., inches, pounds, and seconds). It is always good practice to include the dimensions of all parameters in the  $\bar{p}$  and  $\bar{i}$  equation and check that the dimensions cancel so that the calculated  $\bar{p}$  or  $\bar{i}$  is dimensionless as it should be. The FACEDAP program automatically calculates dimensionless  $\bar{p}$  and  $\bar{i}$  terms as long as the user inputs information in the specific units called out in the program.

**P-I Diagram Input for Reinforced Concrete Beams**

Parameter	Description	Parameter Value for Example Case Below
Peak Pressure (p)	Peak Blast Pressure at Center of Component	-
Specific Impulse (i)	Specific Impulse Applied to Center of Component	-
Span Length (L)	Span Length Between Supports	-
Beam Width (b)	Beam Width	12 in
Beam Thickness (h)	Beam Thickness	12 in
Loaded Width (b <sub>l</sub> )	Loaded Width	10 ft
Total Weight (W)	Total Weight in Pounds of Section + Supported Components	see equation below figure
Concrete Compressive Strength (f' <sub>c</sub> )	Compressive Strength of the Concrete (f' <sub>c</sub> )	4,000 psi
Steel Yield Strength (f <sub>y</sub> )	Yield Strength of the Steel Reinforcement	60,000 psi
Depth to Tensile Steel (d)	Depth to Tensile Steel Reinforcement from Loaded Side	10 in
Area of Tensile Steel (A <sub>s</sub> )*	Area of Tensile Steel Reinforcement within Section Width	2.37 in <sup>2</sup>
Moment of Inertia (I <sub>cr</sub> )	Moment of Inertia of Cracked Cross Section	1,150 in <sup>4</sup>
Gravity Constant (g)	Gravity Constant	386.4 in/sec <sup>2</sup>
Moment Capacity (M <sub>p</sub> )	Moment Capacity of Beam	1.06 E6 lb-in
Young's Modulus (E)	Young's Modulus for Concrete	3.6 E6 psi

• SEE GENERAL NOTES 1 AND 2 <sup>ON PAGE 59 OF USFS MANUAL</sup> AT END OF COMPONENT DESCRIPTIONS

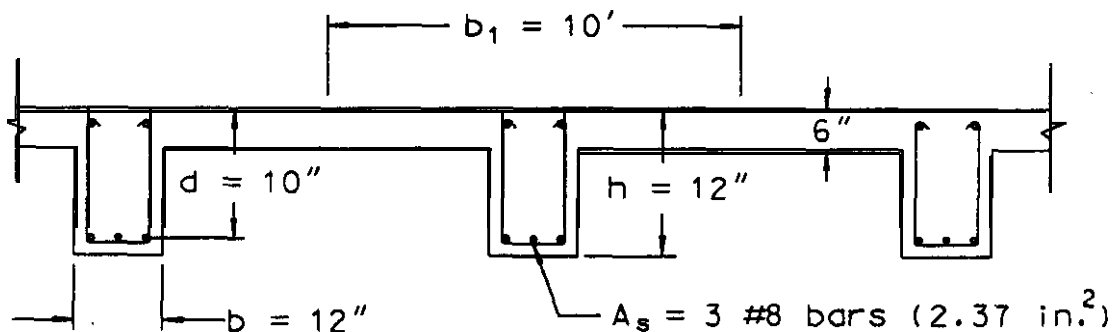
calculated Values

$$M_p = 0.9 b d^2 f_y \rho (1 - 0.59 \rho f_y / f'_c)$$

$$E = 57000 \sqrt{f'_c}$$

$$I_{cr} = \frac{b d^3 (5.5 \rho + 0.083)}{2}$$

$$\rho = \frac{A_s}{b d}$$



$$W = [(10 \text{ ft}) (0.5 \text{ ft}) + (12 \text{ in}) (12 \text{ in} - 6 \text{ in}) / 144] (L) (150 \text{ lb/ft}^3)$$

where L = span length (ft)

## P-I Diagram Input for Reinforced Concrete Beam

Parameter	Description	Parameter Value for Example Case Below
Peak Pressure ( <b>p</b> )	Peak Blast <b>Pressure</b> at Center of Component	
Specific Impulse ( <b>i</b> )	Specific Impulse <b>Applied</b> to Center of Component	
Span Length ( <b>L</b> )	Span Length Between <b>Supports</b>	
Beam Width ( <b>b</b> )	Beam Width	12 in
Beam Thickness ( <b>h</b> )	Beam Thickness	12 in
Loaded Width ( <b>b<sub>l</sub></b> )	Loaded Width	10 ft
Total Weight ( <b>W</b> )	Total Weight in Pounds of Section + Supported Components	see equation below figure
Concrete Compressive Strength ( <b>f'<sub>c</sub></b> )	Compressive Strength of the Concrete ( <b>f'<sub>c</sub></b> )	4,000 psi
Steel Yield Strength ( <b>f<sub>y</sub></b> )	Yield Strength of the Steel Reinforcement	60,000 psi
Depth to Tensile Steel ( <b>d</b> )	Depth to Tensile Steel Reinforcement from Loaded Side	10 in
Area of Tensile Steel ( <b>A<sub>s</sub></b> )*	Area of Tensile Steel Reinforcement within Section Width	2.37 in <sup>2</sup>
Moment of Inertia ( <b>I<sub>cr</sub></b> )	Moment of Inertia of Cracked Cross Section	1,150 in <sup>4</sup>
Gravity Constant ( <b>g</b> )	Gravity Constant	386.4 in/sec <sup>2</sup>
Moment Capacity ( <b>M<sub>p</sub></b> )	Moment Capacity of Beam	1.06 E6 lb-in
Young's Modulus ( <b>E</b> )	Young's Modulus for Concrete	3.6 E6 psi

\* SEE GENERAL NOTES 1 AND 2 AT END OF COMPONENT DESCRIPTIONS

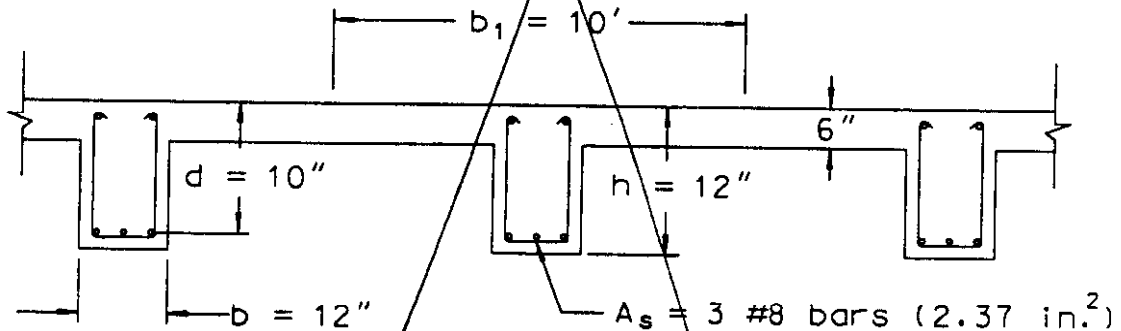
*Calculated Values*

$$M_p = 0.9 b d^2 f_y \rho (1 - 0.59 \rho f_y / f'_c)$$

$$E = 57000 \sqrt{f'_c}$$

$$I_{cr} = \frac{b d^3 (5.5 \rho + 0.083)}{2}$$

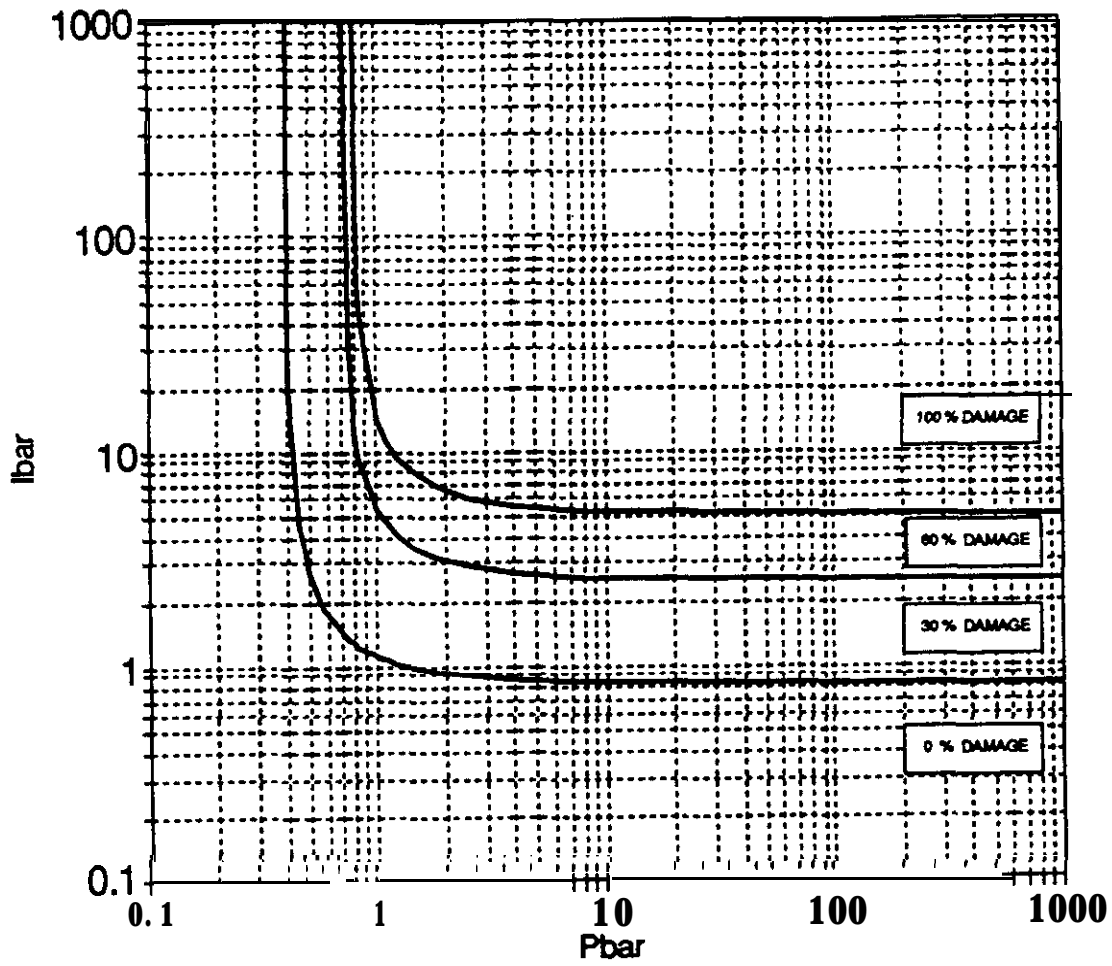
$$\rho = \frac{A_s}{b d}$$



$$W = [(10 \text{ ft}) (0.5 \text{ ft}) + (12 \text{ in}) (12 \text{ in} - 6 \text{ in}) / 144] (L) (150 \text{ lb/ft}^3)$$

where L = span length (ft)

## Reinforced Concrete Beams



$$I_{bar} = \frac{ib_1}{\psi_i M_p} \sqrt{\frac{EI_{agg} L}{W}}$$

$$P_{bar} = \frac{pb_1 L^2}{\psi_p M_p}$$

Boundary Conditions	$\psi_p$	$\psi_i$
Simple-Simple	10.00	0.913
Fixed-Fixed	23.10	0.861

**P-I Diagram Input for One-Way Reinforced Concrete Slabs**

Parameter	Description	Parameter Value for Example Case Below
Peak Pressure (p)	Peak Blast Pressure at Center of Component	
Specific Impulse (i)	Specific Impulse Applied to Center of Component	-
Span Length (L)	Span Length Between Supports	-
Section Width (b)	Section Width (Used for all Section Property Calculations)	12 in
Slab Thickness (h)	Slab Thickness	6 in
Concrete Compressive Strength (f'c)	28 Day Compressive Strength of the Concrete (f'c)	4,000 psi
Steel Yield Strength (fy)	Yield Strength of the Steel Reinforcement	60,000 psi
Depth to Tensile Steel (d)	Depth to Tensile Steel Reinforcement	4.5 in
Area of Tensile Steel (As)*	Area of Tensile Steel Reinforcement within Section Width	0.16 in <sup>2</sup>
Concrete Density (γ)	Weight Density of Concrete	150 lb/ft <sup>3</sup>
Moment of Inertia (Icr)	Moment of Inertia of Cracked Cross Section Within Width	54 in <sup>4</sup>
Gravity Constant (g)	Gravity Constant	386.4 in/sec <sup>2</sup>
Moment Capacity (Mp)	Moment Capacity of Section	3.8 E4 lb-in
Cross Sectional Area (A)	Cross Sectional Area Within Section Width	72 in <sup>2</sup>
Young's Modulus (E)	Young's Modulus for Concrete	3.6 E6 psi

\* SEE GENERAL NOTES 1 AND 2 <sup>ON PAGE 59 OF USER'S MANUAL</sup> AT END OF COMPONENT DESCRIPTIONS

Calculated Values

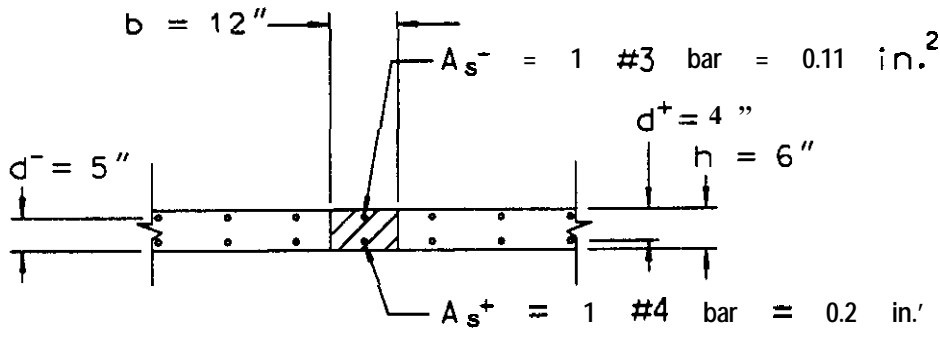
$$M_p = 0.9 b d^2 f_y \rho (1 - 0.59 \rho f_y / f'_c)$$

$$E = 57000 \sqrt{f'_c}$$

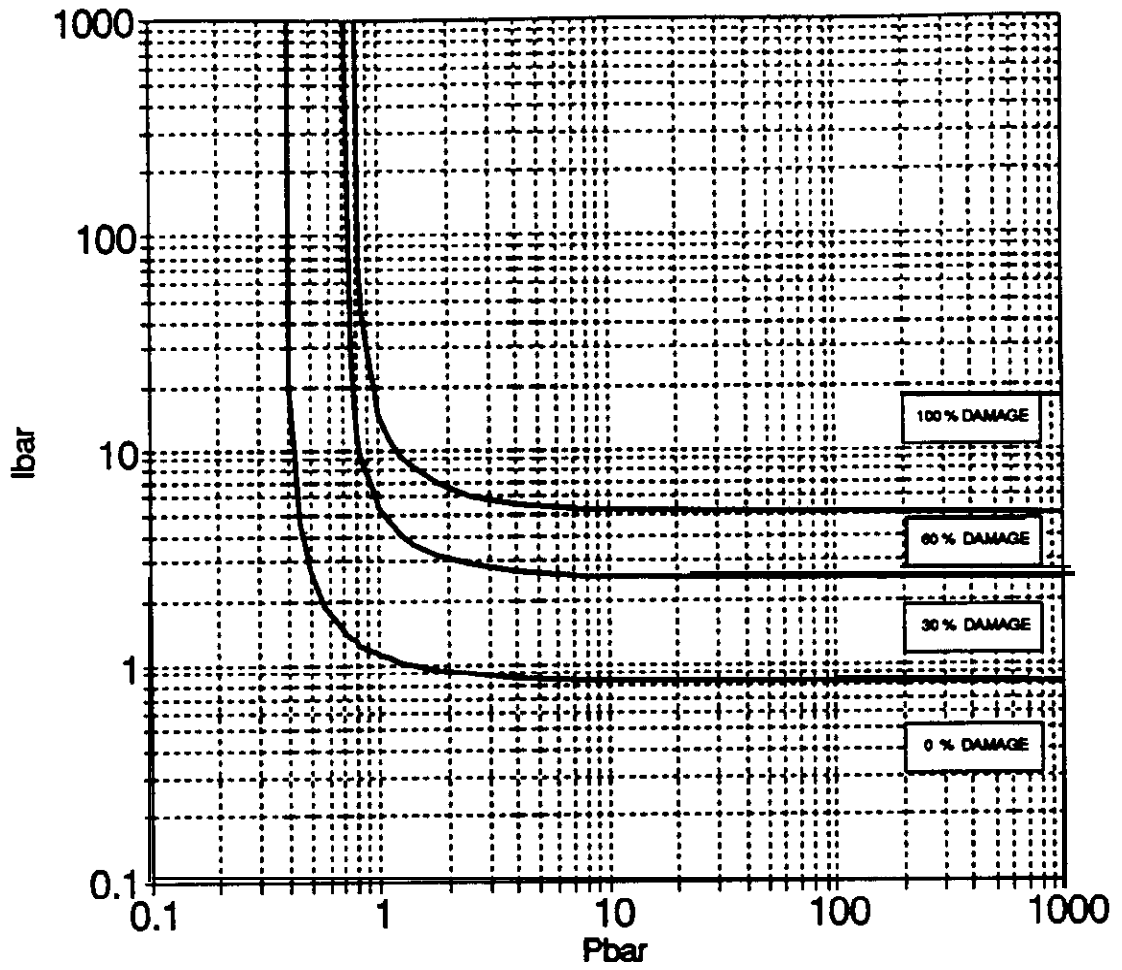
$$I_{cr} = \frac{b d^3 (5.5 \rho + 0.083)}{2}$$

$$\rho = \frac{A_s}{(b d)}$$

$$A = b d$$



## Reinforced Concrete One-Way Slabs



$$I_{bar} = \frac{ib}{\psi_i M_p} \sqrt{\frac{E L_{eff} g}{\gamma A}}$$

$$P_{bar} = \frac{pbL^2}{\psi_p M_p}$$

Boundary Conditions	$\psi_p$	$\psi_i$
Simple-Simple	10.00	0.913
Fixed-Fixed	23.10	0.861

## P-I Diagram Input for Two-Way Reinforced Concrete Slabs

Parameter	Description	Parameter Value for Example Case Below
Parameter ( $p$ )	Peak Blast Pressure at Center of Component	
Specific Impulse ( $I$ )	Specific Impulse Applied to Center of Component	
Short Span Length ( $x$ )	Shorter Span Length Between Supports	
Long Span Length ( $y$ )	Longer Span Length Between Supports	
Section Width ( $b$ )	Section Width (Used for AU Section Property Calculations)	12 in
Slab Thickness ( $h$ )	Slab Thickness	6 in
Concrete Compressive Strength ( $f'_c$ )	28 Day Compressive Strength of the Concrete ( $f'_c$ )	4,000 psi
Steel Yield Strength ( $f_y$ )	Yield Strength of the Steel Reinforcement	60,000 psi
Depth to Tensile Steel ( $d$ )	Depth to Tensile Steel Reinforcement	4 in
Area of Tensile Steel ( $A_s$ )	Area of Tensile Steel Reinforcement within Section Width	0.16 in <sup>2</sup>
Concrete Density ( $\gamma$ )	Weight Density of Concrete	150 lb/ft <sup>3</sup>
Moment of Inertia ( $I_{cr}$ )	Moment of Inertia of Cracked Cross Section Within Width	39 in <sup>4</sup>
Gravity Constant ( $B$ )	Gravity Constant	386.4 in/sec <sup>2</sup>
Arching Response	Arching (Compression Membrane) Response Will Not Occur	No arching
Compression on Block Depth ( $c$ )	Distance from Neutral Axis to Outer Fiber	5.7 in
Moment Capacity ( $M_p$ )	Moment Capacity of Section	3.4 E4 lb-in
Young's Modulus ( $E$ )	Young's Modulus for Concrete	3.6 E6 psi

SEE GENERAL NOTE 3 AT END OF COMPONENT DESCRIPTIONS } ON PAGE 59 OF USER'S MANUAL  
 SEE GENERAL NOTE 4 AT END OF COMPONENT DESCRIPTIONS }

### Calculated Values

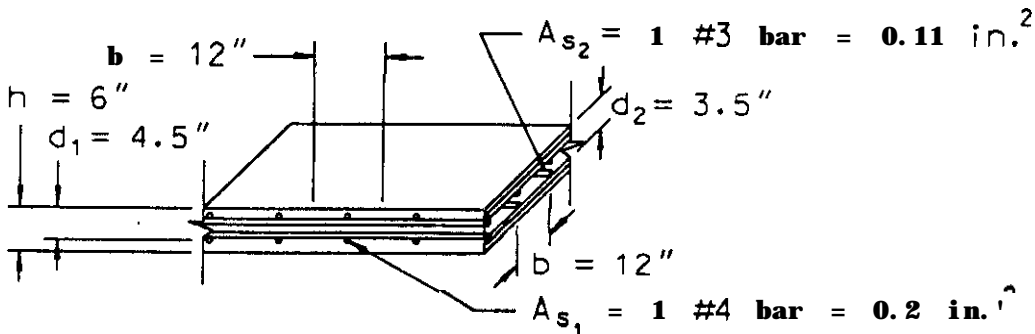
$$c = h - 1.38 \rho f_y / f'_c$$

$$M_p = 0.9 b d^2 f_y \rho (1 - 0.59 \rho f_y / f'_c)$$

$$E = 57000 \sqrt{f'_c}$$

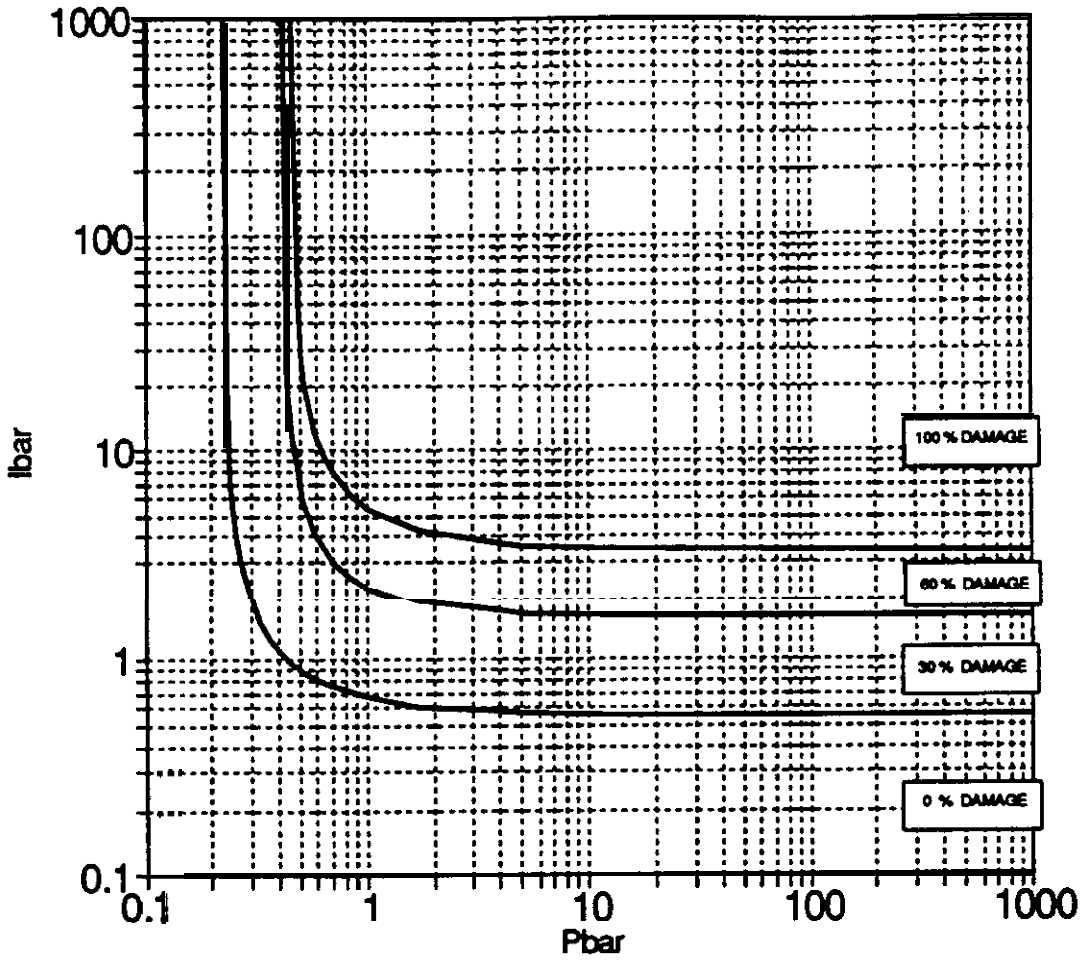
$$I_{cr} = \frac{b d^3 (5.5 \rho + 0.083)}{2}$$

$$\rho = \frac{A_s}{(b d)}$$



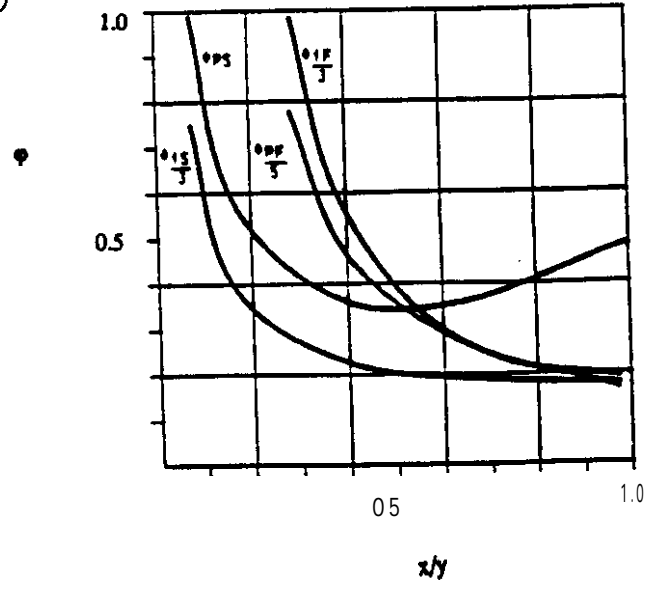
Distance of maximum compression block from neutral axis ( $c$ )

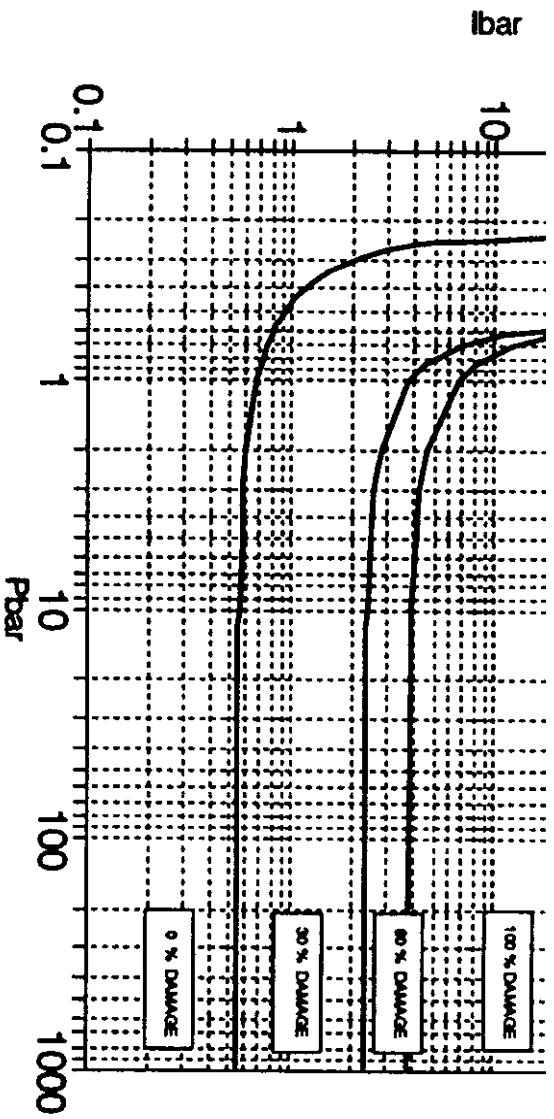
### Reinforced Concrete Two-Way Slabs No Arching



$$I_{bar} = \sqrt{\frac{E_g}{\gamma}} \left( \frac{L_{cr}}{\phi_p M_{p, ch}} \right) i$$

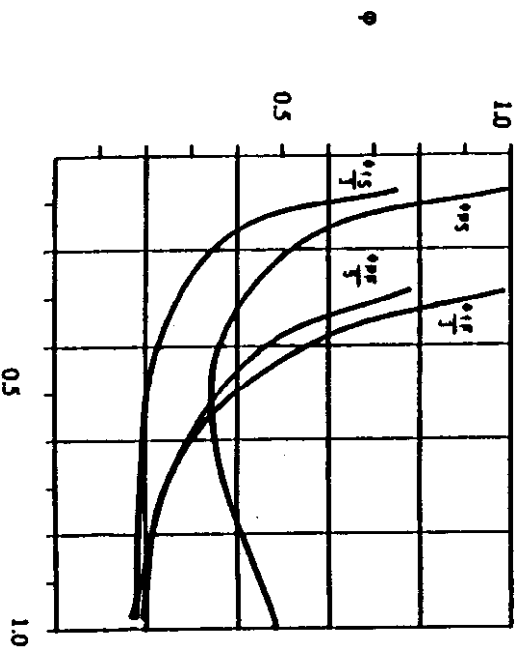
$$P_{bar} = \frac{p x^2 L_{cr}}{4 \phi_p M_{p, ch}^2}$$





$$\bar{l}_{bar} = \sqrt{\frac{Eg}{\gamma} \left( \frac{l_{cr}}{\phi M_p c T_b} \right) i}$$

$$\bar{P}_{bar} = \frac{p x^2 l_{cr}}{4 \phi M_p c T_b^2}$$



## P-4 Diagram Input for Reinforced Concrete Exterior Columns

Parameter	Description	Parameter Value for Example Case Below
Peak Pressure (p)	Peak Blast Pressure at Center of Component	
Specific Impulse (i)	Specific Impulse Applied to Center of Component	
Span Length (L)	Span Length Between Supports	
Column Width (b)	Width of Column Cross Section	12 in
Loaded Width (b <sub>l</sub> )	Width of Area Supported by Component Which is Loaded by Blast	10 ft
Total Weight(W)	Weight of Component Plus Attached Components Within Loaded Width	see equation below figure
Concrete Compressive Strength (f' <sub>c</sub> )	28 Day Compressive Strength of the Concrete (f' <sub>c</sub> )	4,000 psi
Steel Yield Strength (f <sub>y</sub> )	Yield Strength of the Steel Reinforcement	60,000 psi
Depth to Tensile Steel (d)	Depth to Tensile Steel Reinforcement	12 in
Area of Tensile Steel (A <sub>s</sub> )*	Area of Tensile Steel Reinforcement in Column	2.37 in <sup>2</sup>
Moment of Inertia (I <sub>cr</sub> )	Moment of Inertia of Cracked Column Cross Section Resisting Lateral Load	1,799 in <sup>4</sup>
Gravity Constant (g)	Gravity Constant	386.4 in/sec <sup>2</sup>
Moment Capacity (M <sub>p</sub> )	Moment Capacity of Column	1.3 E6 lb-in
Young's Modulus (E)	Young's Modulus for Concrete	3.6 E6 psi

- SEE GENERAL NOTES 1 AND 2 <sup>ON PAGE 59 OF USER'S MANUAL</sup> AT END OF COMPONENT DESCRIPTIONS

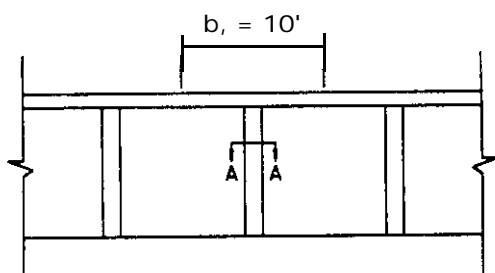
### Calculated Values

$$M_p = 0.9 b d^2 f_y \rho (1 - 0.59 \rho f_y / f'_c)$$

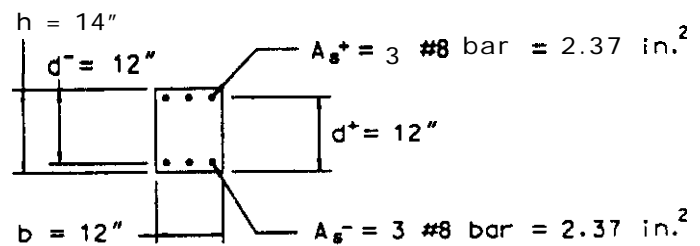
$$E = 57000 \sqrt{f'_c}$$

$$I_{cr} = \frac{b d^3 (5.5 \rho + 0.083)}{2}$$

$$\rho = \frac{4}{(b d)}$$



ELEVATION

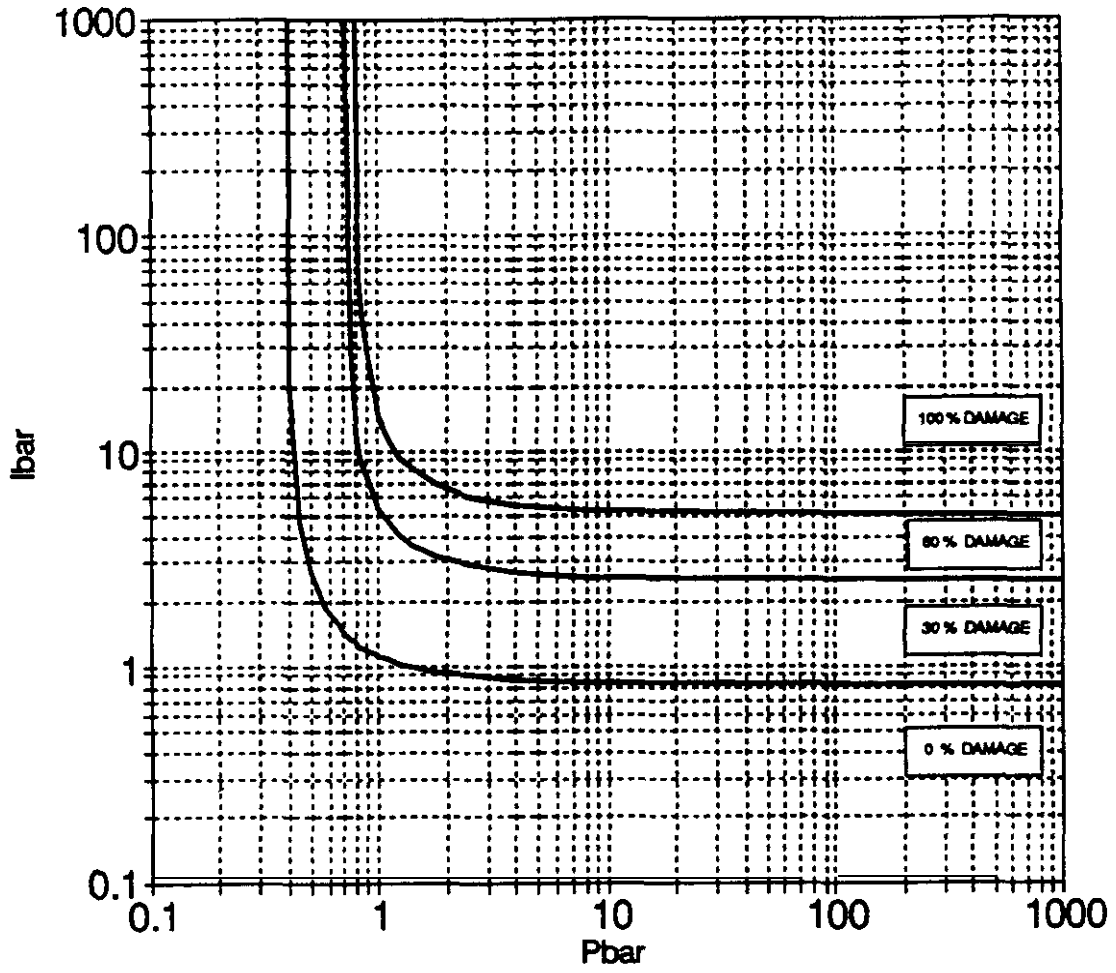


A - A

$$w = [(10 \text{ ft} \cdot 1 \text{ ft}) (t) + (12 \text{ in}) (14 \text{ in}) / 144] (L) (150 \text{ lb/ft}^3)$$

where L = column height (ft)  
t = (concrete) wall panel thickness (ft)

## Reinforced Concrete Exterior Columns



$$I_{bar} = \frac{ib_1}{\psi_p M_p} \sqrt{\frac{EI_{col} L}{W}}$$

$$P_{bar} = \frac{pb_1 L^2}{\psi_p M_p}$$

Boundary Conditions	$\psi_p$	$\psi_i$
Simple-Simple	10.00	0.913
Fixed-Fixed	23.10	0.861

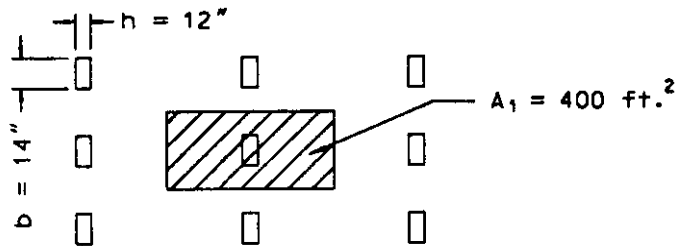
## P-I Diagram Input for Reinforced Concrete Interior Columns

Parameter	Description	Parameter Value for Example Case Below
Peak Pressure (p)	Peak Blast Pressure at Center of Component	-
Specific Impulse (i)	Specific Impulse Applied to Center of Component	-
Smaller Column Dimension (h)	Smaller Column Cross Section Dimension	12 in
Larger Column Dimension (b)	Larger Column Cross Section Dimension	14 in
Column Height (L)	Column Height Between Lateral Supports	-
Loaded Area (A <sub>l</sub> )	Loaded Area Supported by Column	400 ft <sup>2</sup>
Supported Weight per Area (W)	Weight Per Unit Area of Supported Area	see equation below figure
Concrete Compressive Strength (f' <sub>c</sub> )	28 Day Compressive Strength of the Concrete (f' <sub>c</sub> )	4,000 psi
Minimum Moment of Inertia (I)	Moment of Inertia of Cross Section About Weak Bending Axis	2,016 in <sup>4</sup>
Gravity Constant (g)	Gravity Constant	386.4 in/sec <sup>2</sup>
Young's Modulus (E)	Young's Modulus for Concrete	3.6 E6 psi

**Calculated Values**

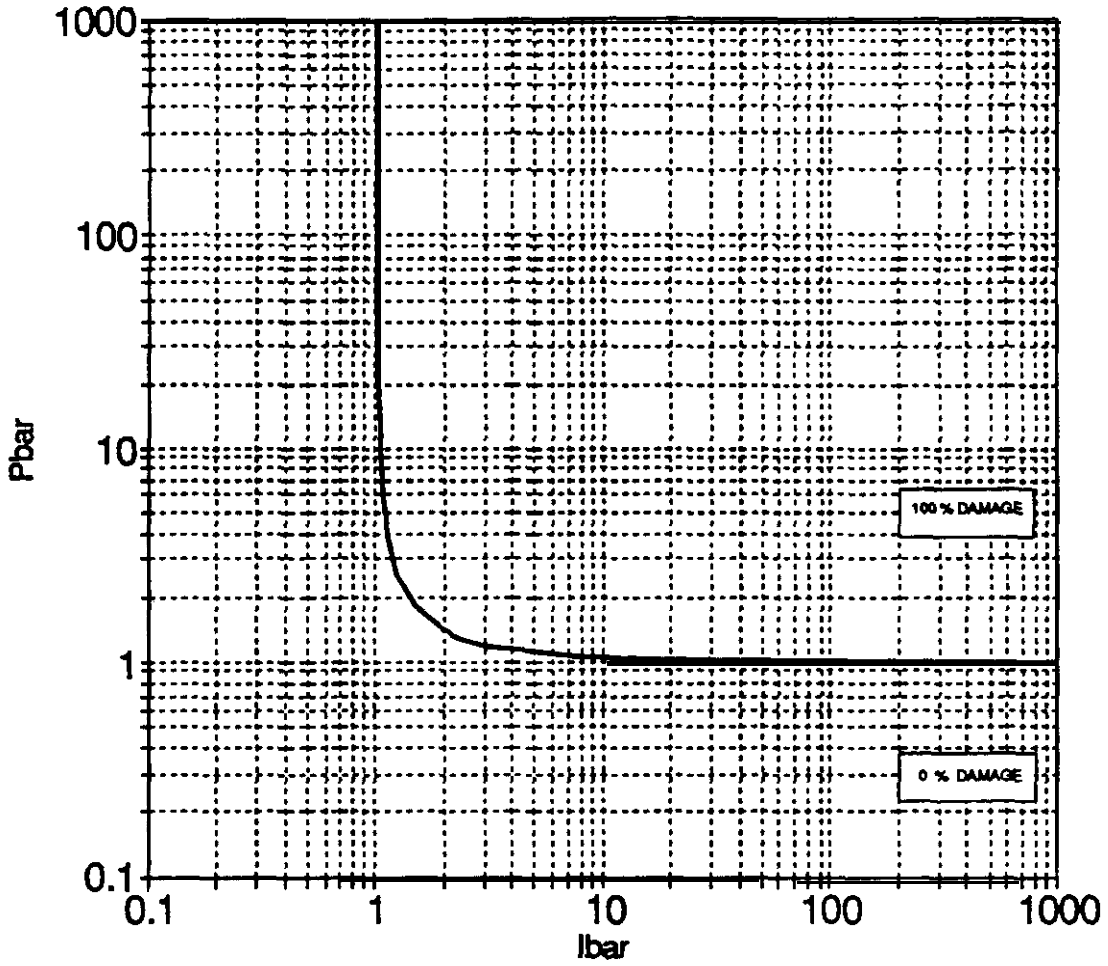
$$I = \frac{bh^3}{12}$$

$$E = 57000\sqrt{f'_c}$$



W = (t) (150 lb/ft<sup>3</sup>) for flat concrete slab roof  
 t = roof slab thickness (ft)

### Reinforced Concrete Interior Columns



$$P_{bar} = \frac{p A_1 L^2}{\alpha_p EI}$$

$$l_{bar} = \frac{ih}{\alpha_1 f_c} \sqrt{\frac{A_1 E_g}{W L}}$$

Boundary Conditions	Side Sway	$\alpha_1$	$\alpha_p$
Fixed-Simple.	No	0.894	20.99
<b>Fixed-Simple</b>	<b>Yes</b>	1.410	2.41
Fixed-Fixed	No	1.410	39.48
<b>Fixed-Fixed</b>	<b>Yes</b>	1.410	9.81
Simple-Simple	No	1.410	9.81
simple-simple	Yes	1.410	2.41

**P-1 Diagram Input for Reinforced Concrete Frames**

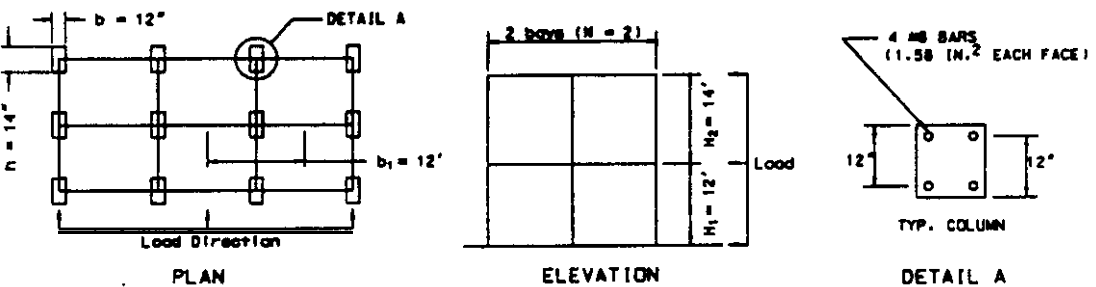
Parameter	Description	Parameter Value for Example Case Below
Peak Pressure (p)	Peak Blast Pressure at Center of Component	-
Specific Impulse (i)	Specific Impulse Applied to Center of Component	-
Loaded Width (b <sub>l</sub> )	Width of Wall Area Supported by Exterior Column of Frame	12 ft
Average Column Width (b)	Average Width Across Cross Section of Frame Columns	12 in
Total Weight (W)	Effective Weight Supported by Frame	see equation below figure
Number of Bays (N)	Number of Bays in the Frame (Must be Less Than 15)	2
Single Story Height (H)	Average Story Height in Frame	13 ft
Number of Stories	Number of Stories in Frame (2 Story Maximum)	2
Concrete Compressive Strength (f' <sub>c</sub> )	28 Day Compressive Strength of Concrete in Frame Columns (f' <sub>c</sub> )	4,000 psi
Steel Yield Strength (f <sub>y</sub> )	Yield Strength of Steel Reinforcement in Frame Columns	60,000 psi
Column Depth to Tensile Steel (d)	Average Depth to Tensile Steel Reinforcement in Frame Columns	12 in
Column Area of Tensile Steel (A <sub>st</sub> )*	Average Area of Tensile Steel in Frame Columns	1.58 in <sup>2</sup>
Column Moment of Inertia (I <sub>cr</sub> )	Average Moment of Inertia (Cracked Section) of Frame Columns	1,486 in <sup>4</sup>
Gravity Constant (g)	Gravity Constant	386.4 in/sec <sup>2</sup>
Moment Capacity (M <sub>p</sub> )	Average Moment Capacity of Frame Columns	9.2 E5 lb-in
Young's Modulus (E)	Young's Modulus of Column Concrete	3.6 E6 psi

• SEE GENERAL NOTES 1 AND 2 <sup>ON PAGE 57 OF DEPT. MANUAL</sup> AT END OF COMPONENT DESCRIPTIONS

Calculated Values

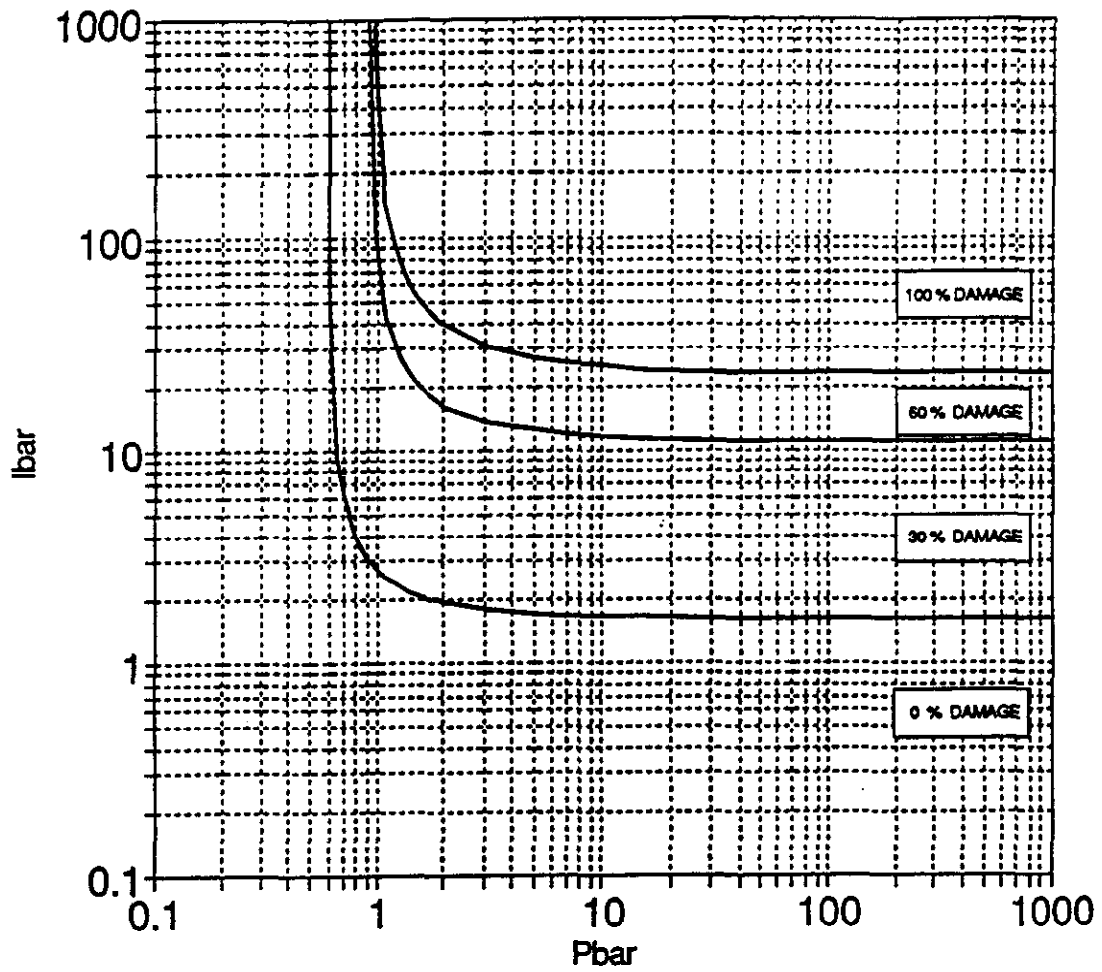
$$M_p = 0.9 b d^2 f_y \rho (1 - 0.59 \rho f_y / f'_c) \quad E = 57000 \sqrt{f'_c}$$

$$I_{cr} = \frac{b d^3 (5.5 \rho + 0.083)}{2} \quad \rho = \frac{4}{(b d)}$$



w = roof weight + 1/3 (wall and column weight) within Loaded Width  
 w = (t<sub>r</sub>) (12 ft) (24 ft) (150 lb/ft<sup>3</sup>) + 1/3 [(2 (t<sub>w</sub>) (12 ft) (26 ft))] + [3 (12 in) (14 in) (26 ft)/144] (150 lb/ft<sup>3</sup>)  
 t<sub>r</sub> = (concrete) roof slab thickness (ft)  
 t<sub>w</sub> = (concrete) wall slab thickness (ft)

# Reinforced Concrete Frames



$$I_{bar} = \frac{\alpha_1 [1 + 0.7 (n - 1)]}{(n + 1)^2} \left( \frac{gE L_c b_1^2 H}{WM_p^2} \right)^{1/2}$$

$$P_{bar} = \frac{\alpha_2 b_1 H^2 p}{(1 + n)M_p}$$

	1 Story Frame	2 Story Frame
$\alpha_1$	0.83	75
$\alpha_2$	0.50	1.5

### P-i Diagram Input for Reinforced Concrete Prestressed Beams

Parameter	Description	Parameter Value for Example Case Below
Peak Pressure (p)	Peak Blast Pressure at Center of Component	
Specific Impulse (i)	<b>Specific Impulse Applied</b> to Center of <b>Component</b>	
Span Length (L)	Span Length Between <b>Supports</b>	-
Beam Flange Width (b)	Beam <b>Flange</b> in <b>Compression</b>	18 in
Loaded Width (b <sub>l</sub> )	Width of Area <b>Supported</b> by Component <b>Which</b> is Loaded by Blast	5 ft
Total Weight(W)	Total Weight of <b>Component</b> Plus <b>Weight</b> of <b>Any Supported Components</b>	see equation below figure on next page
Concrete Compressive Strength (f <sub>c</sub> )	<b>28 Day</b> Compressive Strength of the <b>Concrete</b> (PC)	4,000 psi
Steel Yield Strength (f <sub>y</sub> )	Yield <b>Strength</b> of the Steel Reinforcement	60,000 psi
Prestress Steel Ultimate strength (f <sub>pu</sub> )	<b>Ultimate Strength</b> of the <b>Prestressing Steel</b>	250,000 psi
Depth to Tensile Steel (d)	<b>Depth to Tensile Reinforcement</b> (If Unknown: Beam <b>Thickness</b> - 2")	16 in
Depth to <b>Prestress Steel</b> (d <sub>p</sub> )	<b>Depth to Prestress Steel</b> in Maximum Moment <b>Area</b> (If Unknown: 80% Beam <b>Thickness</b> )	11 in
Area of Tensile Steel (A <sub>s</sub> )	<b>Area of Non-Prestressed Tensile Steel</b> (If Unknown: 0.5% Beam Area)	0.88 in <sup>2</sup>
Area of <b>Compression Steel</b> (A <sub>s</sub> )	<b>Area of Non-Prestressed Compression Steel</b> (If Unknown: 0.5% of Beam Area)	0.93 in <sup>2</sup>
Area of <b>Prestress Steel</b> (A <sub>p</sub> )	Area of <b>Non-Prestressed Compression Steel</b> (If Unknown: 0.5% Beam Area)	0.58 in <sup>2</sup>
Gross Moment of Inertia (I <sub>g</sub> )	<b>Uncracked</b> Moment of Inertia of <b>Cross Section</b>	6.005 in <sup>4</sup>
Gravity Constant(B)	Gravity Constant	386.4 in/sec <sup>2</sup>
<b>Prestressed Steel Ratio</b> (ρ <sub>p</sub> )	<b>Steel Ratio of Prestressing Steel</b>	0.002
<b>Non-Prestressed Steel Ratio</b> (ρ)	Steel Ratio of <b>Non-Prestressed Tension Steel</b>	0.003
Compression Steel Ratio (ρ')	Steel Ratio of <b>Non-Prestressed Compression Steel</b>	0.003
Effective Moment of <b>Inertia</b> (I <sub>cr</sub> )	Moment of Inertia of Cracked <b>Cross Section</b>	3,520 in <sup>4</sup>
Effective <b>Prestress Steel Strength</b> (f <sub>ps</sub> )	Effective Yield Strength in <b>Prestressing Steel</b>	230,000 psi
<b>Young's Modulus</b> (E)	<b>Young's Modulus</b> of Concrete	3.6 E6 psi
Moment Capacity (M <sub>p</sub> )	Moment <b>Capacity</b> of Beam	2.8 E6 lb-in

**Calculated Values**

$$E = 57000 \sqrt{f'_c}$$

$$\rho = \frac{A_s}{(bd)}$$

$$f_{pr} = \left\{ \rho_r \left( \frac{f_{pr}}{f'_c} \right) + \left( \frac{d}{d_p} \frac{f_y}{f'_c} \right) (\rho - \rho_r) \right\}$$

$$\rho' = \frac{A'_s}{(bd)}$$

If  $f_{pr} < 0.17$ ,  $f_{pr} = 0.17$

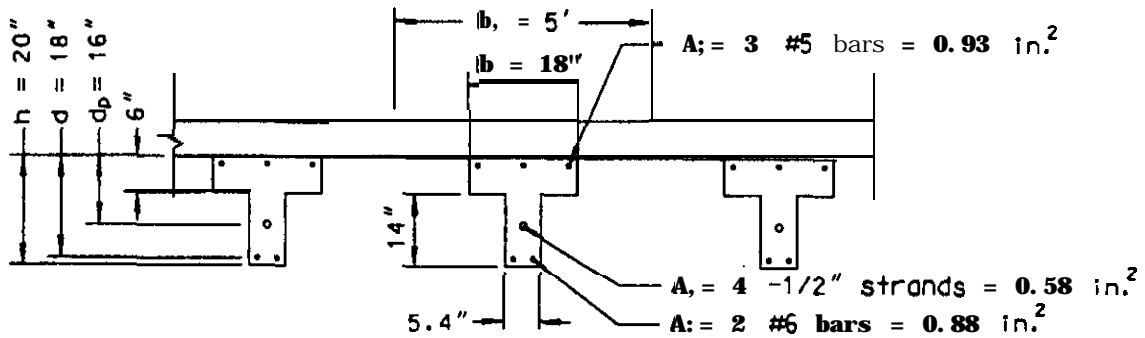
$$f_{pr} = f_{pr} [1 - 0.47 (f_{pr})]$$

$$\rho_p = \frac{A_{ps}}{(bd_p)}$$

$$a = (A_{ps} f_{ps} + A_s f_y) / (0.85 f'_c b)$$

$$I_{cr} = [7A_{ps} d_p^2 (1 - \sqrt{\rho_p}) + I_g] / 2$$

$$M_p = A_{ps} f_{ps} \left( d_p - \frac{a}{2} \right) + A_s f_y \left( d - \frac{a}{2} \right)$$



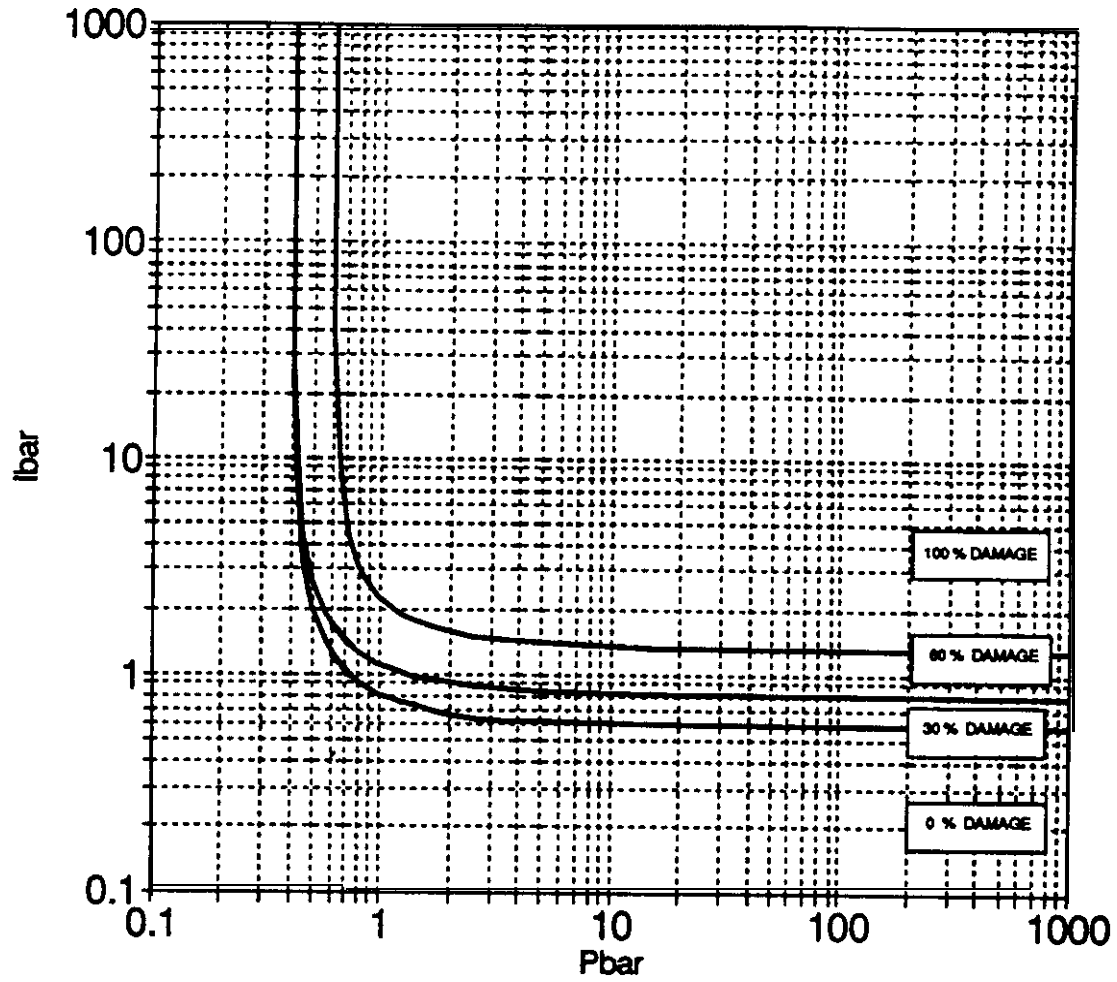
$$W = [(5 \text{ ft}) (t) + A_b] (L) (150 \text{ lb/ft}^3)$$

$L$  = span length (ft)

$A_b$  = cross sectional area of beam (ft<sup>2</sup>)

$t$  = (concrete) slab thickness (ft)

## Reinforced Concrete Prestressed Beams



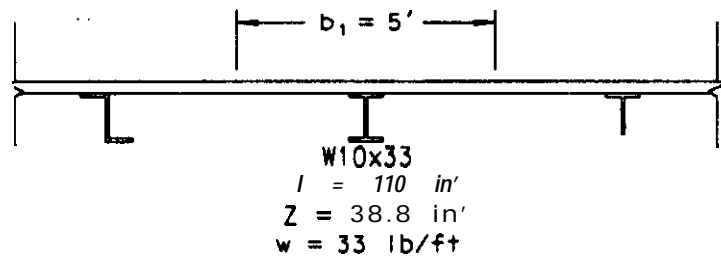
$$I_{bar} = \frac{ib_1}{\psi_i M_p} \sqrt{\frac{E_c s L}{W}}$$

$$P_{bar} = \frac{pb_1 L^2}{\psi_p M_p}$$

Boundary Conditions	$\psi_p$	$\psi_i$
Simple-Simple	10.00	0.913
Fixed-Fixed	23.10	0.861

## P-I Diagram Input for Steel Beams

Parameter	Description	Parameter Value for Example Case Below
Peak Pressure ( <b>p</b> )	Peak Blast Pressure at Center of Component	
Specific Impulse ( <b>i</b> )	Specific Impulse. Applied to Center of Component	
Span Length ( <b>L</b> )	Span Length Between Supports	
Loaded Width ( <b>b<sub>l</sub></b> )	Width of Area Supported by Component Which is Loaded by Blast	5 ft
Total Weight ( <b>W</b> )	Total Weight of Component Plus Weight of Any Supported Components	see equation below figure
Steel Yield Strength ( <b>σ<sub>y</sub></b> )	Yield Strength of Beam	36,000 psi
Plastic Section Modulus ( <b>Z</b> )	Plastic section Modulus	38.8 in'
Moment of Inertia ( <b>I</b> )	Moment of Inertia of Cross Section	170 in <sup>4</sup>
Gravity Constant ( <b>g</b> )	Gravity constant	386.4 in/sec <sup>2</sup>
Young's Modulus ( <b>E</b> )	Young's Modulus for Beam	29 E6 psi

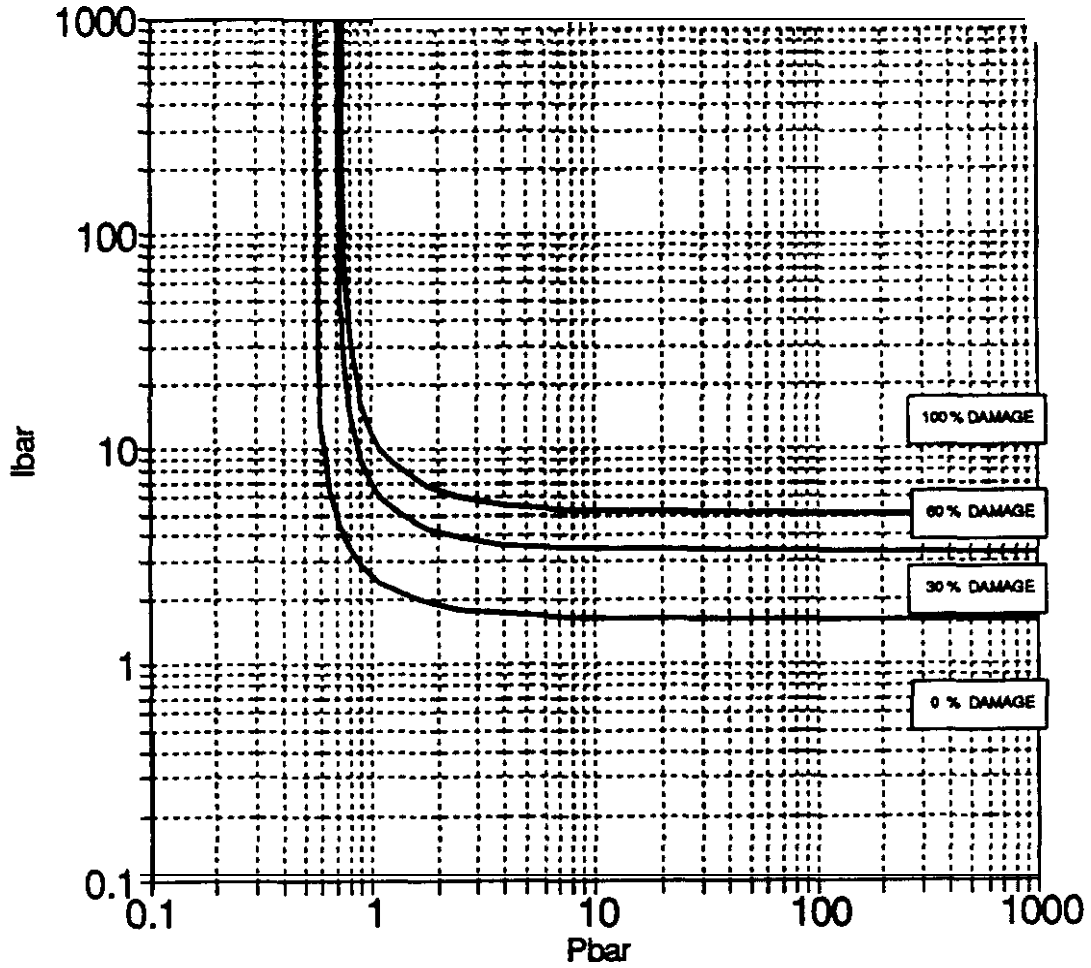


$$w = [(W_p) (5 \text{ ft}) + (33 \text{ lb/ft})] (L)$$

$W_p$  = areal weight of paneling and insulation supported by beams (lb/ft<sup>2</sup>)

$L$  = span length (ft)

**Steel Beams**  
No Tension Membrane

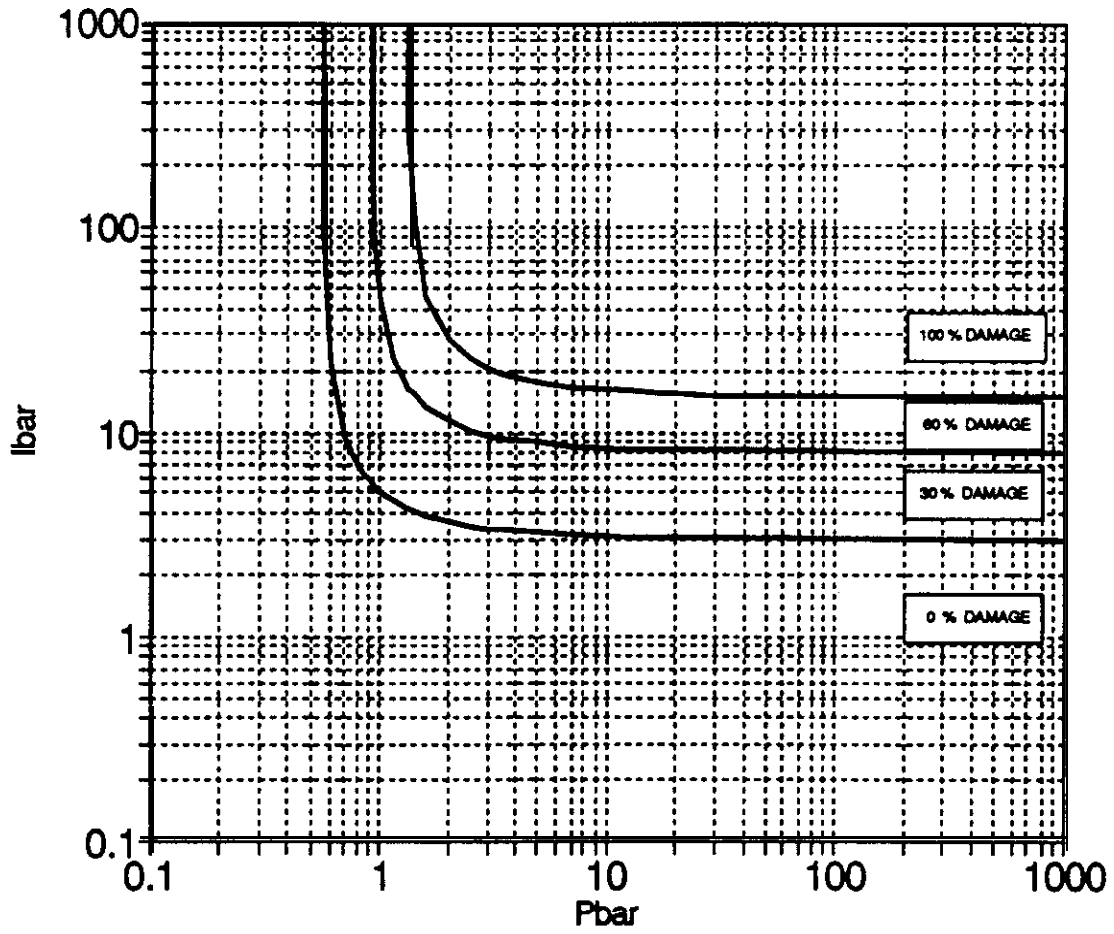


$$Ibar = \frac{ib_1}{\psi_i \sigma_y Z} \sqrt{\frac{EiGL}{W}}$$

$$Pbar = \frac{pb_1 L^2}{\psi_p \sigma_y Z}$$

Boundary Conditions	$\psi_p$	$\psi_i$
Simple-Simple	10.00	0.913
Fixed-Fixed	23.10	0.861

steel Beams  
With Tension Membrane



$$Ibar = \frac{ib_1}{\psi_i \sigma_y Z} \sqrt{\frac{EIgL}{W}}$$

$$Pbar = \frac{pb_1 L^2}{\psi_p \sigma_y Z}$$

Boundary Conditions	$\psi_p$	$\psi_i$
Simple-Simple	10.00	0.913
Fixed-Fixed	23.10	0.861

## P-I Diagram Input for Metal Stud Walls

Parameter	Description	Parameter Value for Example Case Below
Peak Pressure (p)	Peak Blast Pressure at Center of Component	
Specific Impulse (i)	Specific Impulse Applied to Center of Component	-
Span Length (L)	Span Length Between Supports	-
Section Width (b <sub>1</sub> )	Section Width (Used for all Section Property Calculations)	16 in
Wall Thickness (h)	Total Wall Thickness	6.6 in
Total Weight (W)	Total Weight of Component Plus Attached Components Within Loaded Width	see equation below figure
Yield Strength (a)	Yield Strength of Metal Stud	50,000 psi
Elastic section Modulus (S)	Elastic Section Modulus of Metal stud	0.85 in'
Moment of Inertia (I)	Moment of Inertia of Stud	2.55 in <sup>4</sup>
Gravity Constant (g)	Gravity Constant	386.4 in/sec <sup>2</sup>
Young's Modulus (E)	Young's Modulus for stud	29 E6 psi

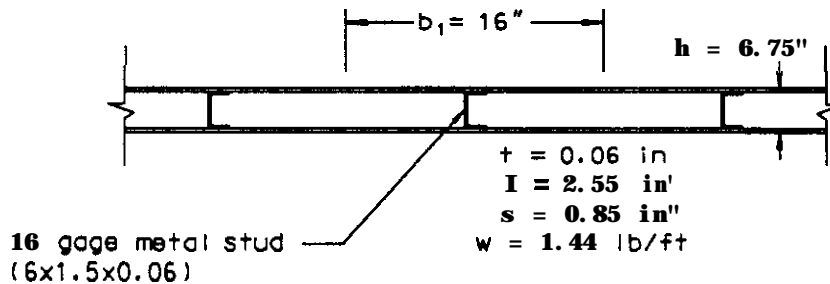
**Calculated Values**

$$S = 0.08 (h + h^2/10)$$

$$I = 0.036 (h^2 + h^3/10)$$

**Note:** These calculated values assume a metal stud thickness equal to 0.06", a section depth equal to (0.9)(h), an unstiffened flange width equal to 1.5", and a "C" or "Z" shaped section.

*Width of area supported by Component which is Loaded by Blast*  
(errata)

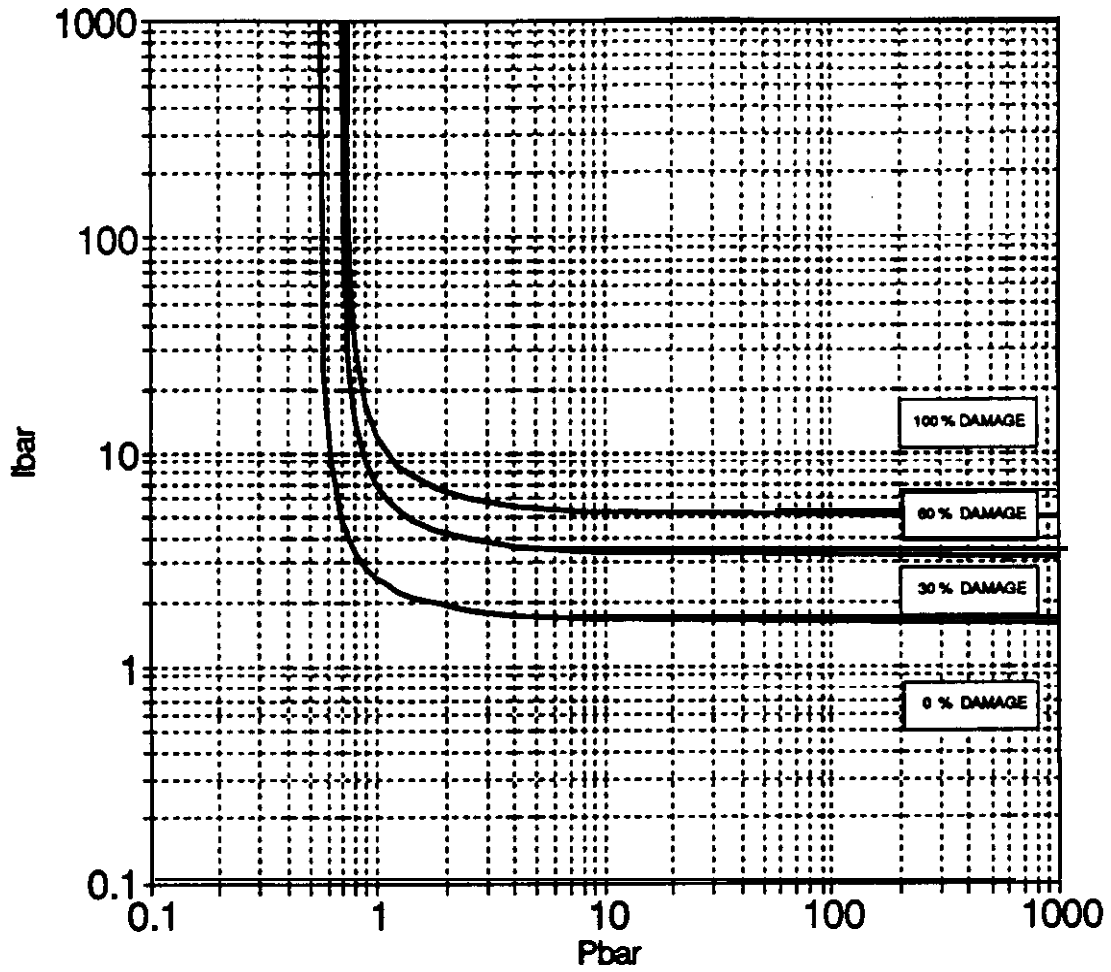


$$W = [W_p (1.33 \text{ ft}) + (1.44 \text{ lb/ft})] (L)$$

$$W_p = \text{areal weight of paneling and insulation supported by studs (lb/ft}^2\text{)}$$

$$L = \text{span length (ft)}$$

### Metal Stud Walls



$$I_{bar} = \frac{i b_1}{\psi_i \sigma_y S} \sqrt{\frac{E I_g L}{W}}$$

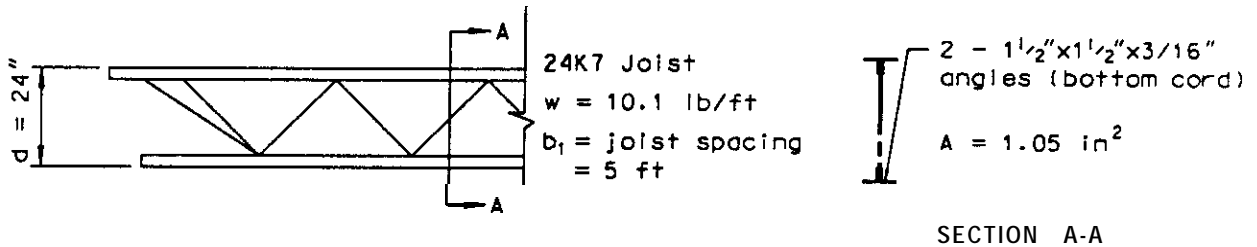
$$P_{bar} = \frac{p b_1 L^2}{\psi_p \sigma_y S}$$

Boundary Conditions	$\psi_p$	$\psi_i$
Simple-Simple	10.00	0.913
Fixed-Fixed	23.10	0.861

### P-I Diagram Input for Steel Open Web Joists

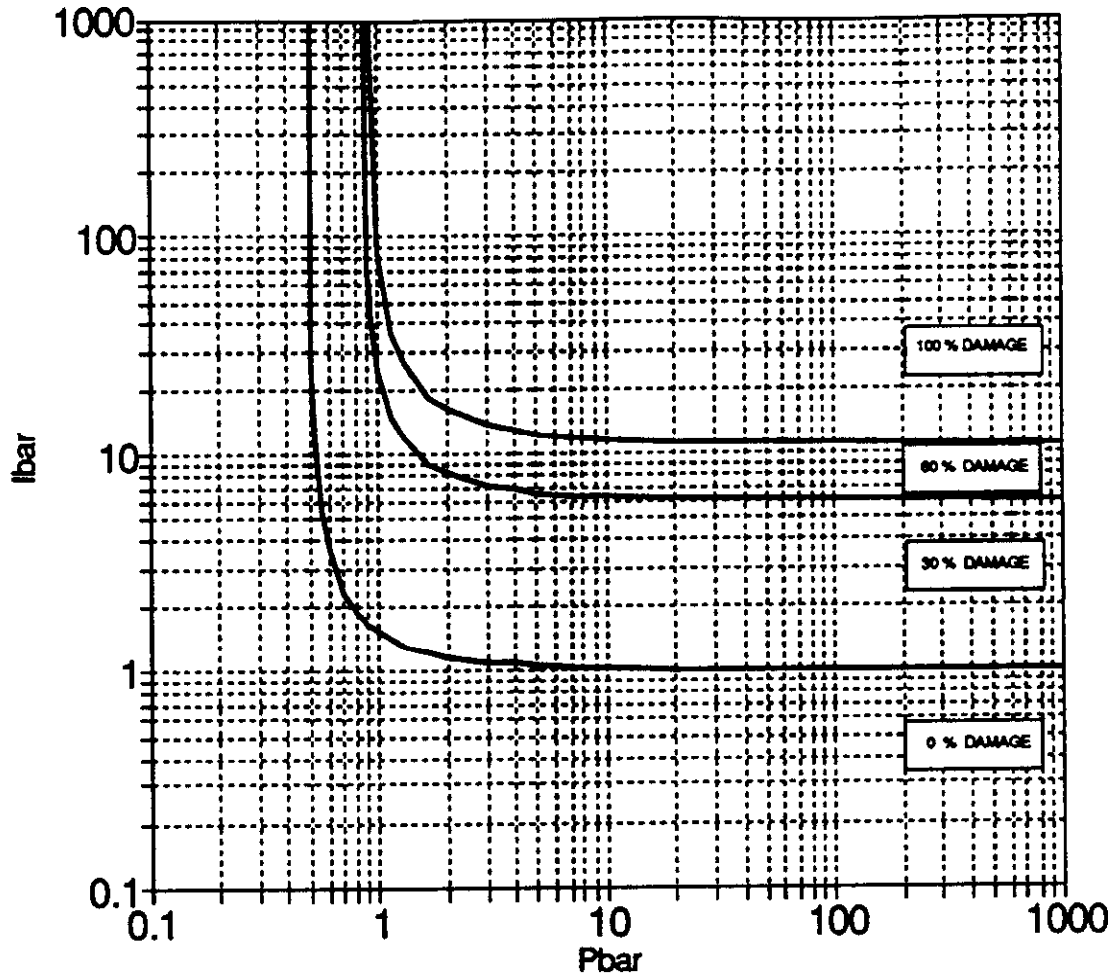
Parameter	Description	Parameter Value for Example Case Below
Peak Pressure (p)	Peak <b>Blast Pressure</b> at Center of Component	-
Specific Impulse (i)	<b>Specific Impulse</b> Applied to Center of <b>Component</b>	-
Span Length (L)	Span Length <b>Between</b> Supports	-
Loaded Width (b)	Width of Area <b>Supported</b> by Component	5 ft
Joist Depth (d)	<b>Distance Between</b> Top and Bottom Chord of Joist	24 in
Area of Bottom Chord (A)	<b>Cross Sectional Area of Joist Bottom Chord at Midspan</b>	1.05 in <sup>2</sup>
Total Weight (W)	Total Weight of the Joist and Deck Within <b>the Loaded Width</b>	see equation below figure
Yield Strength (σ <sub>y</sub> )	Yield <b>Strength</b> of Bottom Chord	50,000 psi
Bending Stiffness • (K)	Joist <b>Bending Stiffness</b>	1.06 E4 lb/in for 30 ft span
Gravity Constant(s)	Gravity constant	386.4 in/sec <sup>2</sup>

\* SEE GENERAL NOTE 6 AT END OF COMPONENT DESCRIPTIONS } ON PAGE 59 OF USER'S MANUAL  
 † SEE GENERAL NOTE 5 AT END OF COMPONENT DESCRIPTIONS



$$\begin{aligned}
 W &= [(t) (5 \text{ ft}) (150 \text{ lb/ft}^3) + (10.1 \text{ lb/ft})] (L) \\
 t &= \text{(concrete) roof slab thickness} \\
 L &= \text{span length (ft)}
 \end{aligned}$$

# Open Web Steel Joists



$$I_{bar} = \left[ \frac{ib_1 L^2}{7.1 \sigma_y Ad} \right]^2 \frac{Kg}{W}$$

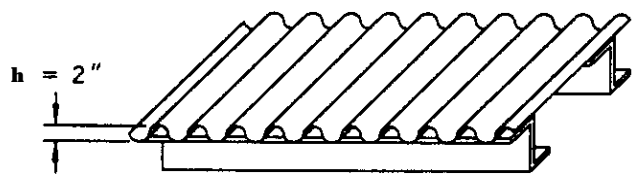
$$P_{bar} = \frac{pb_1 L^2}{8\sigma_y Ad}$$

**P-I Diagram Input for Steel Corrugated Decking**

Parameter	Description	Parameter Value for Example Case Below
Peak Pressure (p)	Peak Blast Pressure at Center of Component	
Specific Impulse (i)	Specific Impulse Applied to Center of Component	
Span Length (L)	Span Length Between Supports	
Decking Uncoated Thickness (t)	Uncoated Thickness of Decking	0.023 in
Rib Height (h)	Height of Corrugations	2 in
Total Weight(W)	Weight of Decking and Any Attached Material Within 1 ft Width	see equation below figure
Yield Strength (σ <sub>y</sub> )	Yield Strength of Decking	40,000 psi
Elastic Section Modulus (S)	Elastic Section Modulus of Decking Per Foot	0.29 in <sup>3</sup> /ft
Moment of Inertia m	Moment of Inertia of Decking Cross Section Pa Foot	0.343 in <sup>4</sup> /ft
Gravity Constant (g)	Gravity Constant	386.4 in/sec <sup>2</sup>
Young's Modulus (E)	Young's Modulus for Decking	29 E6 psi
Section Width (b)	Section Width (Used to Calculate All Sectional Properties)	12in

**Calculated Values**       $S = 4.5 ht$        $I = 2.4 th^2$

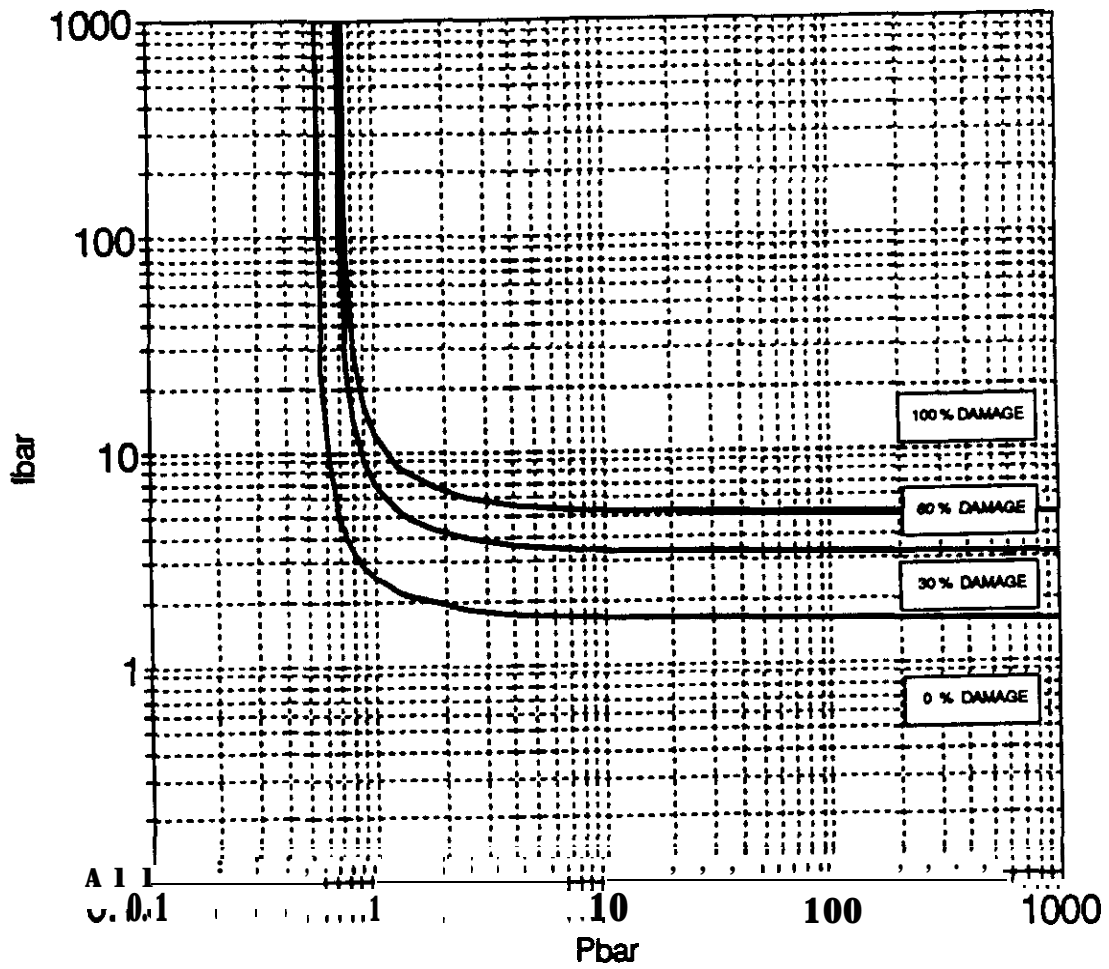
**Note:** These *calculated values* assume an *effective flange width* 0.375 times the *section width*. This is a good approximation based on comparisons with *actual section properties* reported in *manufacturer's literature*. A 12" *section width* is assumed.



Vulcraft 2VL22 Deck  
 t = 0.023 in (22 gage)  
 I = 0.343 in<sup>4</sup>/ft  
 S = 0.29 in<sup>3</sup>/ft  
 w = 1.7 lb/ft<sup>2</sup>

$W = [(1.7 \text{ lb/ft}^2) + (W^1)] (1 \text{ ft}) (L)$   
 $W^1 = \text{areal weight of insulation, etc., attached to decking (lb/ft}^2)$   
 $L = \text{span length (ft)}$

### Corrugated Steel Deck



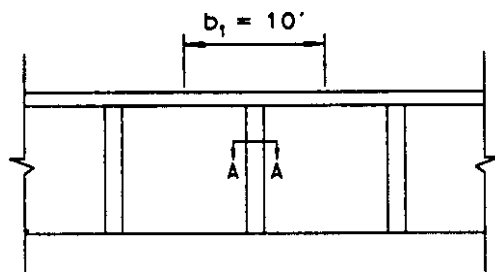
$$i_{bar} = \frac{ib}{\psi_i \sigma_y S} \sqrt{\frac{EI_g L}{W}}$$

$$P_{bar} = \frac{pb L^2}{\psi_p \sigma_y S}$$

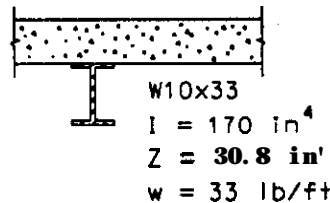
Boundary Conditions	$\psi_p$	$\psi_i$
Simple-Simple	10.00	0.913
Fixed-Fixed	23.10	0.861

### P-I Diagram Input for Steel Exterior Columns

Parameter	Description	Parameter Value for Example Case Below
Peak Pressure (p)	Peak Blast Pressure at Center of Component	-
Specific Impulse (i)	Specific Impulse Applied to Center of Component	-
Span Length (L)	Span Length Between Supports	-
Loaded Width (b <sub>l</sub> )	Width of Area Supported by Component Which is Loaded by Blast	10 ft
Total Weight (W)	Total Weight of Component Plus Weight of Any Supported Components	see equation below figure
Yield Strength (σ <sub>y</sub> )	Yield Strength of Column	36,000 psi
Plastic Section Modulus (Z)	Plastic Section Modulus of Column	38.8 in <sup>3</sup>
Moment of Inertia (I)	Moment of Inertia of Column Cross Section Resisting Lateral Load	170 in <sup>4</sup>
Gravity Constant (g)	Gravity Constant	386.4 in/sec <sup>2</sup>
Young's Modulus (E)	Young's Modulus of Column	29 E6 psi



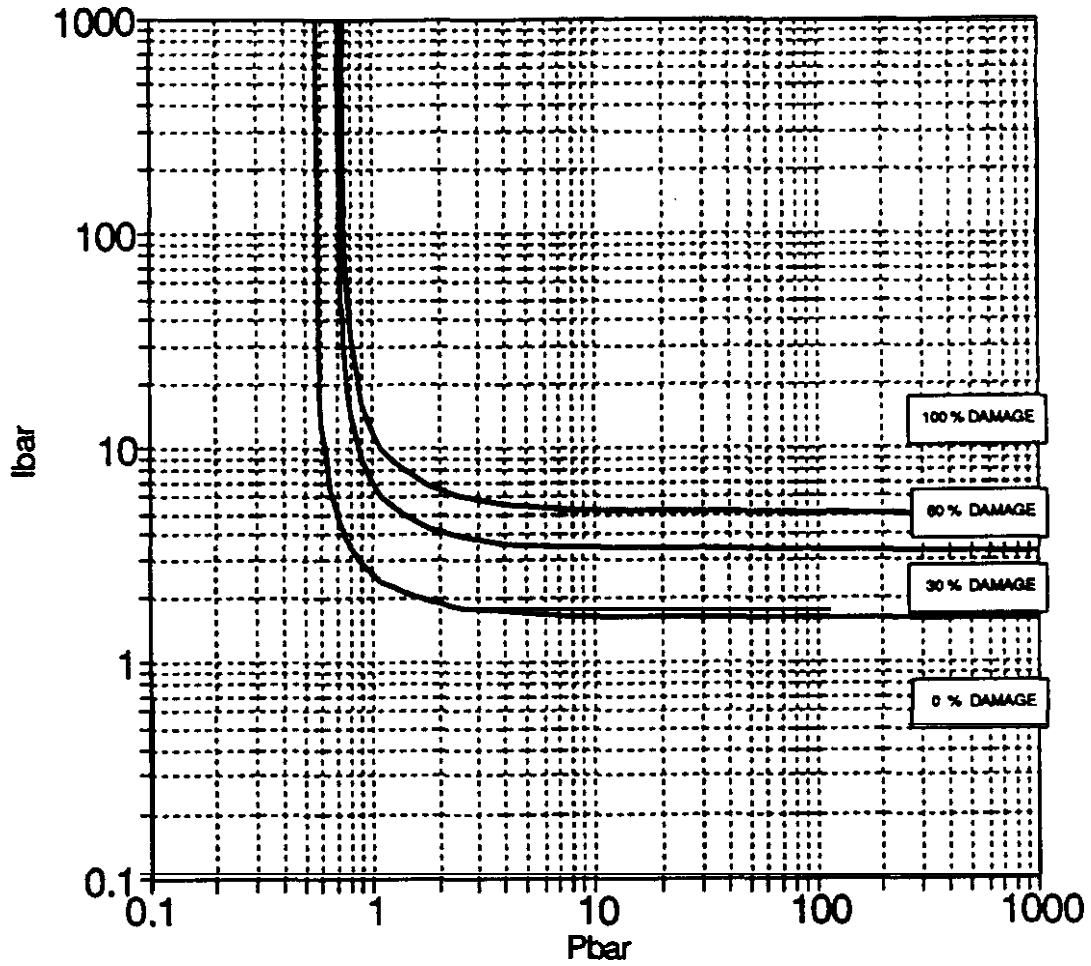
ELEVATION



A - A

$$\begin{aligned}
 w &= [(10 \text{ ft}) (t) (150 \text{ lb/ft}^3) + 33 \text{ lb/ft}] (L) \\
 t &= (\text{concrete}) \text{ wall slab thickness (ft)} \\
 L &= \text{span length (ft)}
 \end{aligned}$$

Steel Exterior Columns  
No Tension Membrane

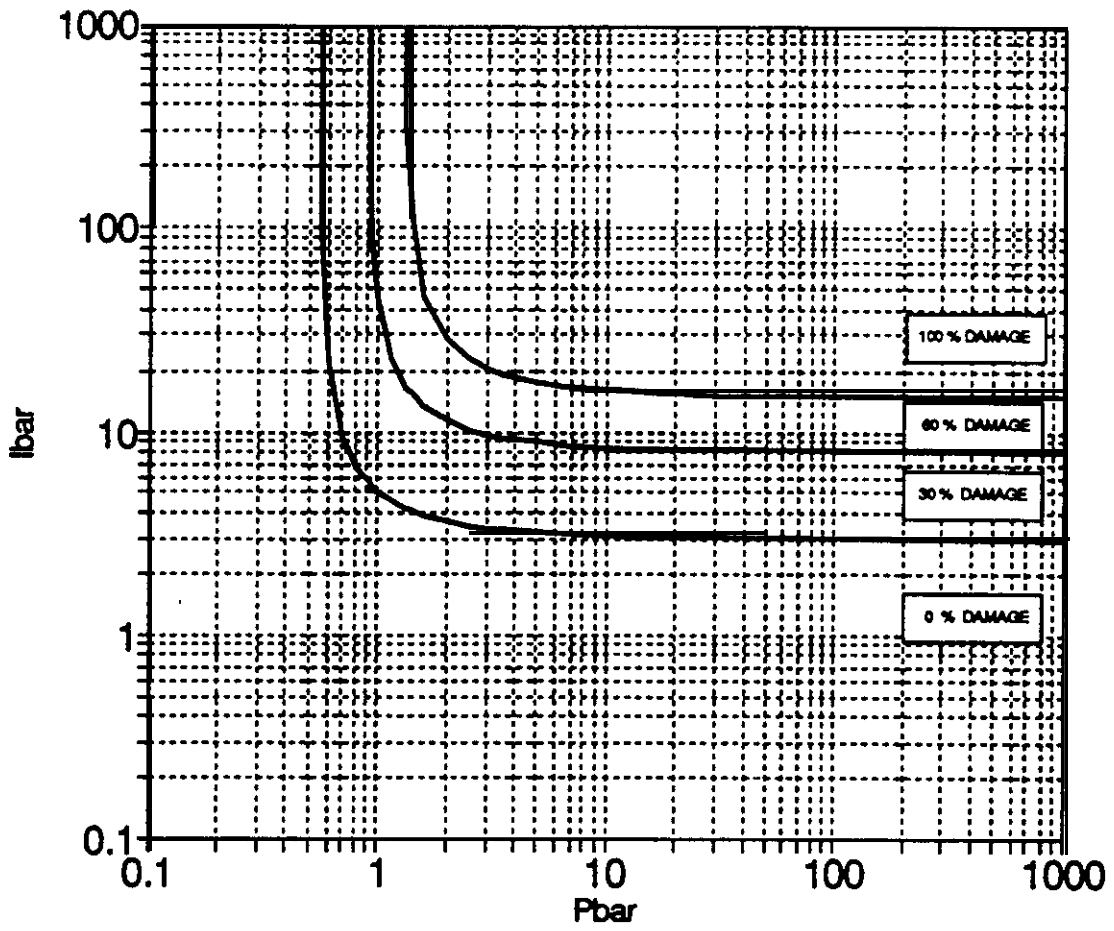


$$I_{bar} = \frac{i b_1}{\psi_i \sigma_y Z} \sqrt{\frac{E I_g L}{W}}$$

$$P_{bar} = \frac{p b_1 L^2}{\psi_p \sigma_y Z}$$

Boundary Conditions	$\psi_p$	$\psi_i$
Simple-Simple	10.00	0.913
Fixed-Fixed	23.10	0.861

### Steel Exterior Columns With Tension Membrane



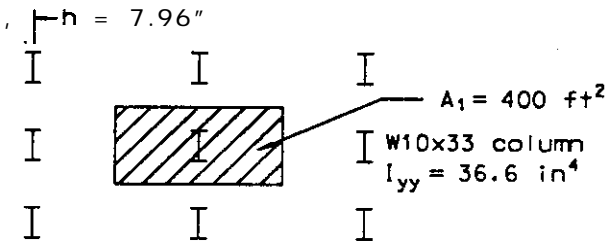
$$I_{bar} = \frac{ib}{\psi_i \sigma_y Z} \sqrt{\frac{EI_g L}{W}}$$

$$P_{bar} = \frac{pb L^2}{\psi_p \sigma_y Z}$$

Boundary Conditions	$\psi_p$	$\psi_i$
Simple-Simple	10.00	0.913
<b>Fixed-Fixed</b>	23.10	0.861

**P-1 Diagram Input for Steel Interior Columns**

Parameter	Description	Parameter Value for Example Case Below
Peak Pressure (p)	Peak Blast Pressure at Center of Component	
Specific Impulse (i)	Specific Impulse Applied to Center of Component	
Smaller Column Dimension (h)	Column Thickness About Weak Axis	7.96 in
Column Height(L)	Column Height Between Lateral Supports	
Loaded Area (A <sub>1</sub> )	Loaded Area Supported by Column	400 ft <sup>2</sup>
Supported Weight pa Area (W)	Weight Per Unit Area of Supported Area	see equation below figure
Yield Strength(a.)	Yield Strength of Column	36,000 psi
Minimum Moment of Inertia (I <sub>yy</sub> )	Column Moment of Inertia About the Weak Bending Axis	36.6 in <sup>4</sup>
Gravity Constant (g)	Gravity Constant	386.4 in/sec <sup>2</sup>
Young's Modulus (E)	Young's Modulus of Column	29 E6 psi

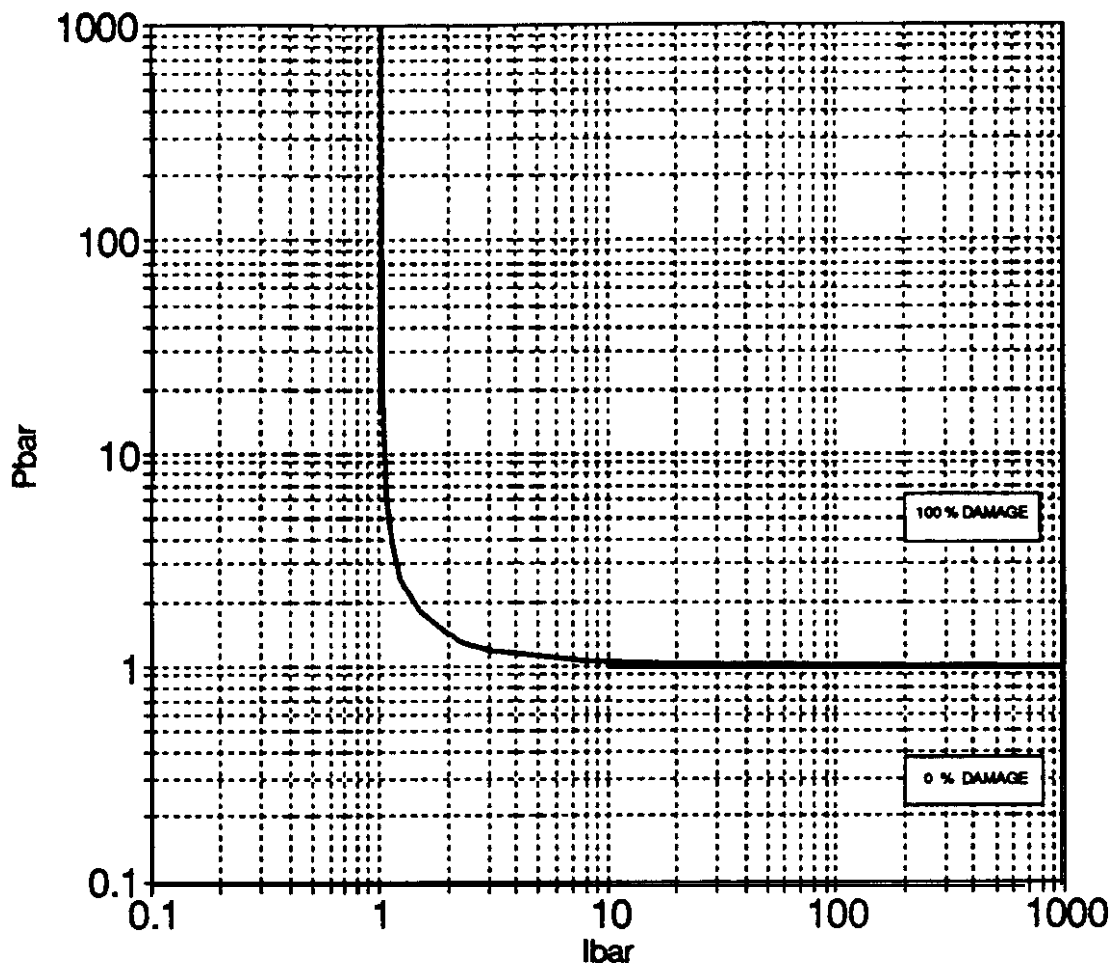


PLAN VIEW

$$w = (t) (150 \text{ lb/ft}^3)$$

$$t = (\text{concrete}) \text{ roof slab thickness}$$

### Steel Interior Columns



$$P_{bar} = \frac{p A_1 L^2}{\alpha_y E I_{yy}}$$

*errata*

$$I_{bar} = \frac{i h}{\alpha_1 \alpha_y} \sqrt{\frac{E A_1 g}{W I_{yy}}}$$

*errata*

$W I_{yy} L$

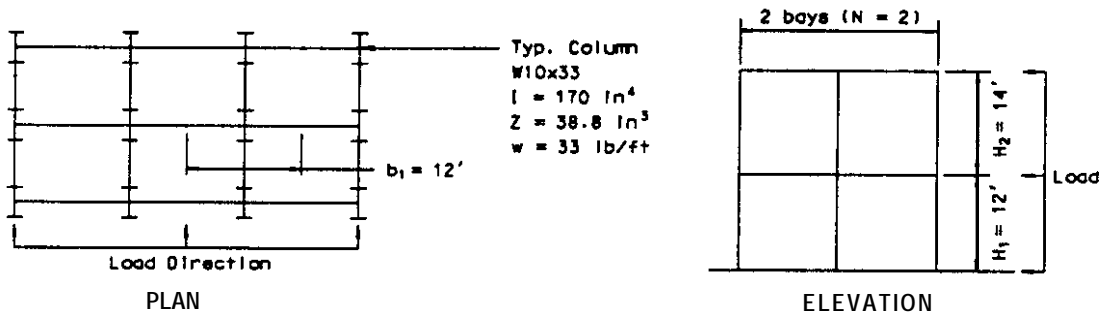
Boundary Conditions	Side Sway	$\alpha_1$	$\alpha_y$
Fixed-Simple	No	0.894	20.99
Fixed-simple	Yes	1.410	2.41
Fixed-Fixed	No	1.410	39.48
Fixed-Fixed	Yes	1.410	9.81
Simple-Simple	No	1.410	9.81
Simple-Simple	Yes	1.410	2.41

## P-I Diagram Input for Steel Frames

Parameter	Description	Parameter Value for Example Case Below
Peak Pressure (p)	Peak Blast Pressure at Center of Component	-
Specific Impulse (i)	Specific Impulse Applied to Center of Component	-
Loaded Width (b <sub>l</sub> )	Width of Wall Area Supported by Exterior Column of Frame	12 ft
Total Weight (W)	Effective Weight Supported by Frame	see equation below figure
Number of Bays (N)	Number of Bays in the Frame (Must be Less Than 15)	2
Single Story Height (H)	Average Story Height	13 ft
Number of Stories	Number of Stories in Frame (2 Story Maximum)	2
Steel Yield Strength (σ <sub>y</sub> )	Yield Strength of Frame Columns	36,000 psi
Column Plastic Section Modulus (Z)	Average Plastic Section Modulus of Frame Columns	38.8 in <sup>3</sup>
Column Moment of Inertia (I)	Average Moment of Inertia of Frame Columns Resisting Lateral Load	170 in <sup>4</sup>
Gravity Constant (g)	Gravity Constant	386.4 in/sec <sup>2</sup>
Moment Capacity (M <sub>p</sub> )	Average Moment Capacity of Frame Columns	1.4 E9 lb-in
Young's Modulus (E)	Young's Modulus for Frame Columns	29 E6 psi

Calculated Values

$$M_p = \sigma_y Z$$

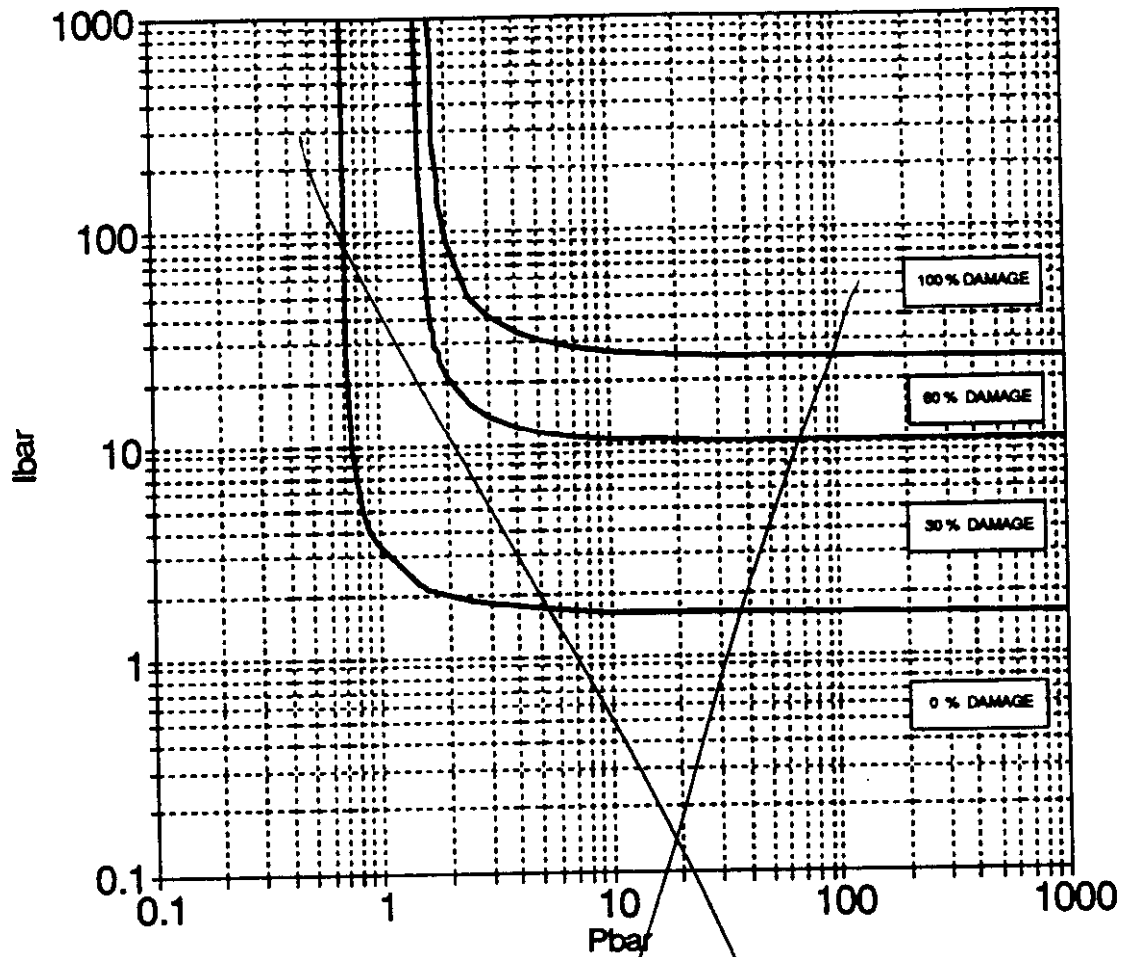


$$W = \text{roof weight} + 1/3 (\text{wall and column weight}) \text{ within Loaded Width}$$

$$w = (t_s)(12 \text{ ft})(24 \text{ ft})(150 \text{ lb/ft}^3) + 1/3 \{ [2(t_w)(12 \text{ ft})(26 \text{ ft})(150 \text{ lb/ft}^3)] + [3(33 \text{ lb/ft})(26 \text{ ft})] \}$$

where  $t_s$  = (concrete) m of slab thickness (ft)  
 $t_w$  = (concrete) wall thickness (ft)

# Steel Frames



$$I_{bar} = \frac{\alpha_1 [1 + 0.7(n - 1)]}{(n + 1)^2} \left( \frac{gE I_{eff} b_1^2 H}{WM_p^2} \right) i^2$$

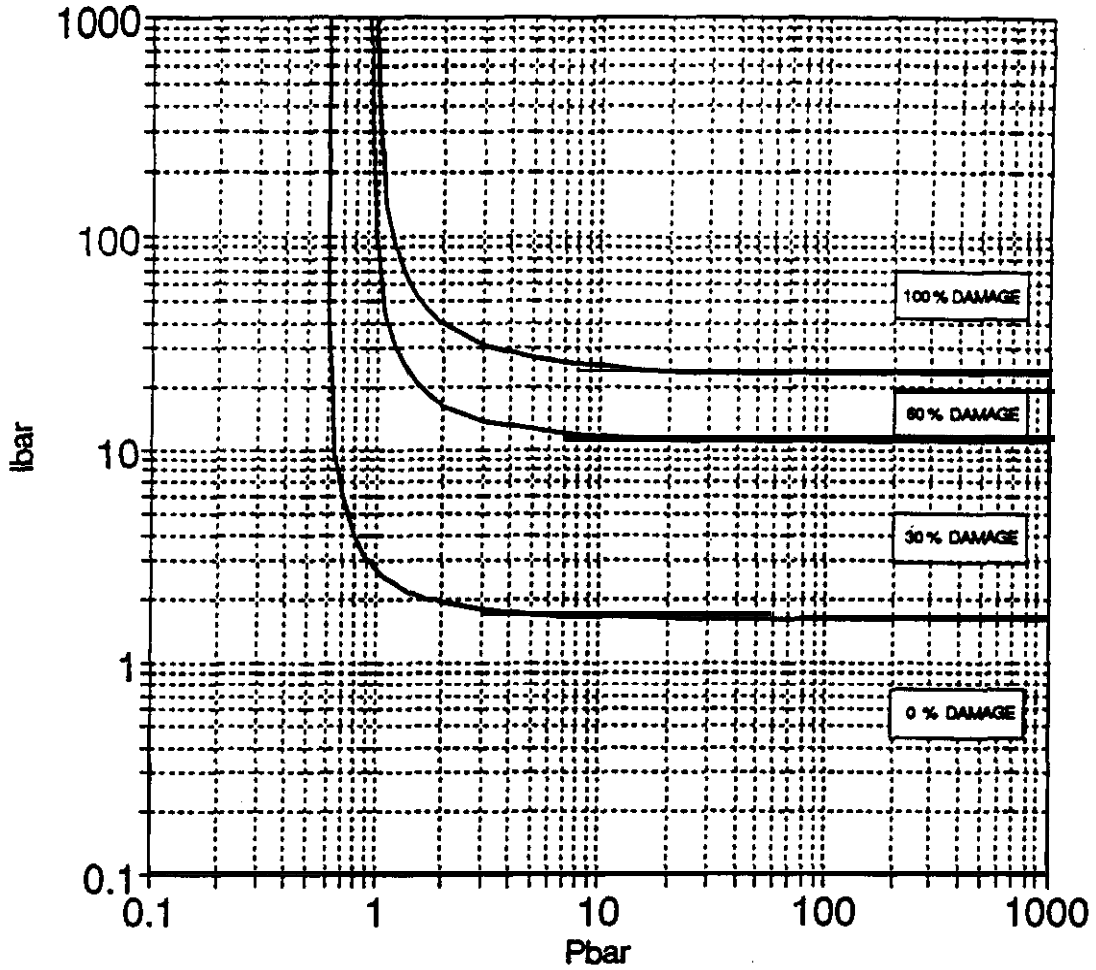
$$P_{bar} = \frac{\alpha_p b_1 H^2 p}{(1 + n)M_p}$$

1 Story Frame

2 Story Frame

	1 Story Frame	2 Story Frame
$\alpha_1$	0.83	7.5
$\alpha_p$	0.50	1.5

# Steel Frames



*evirati*

$$I_{bar} = \frac{\alpha_1 [1 + 0.7 (n - 1)]}{(n + 1)^2} \left( \frac{gE \overset{I}{\cancel{I}} b_1^3 H}{WM_p^2} \right) i^2 \qquad P_{bar} = \frac{\alpha_2 b_1 H^2 p}{(1 + n)M_p}$$

	1 Story Frame	2 Story Frame
$\alpha_1$	0.83	7.5
$\alpha_2$	0.50	15

**P-1 Diagram Input for Masonry One-Way Unreinforced Walls**

Parameter	Description	Parameter Value for Example Case Below
Peak Pressure (p)	Peak Blast Pressure at Center of Component	
Specific Impulse (i)	Specific Impulse Applied to Center of Component	
Span Length (L)	Span Length Between Supports	
Section Width (b)	Section Width (Used for all Section Property Calculations)	16 in
Wall Thickness (h)	Wall Thickness	8 in
Masonry Compressive Strength (f <sub>m</sub> )	Compressive Strength of Masonry Wall	1,350 nsi
Masonry Tensile Strength (f <sub>t</sub> )	Tensile Strength of Masonry Wall	200 psi
Weight/Unit Loaded Area (W)	Weight per Unit of Surface Area Loaded by Blast Pressure - Accounting for Voids	see equation below figure
Masonry Shell Thickness (t)	Masonry Shell Thickness (Usually 1.25" for CMU, 0.75" for Thickness of Masonry Block)	1.25 in
Section Modulus (S)	Elastic Section Modulus Within Section Width	135 in <sup>3</sup>
Moment of Inertia (I)	Moment of Inertia of Cross Section Within Section Width	455 in <sup>4</sup>
Gravity Constant (g)	Gravity Constant	386.4 in/sec <sup>2</sup>
Young's Modulus (E)	Young's Modulus for Masonry	1.35 E6 psi

errata

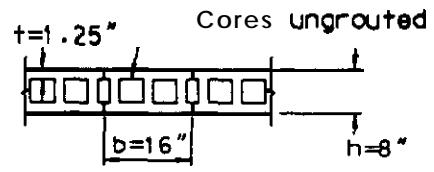
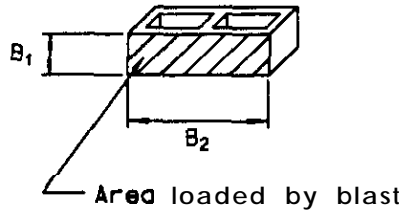
**Calculated Values**

$$S = t b (h-t)$$

$$I = \frac{tb (h-t)^2}{2}$$

$$E = 1000 f_m$$

Note: These formulas assume the wall is ungrouted. If it is known that the wall is grouted input  $S = \frac{bh^2}{6}$ ,  $I = \frac{bh^3}{12}$



CROSS-SECTION

- W = W<sub>B</sub> / [(B<sub>1</sub>) (B<sub>2</sub>)]
- W<sub>B</sub> = weight of block (including grout if voids grouted) (lb)
- B<sub>1</sub>, B<sub>2</sub> = dimensions of block area loaded by blast (ft)

## P-4 Diagram Input for Masonry One-Way Unreinforced Walls

Parameter	Description	Parameter Value for Example Case Below
Peak Pressure (p)	Peak Blast Pressure at Center of Component	-
Specific Impulse (i)	Specific Impulse Applied to Center of Component	-
Span Length (L)	Span Length Between Supports	-
Section Width (b)	Section Width (Used for all Section Property Calculations)	16 in
Wall Thickness (h)	Wall Thickness	8 in
Masonry Compressive Strength ( $f_m$ )	Compressive Strength of Masonry Wall	1,350 psi
Masonry Tensile Strength ( $f_t$ )	Tensile Strength of Masonry Wall	200 psi
Weight/Unit Loaded Area (W)	Weight per Unit of Surface Area Loaded by Blast Pressure - Accounting for Voids	see equation below figure
Masonry Shell Thickness (t)	Masonry Shell Thickness (Usually 1.25" for CMU, 0.75" for Thickness)	1.25 in
Section Modulus (S)	Elastic Section Modulus Within Section Width	135 in <sup>3</sup>
Moment of Inertia (I)	Moment of Inertia of Cross Section Within Section Width	455 in <sup>4</sup>
Gravity Constant (g)	Gravity Constant	386.4 in/sec <sup>2</sup>
Young's Modulus (E)	Young's Modulus for Masonry	1.35 E6 psi

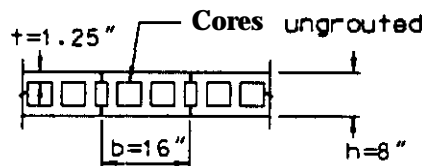
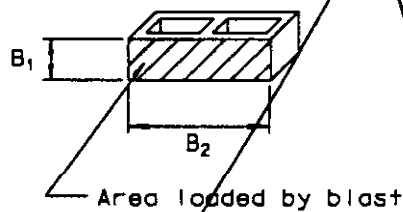
**Calculated Values**

$$S = t b (h-t)$$

$$I = \frac{tb (h-t)^2}{2}$$

$$E = 1000 f_m$$

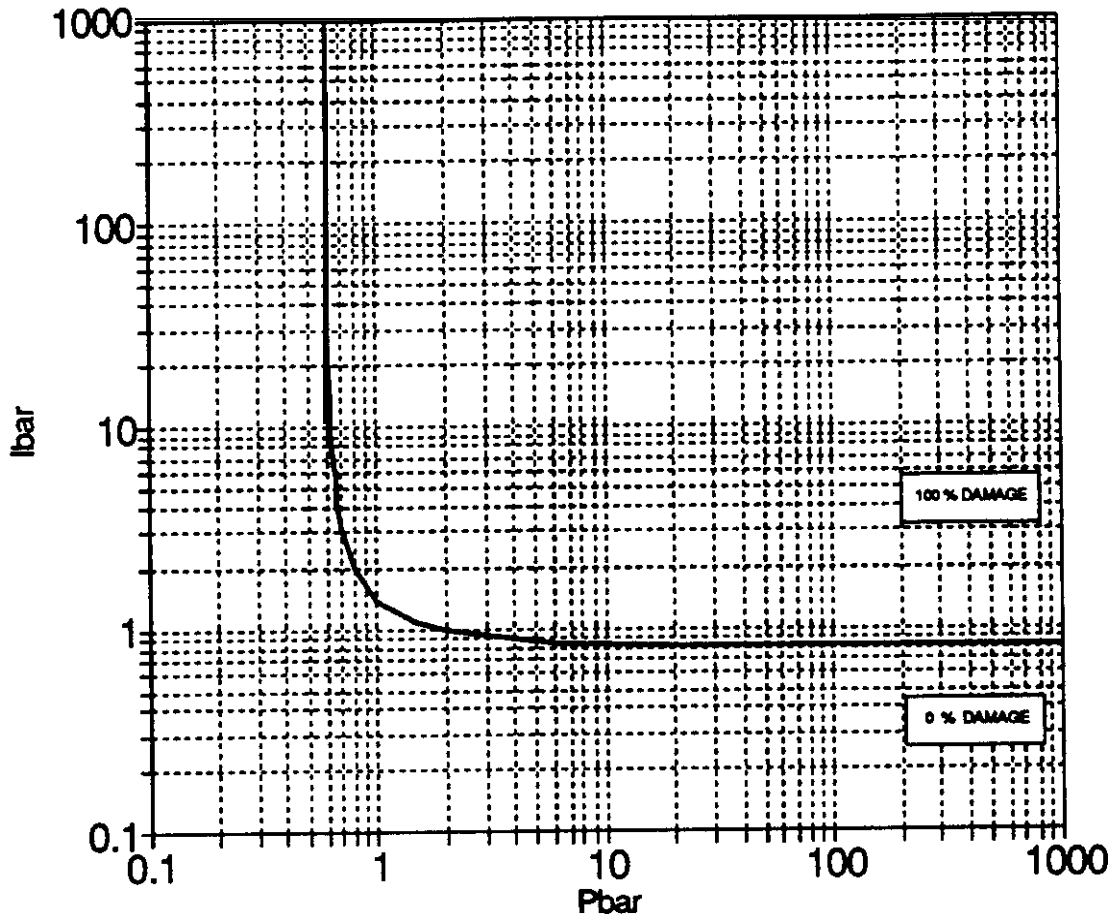
Note: These formulas assume the wall is ungrouted. If it is known that the wall is grouted input  $S = \frac{bt^3}{6}$ ,  $I = \frac{bt^3}{12}$



$$W = W_B / [(B_1) (B_2)]$$

$W_B$  = weight of block (including grout if voids grouted) (lb)  
 $B_1, B_2$  = dimensions of block area loaded by blast (ft)

### Masonry Unreinforced One-Way Slabs No Arching

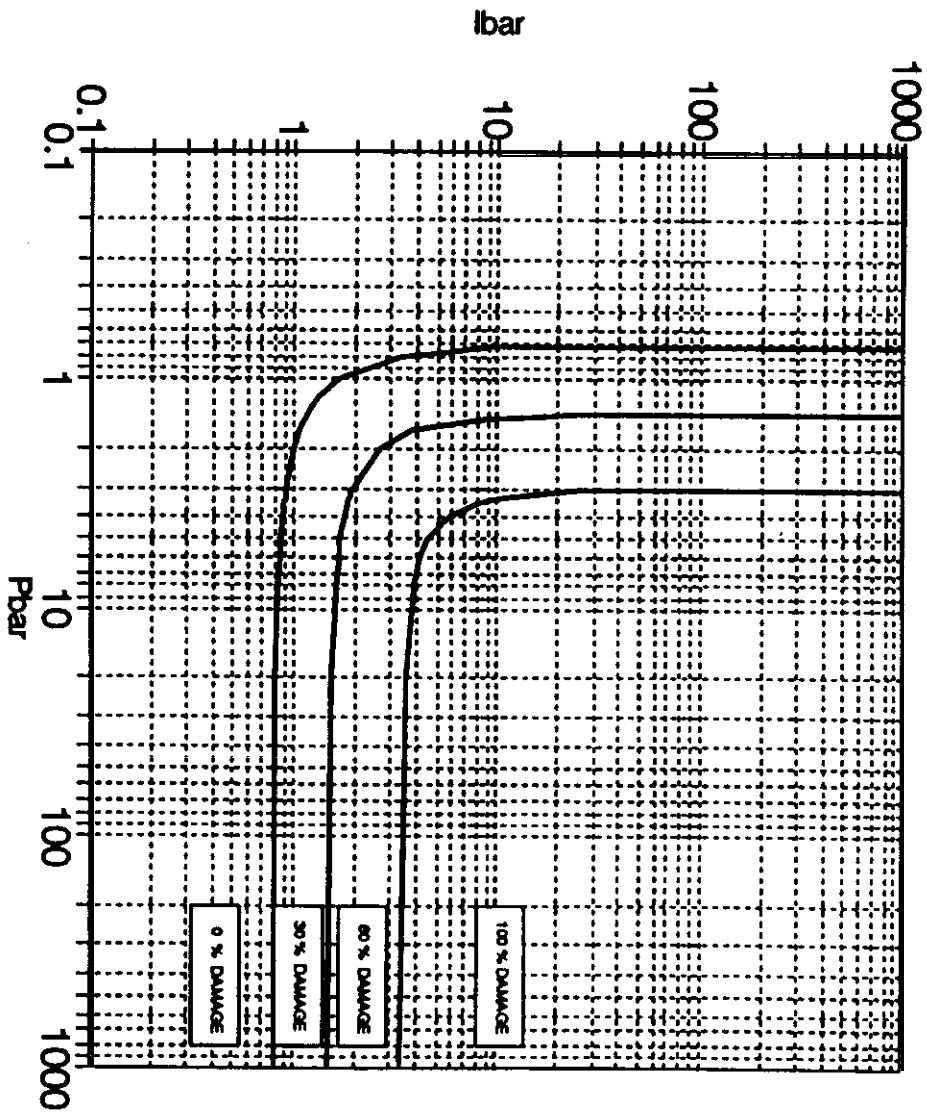


$$I_{bar} = \frac{ib}{\psi_i f_i S} \sqrt{\frac{EI_g}{Wb}}$$

$$P_{bar} = \frac{pb L^2}{\psi_p f_i S}$$

Boundary Conditions	$\psi_p$	$\psi_i$
Simple-Simple	10.00	0.913
Fixed-Fixed	23.10	0.861

### Masonry Unreinforced One-Way Slab With Arching



$$I_{bar} = \frac{lb}{w_l f_t S} \sqrt{\frac{EIg}{Wb}}$$

$$P_{bar} = \frac{pb L^2}{w_p f_t S}$$

Boundary condition

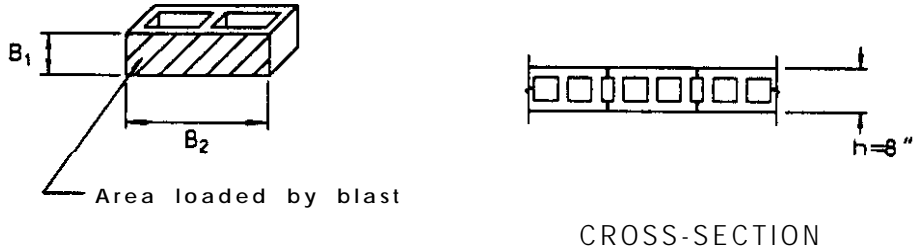
fixed

861

**P-1 Diagram Input for Masonry Two-Way Unreinforced Walls**

Parameter	Description	Parameter Value for Example Case Below
Peak Pressure (p)	Peak Blast Pressure at Center of Component	
Specific Impulse (i)	Specific Impulse Applied to Center of Component	
Short Span Length (x)	Shorter Span Length Between Supports	
Long Span Length (y)	Longer Span Length Between Supports	
wall Thickness (h)	Wall Thickness	8 in
Masonry Compressive Strength (f <sub>m</sub> )	Compressive Strength of Masonry Wall	1,350 psi
Masonry Tensile Strength (f <sub>t</sub> )	Tensile Strength of Masonry Wall	200 psi
Weight/Unit Loaded Area (W)	Weight per Unit of Surface Area Loaded by Blast Pressure - Accounting for voids	see equation below figure
Gravity Constant (g)	(Gravity Constant)	386.4 in/sec <sup>2</sup>
Young's Modulus (E)	Young's Modulus for Masonry	1.35E6 psi

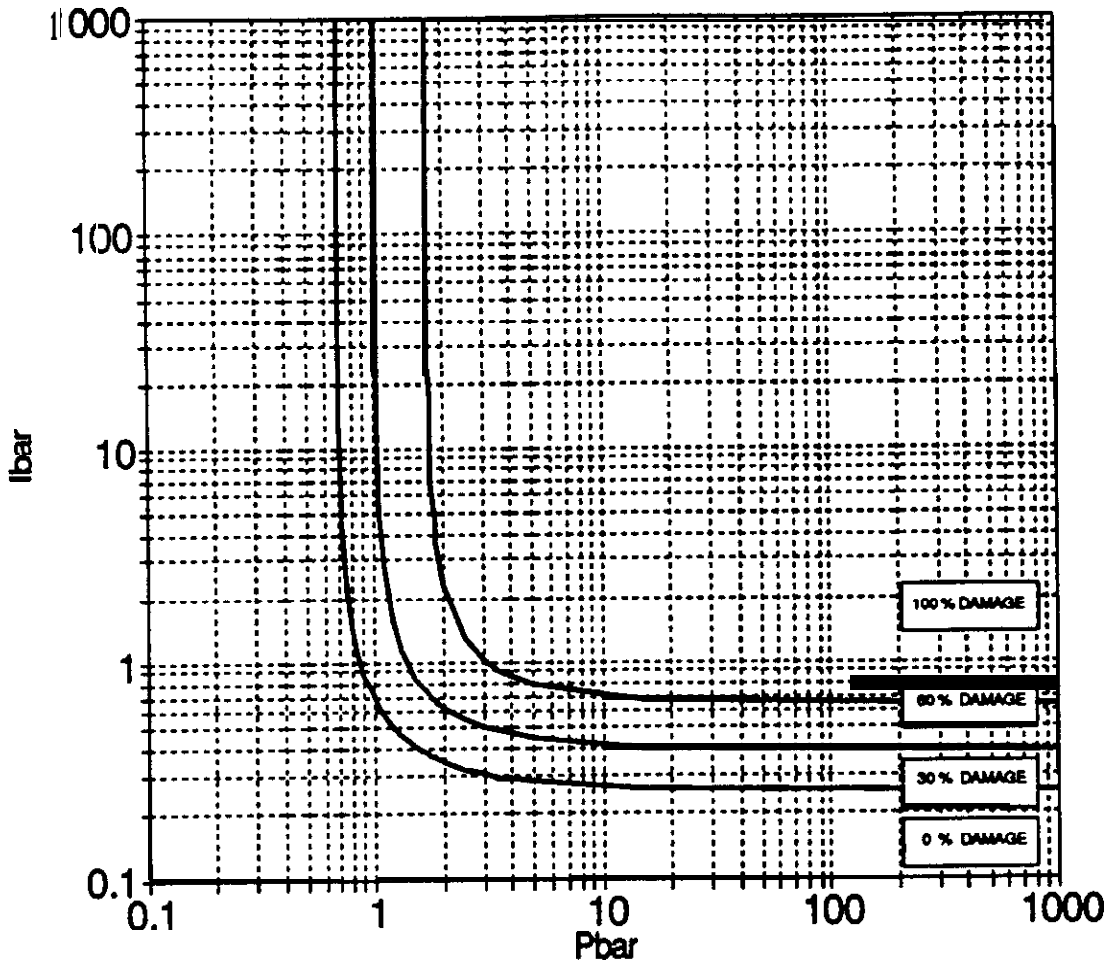
**Calculated Values**                       $E = 1000 f_m$



$$W = W_B / [(B_1)(B_2)]$$

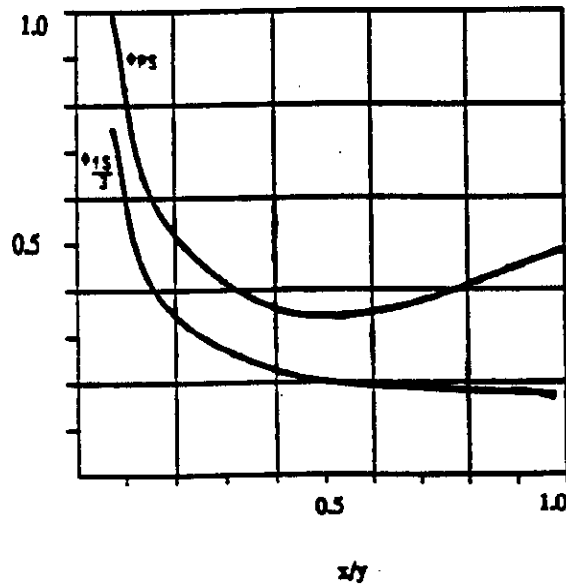
$W_B$  = weight of block (including grout if voids grouted) (lb)  
 $B_1, B_2$  = dimensions of block area loaded by blast (ft)

# Masonry Unreinforced Two-Way Slabs



$$I_{bar} = \frac{i}{\psi_1 \gamma_v h} \sqrt{\frac{Egh}{W}}$$

$f_t$



$$P_{bar} = \frac{px^2}{4\psi p \gamma_v h^2}$$

$f_t$

*errata*

**P-1 Diagram Input for Masonry One-Way Reinforced Wall**

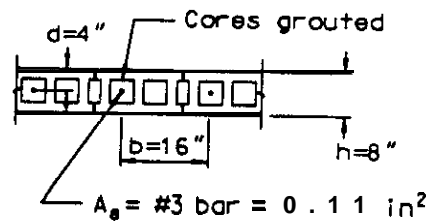
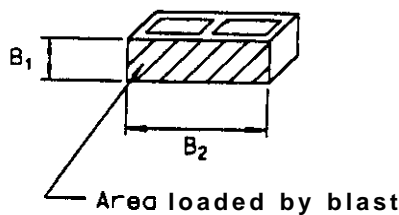
Parameter	Description	Parameter Value for Example Case Below
Peak Pressure (p)	Peak Blast Pressure at Center of Component	
Specific Impulse (i)	Specific Impulse Applied to Center of Component	-
Span Length (L)	Span Length Between Supports	-
Section Width (b)	Section Width (Used for all Section Property Calculations)	16 in
Wall Thickness (h)	Wall Thickness	8 in
Masonry Compressive Strength (f <sub>m</sub> )	Compressive Strength of Masonry Wall	1350 psi
Steel Yield Strength (f <sub>y</sub> )	Yield Strength of the Steel Reinforcement	60,000 psi
Depth to Tensile Steel (d)	Depth to Tensile Steel Reinforcement	4 in
Area of Tensile Steel (A <sub>s</sub> )*	Area of Tensile Steel Reinforcement Within Section Width	0.11 in <sup>2</sup>
Weight/Unit Loaded Area (W)	Weight per Unit of Surface Area Loaded by Blast Pressure	see equation below figure
Moment of Inertia (I <sub>cr</sub> )	Moment of Inertia of Cracked Cross Section Within Section Width	344 in <sup>4</sup>
Gravity Constant (g)	Gravity Constant	386.4 in/sec <sup>2</sup>
Moment Capacity (M <sub>p</sub> )	Moment Capacity of Section	2.2 E4 lb-in
Young's Modulus (E)	Young's Modulus of Section	1.35 E6 psi

ON PAGE 59 OF USER'S MANUAL  
 \* SEE GENERAL NOTES 1 AND 2 AT END OF COMPONENT DESCRIPTIONS

**Calculated Values**

$$I_{cr} = \frac{bh^3}{24} + 0.0025 (b)(d)^3 \quad M_p = 0.9 bd^2 f_y \rho (1 - 0.59 \rho f_y / f_m)$$

$$E = 1000 f_m \quad \rho = \frac{A_s}{(bd)}$$

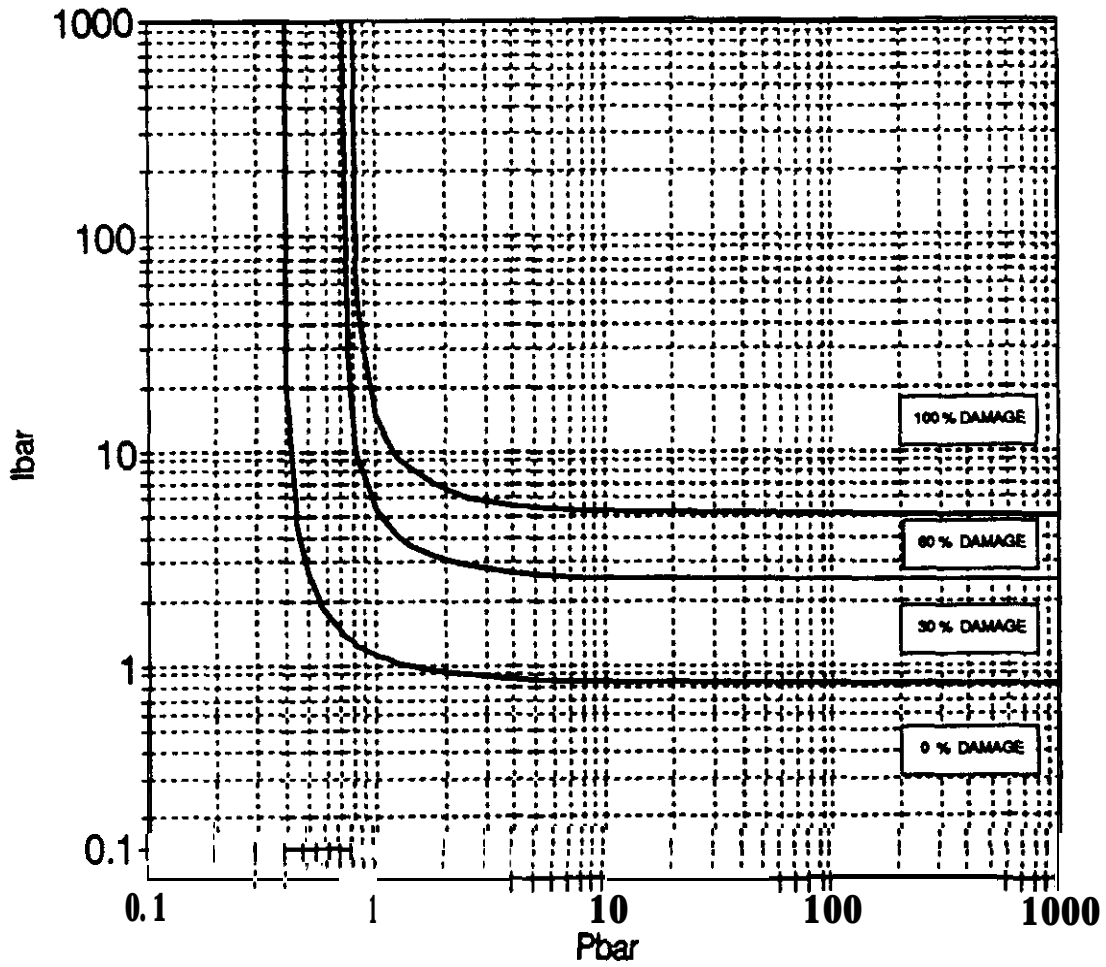


CROSS-SECTION

$$W = W_B / [(B_1) (B_2)]$$

W<sub>B</sub> = weight of block (including grout if voids grouted) (lb)  
 B<sub>1</sub>, B<sub>2</sub> = dimensions of block area loaded by blast (ft)

## Masonry Reinforced One-Way Slabs



$$I_{bar} = \frac{ib}{\psi_i M_p} \sqrt{\frac{E L_{eff} g_c'}{Wb}}$$

$$P_{bar} = \frac{pb L^2}{\psi_p M_p}$$

Boundary Conditions	$\psi_p$	$\psi_i$
Simple-Simple	10.00	0.913
Fixed-Fixed	23.10	0.861

## P-1 Diagram Input for Masonry Two-Way Reinforced Walls

Parameter	Description	Parameter Value for Example Case Below
Peak Pressure (p)	Peak Blast Pressure at Center of Component	
Specific Impulse (i)	Specific Impulse Applied to Center of Component	
Short Span Length (x)	Shorter Span Length Between Supports	
Long Span Length (y)	Longer Span Length Between Supports	
Section Width (b)	section Width (Used for all Section Property Calculations)	16in
Wall Thickness (h)	wall Thickness	8 in
Masonry Compressive Strength (f <sub>m</sub> )	Compressive Strength of Masonry Wall	1350 psi
Steel Yield Strength (f <sub>y</sub> )	Yield Strength of the Steel Reinforcement	60,000 psi
Depth to Tensile Steel (d)'	Depth to Tensile Steel Reinforcement	5.5 in
Area of Tensile Steel (A <sub>s</sub> )*	Area of Tensile Steel Reinforcement Within Section Width	0.11 in <sup>2</sup>
weight/unit Loaded Area (W)	Weight per Unit of Surface Area Loaded by Blast Pressure	see equation below figure
Moment of Inertia (I <sub>m</sub> )	Moment of Inertia of Cracked Cross Section Within Section Width	348 in <sup>4</sup>
Gravity Constant (g)	Gravity Constant	386.4 in/sec <sup>2</sup>
Moment Capacity (M <sub>p</sub> )	Moment Capacity of Section	32 E4 lb-in
Young's Modulus (E)	Young's Modulus for Masonry	1.35 E6 psi

SEE GENERAL NOTE 3 AT END OF COMPONENT DESCRIPTIONS

SEE GENERAL NOTE 4 AT END OF COMPONENT DESCRIPTIONS

*Refer to TWO-WAY Reinforced Concrete Slab Descriptions for explanation of Parameter.*  
*ON PAGE 59 OF USER'S MANUAL*

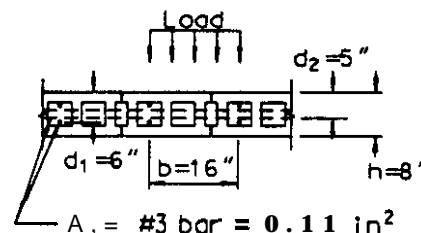
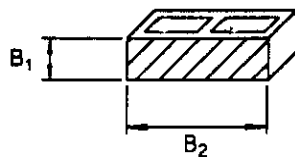
Calculated Values

$$I_{cr} = \frac{bh^3}{24} + 0.0025 (b)(d)'$$

$$M_p = 0.9 b d^2 f_y \rho (1 - 0.59 \rho f_y / f'_c)$$

$$E = 1000 f'_m$$

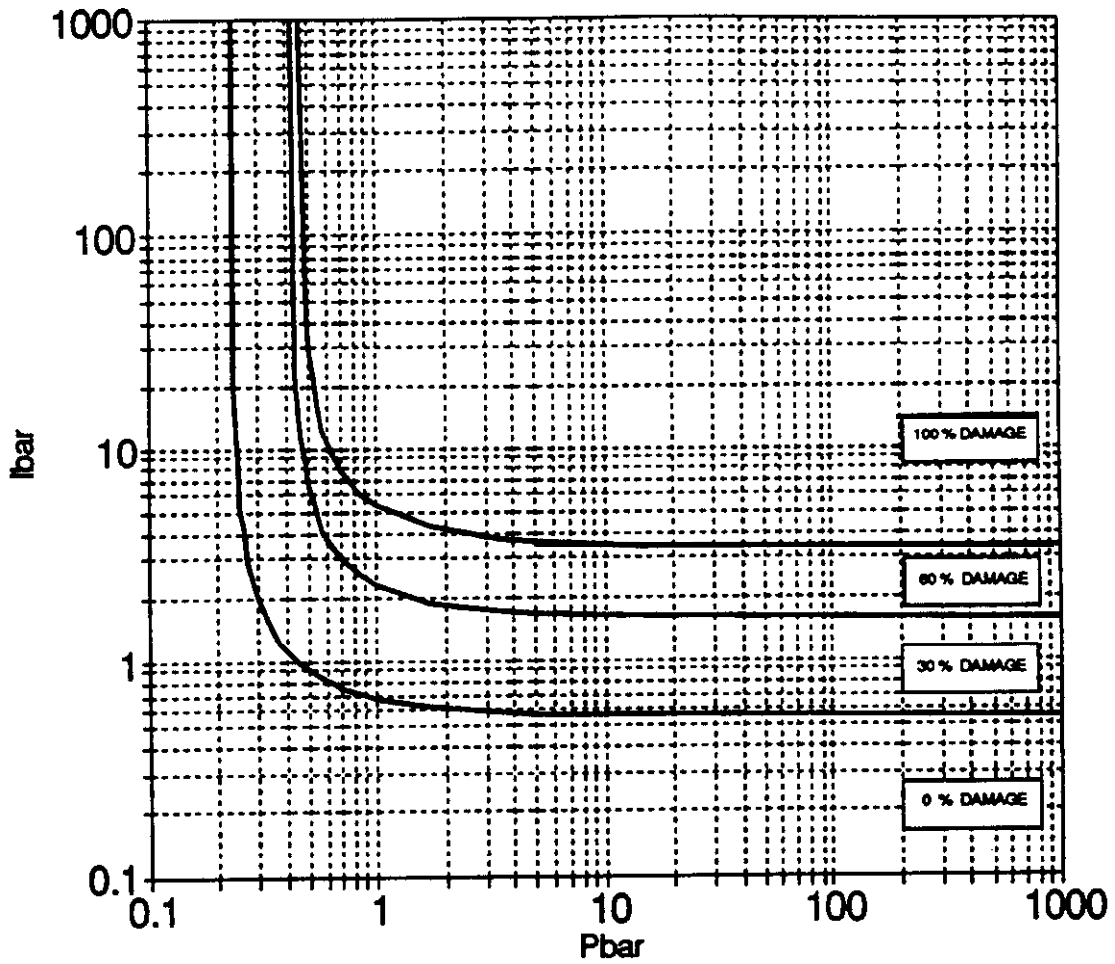
$$\rho = \frac{A_s}{(bd)}$$



CROSS-SECTION

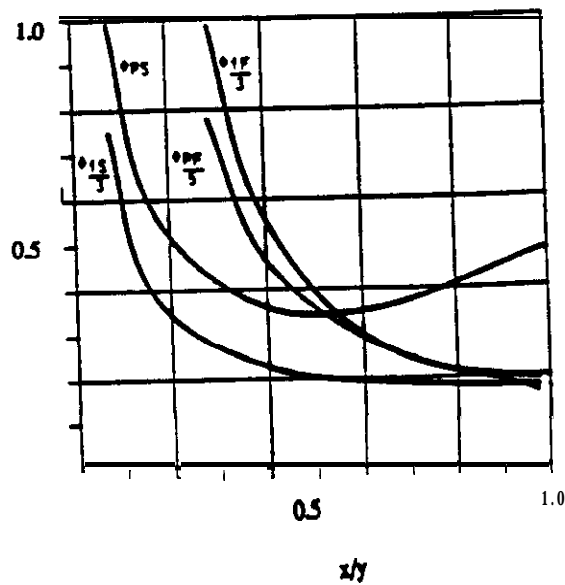
- W = W<sub>B</sub> / [(B<sub>1</sub>) (B<sub>2</sub>)]
- W<sub>B</sub> = weight of block (including grout if voids grouted) (lb)
- B<sub>1</sub>, B<sub>2</sub> = dimensions of block area loaded by blast (ft)

# Masonry Reinforced Two-Way Slabs



$$I_{bar} = \sqrt{\frac{E g h}{W}} \left( \frac{I_{eR}}{\psi_p M_p c h} \right) i$$

$$P_{bar} = \frac{p x^2 I_{eR}}{4 \psi_p M_p c h^2}$$



## P-I Diagram Input for Masonry Pilasters

Parameter	Description	Parameter Value for Example Case Below
Peak Pressure (p)	Peak Blast Pressure at Center of Component	-
Specific Impulse (i)	Specific Impulse Applied to Center of Component	-
Span Length (L)	Span Length Between Supports	-
Pilaster Width (b)	Width of Pilaster Cross Section	16 in
Pilaster Thickness (h)	Thickness of Pilaster Cross Section (Perpendicular to Loaded Area)	16 in
Loaded Width (b <sub>l</sub> )	Width of Area Supported by Pilaster Which is Loaded by Blast	12 ft
Total Weight (W)	Total Weight of Pilaster Plus Attached Components Within Loaded Width	see equation below figure
Masonry Compressive Strength (f <sub>m</sub> )	Compressive Strength of Pilaster	1,350 psi
Steel Yield Strength (f <sub>y</sub> )	Yield Strength of the Steel Reinforcement	60,000 psi
Depth to Tensile Steel (d)	Depth to Tensile Steel Reinforcement	12 in
Area of Tensile Steel (A <sub>s</sub> )	Area of Tensile Steel Reinforcement	1.32 in <sup>2</sup>
Moment of Inertia (I <sub>cr</sub> )	Moment of Inertia of Cracked Pilaster Cross section Resisting Lateral Load	1,670 in <sup>4</sup>
Gravity Constant (g)	Gravity Constant	386.4 in/sec <sup>2</sup>
Moment Capacity (M <sub>p</sub> )	Moment Capacity of Pilaster	8.0 ES lb-ii
Young's Modulus (E)	Young's Modulus of Pilaster	1.35E6 psi

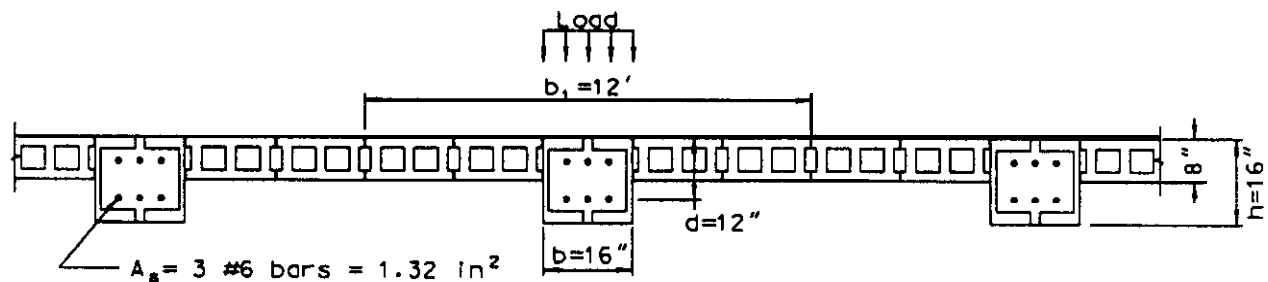
### Calculated Values

$$I_{cr} = \frac{bd^3 (5.5\rho + 0.083)}{2}$$

$$\rho = \frac{4}{(bd)}$$

$$M_p = 0.9 bd^2 f_y \rho (1 - 0.59 \rho f_y / f_m)$$

$$E = 1000 f_m$$

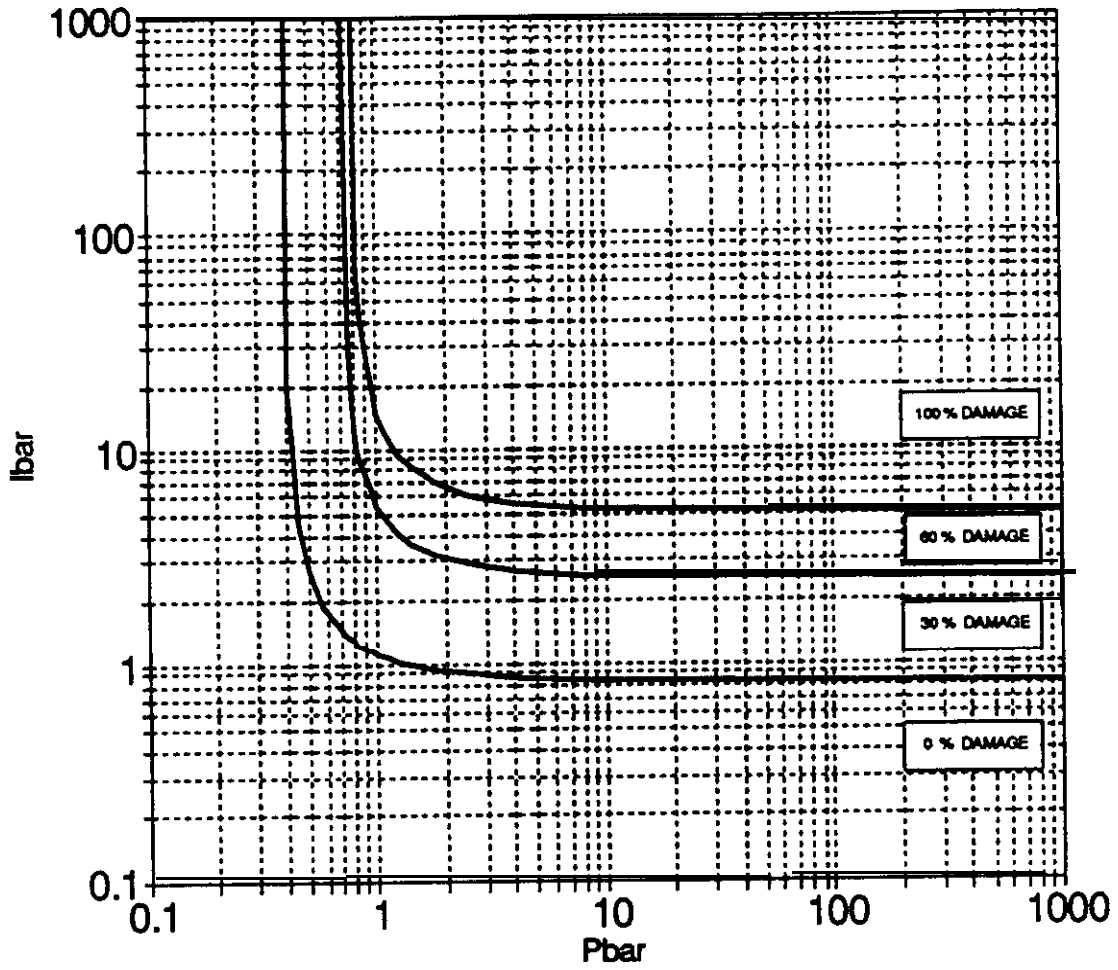


$$W = [W^1 (12 \text{ ft}) + [(16 \text{ in} \cdot 8 \text{ in}) (16 \text{ in})/144] (120 \text{ lb/ft}^2)] (L)$$

$$W^1 = \text{areal weight of wall per unit area (lb/ft}^2) - \text{calculate as shown for other masonry components}$$

$$L = \text{pilaster height (ft)}$$

### Masonry Pilasters



$$Ibar = \frac{ib_1}{\psi_1 M_p} \sqrt{\frac{EI_{agg}L}{W}}$$

$$Pbar = \frac{pb_1 L^2}{\psi_p M_p}$$

Boundary Conditions	$\psi_p$	$\psi_i$
Simple-Simple	10.00	0.913
Fixed-Fixed	23.10	0.861

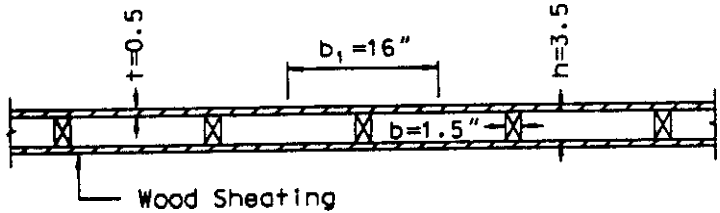
**P-1 Diagram Input for Wood Walls**

Parameter	Description	Parameter Value for Example Case Below
Peak Pressure (p)	Peak Blast Pressure at Center of Component	
Specific Impulse(i)	Specific Impulse Applied to Center of Component	
Span Length (L)	Span Length Between Supports	
Stud Width(b)	Actual Wall Stud Width (Usually Nominal Width-0.5")	1.5 in
Stud Depth (h)	Actual Wall Stud Depth (Usually Nominal Depth + 0.5")	3.5 in
Loaded Width(b <sub>l</sub> )	Loaded width (Stud Spacing) Used for all section Properties	16in
Total Weigh(W)	Total Weight of Stud Plus Attached Components Within Loaded Width	see equation below figure
Wood Yield Strength (f <sub>y</sub> )	Full Modulus of Rupture Strength of Wall Stud (Approximately 25 Times Allowable Design Stress)	
Modulus of Elasticity (E)	Modulus of Elasticity of Stud	1.2E6 psi
Wall Sheathing Thickness (t)	Average Thickness of Interior and Exterior Wall Sheathing Attached to stud	0.5 in
SNd+ Sheath Moment of Inertia (I)	Moment of Inertia of Stud (& Sheathing Each Side if Composite)	69 in <sup>4</sup> 37.4 in <sup>4</sup>
Gravity Constant (g)	Gravity Constant	386.4 in/sec <sup>2</sup>

**Calculated Values**

$$I = \frac{(b_l/2)(h+t)^2}{2} + \frac{bh^3}{12}$$

**Notes:** The formula above assumes *one-fourth* of the sheathing span between studs acts compositively with studs. If sheathing is not composite with wall studs input  $I = \frac{bh^3}{12}$  and  $t = 0$

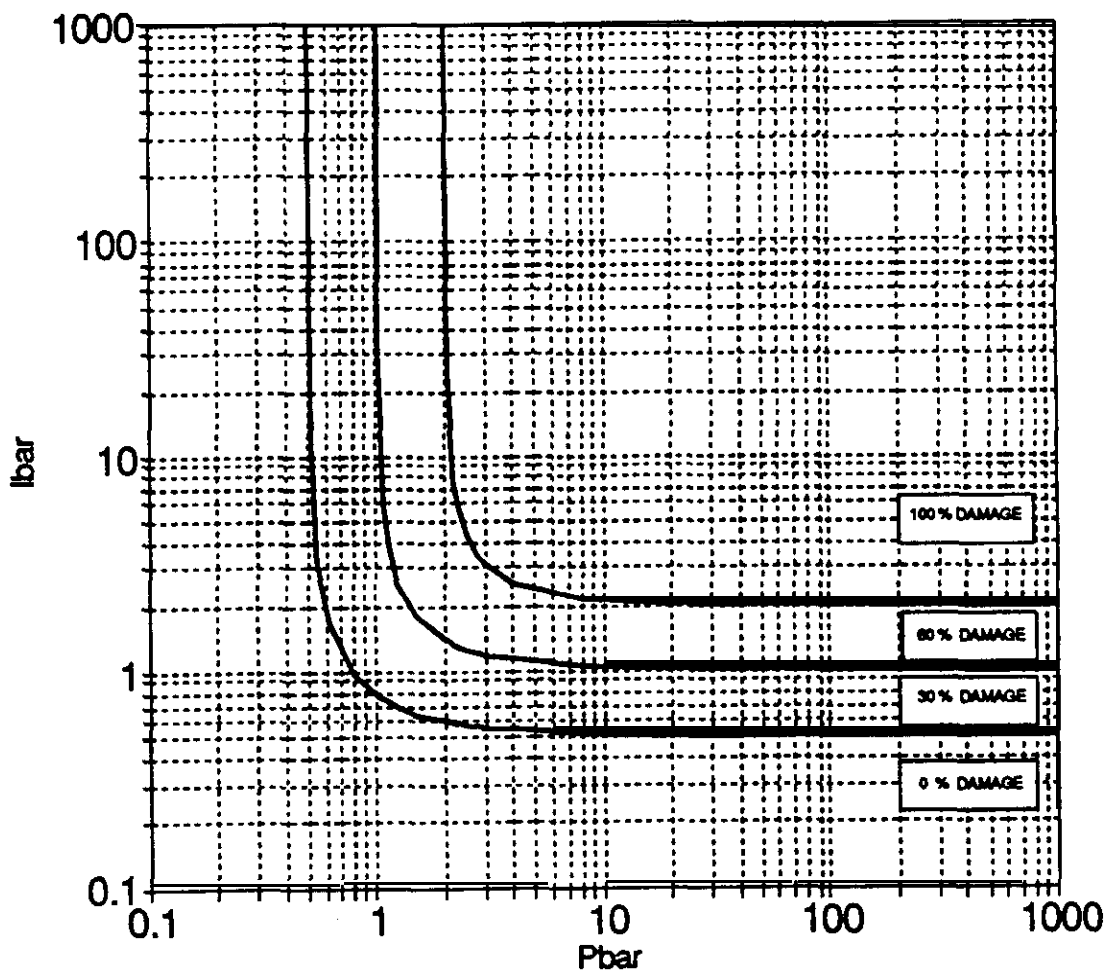


SECTION

$$W = \left[ W' (16 \text{ in}/12) + [(1.5 \text{ in}) (3.5 \text{ in})/144] (\gamma_w) \right] L$$

$W'$  = areal weight of both faces of sheathing and wall insulation (lb/ft<sup>2</sup>)  
 $L$  = wall height(ft)  
 $\gamma_w$  = density of wood in stud (lb/ft<sup>3</sup>)

### Wood Walls



$$I_{bar} = \frac{i b_1 h}{\alpha_1 f_y} \sqrt{\frac{E L g}{W I}}$$

$$P_{bar} = \frac{p b_1 h L^2}{\alpha_p I f_y}$$

Boundary Conditions	$\alpha_1$	$\alpha_p$
Simple-Simple	1.4610	8.0
Fixed-Fii	0.8944	12.0

## P-I Diagram Input for Wood Roofs

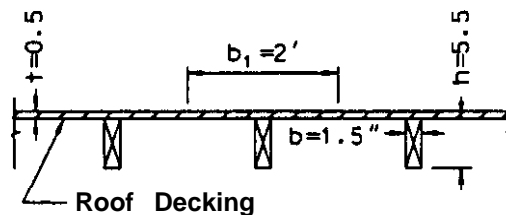
Parameter	Description	Parameter Value for Example Case Below
Peak Pressure (p)	Peak Blast Pressure at Center of Component	
specific Impulse (i)	Specific Impulse Applied to Center of Component	
Span Length (L)	Span Length Between Supports	
Joist Width (b)	Actual Roof Joist Width (Usually Nominal Width + 0.5")	1.5 in
Joist Depth (h)	Actual Roof Joist Depth (Usually Nominal Depth + 0.5")	5.5 in
Loaded Width (b <sub>l</sub> )	Loaded Width (Joist Spacing) Used for All Section Properties	24 in
Total Weight (W)	Total Weight of Joist + Weight of Attached Components Within Loaded Width	see equation below figure
Wood Yield Strength (f <sub>y</sub> )	Full Modulus of Rupture Strength of Joist (Approximately 25 Times Allowable Stress)	
Modulus of Elasticity (E)	Modulus of Elasticity of Joist	1.2E6 psi
Roof Decking Thickness (t)	Wood Thickness of the Roof Decking	0.5 in
Joist + Deck Moment of Inertia (I)	Moment of Inertia of Joist (and Deck if Composite)	64.8 in <sup>4</sup> 45
Gravity constant (g)	Gravity Constant	386.4 in/sec <sup>2</sup>

### Calculated Values

$$I = (b_l t / 2) \left( \bar{y} - \frac{t}{2} \right)^2 + \frac{h^3 b}{12} + hb \left( t + \frac{h}{2} - \bar{y} \right)^2$$

where  $\bar{y} = \left[ b_l \frac{t^2}{4} + bh \left( t + \frac{h}{2} \right) \right] / [b_l t / 2 + bh]$

Notes: The formula above <sup>half</sup>assumes one-fourth of the decking span between studs acts compositively with studs. If decking is not composite with roof joists, input  $I = \frac{b_l^3 t^3}{12}$  and  $t = 0$ .

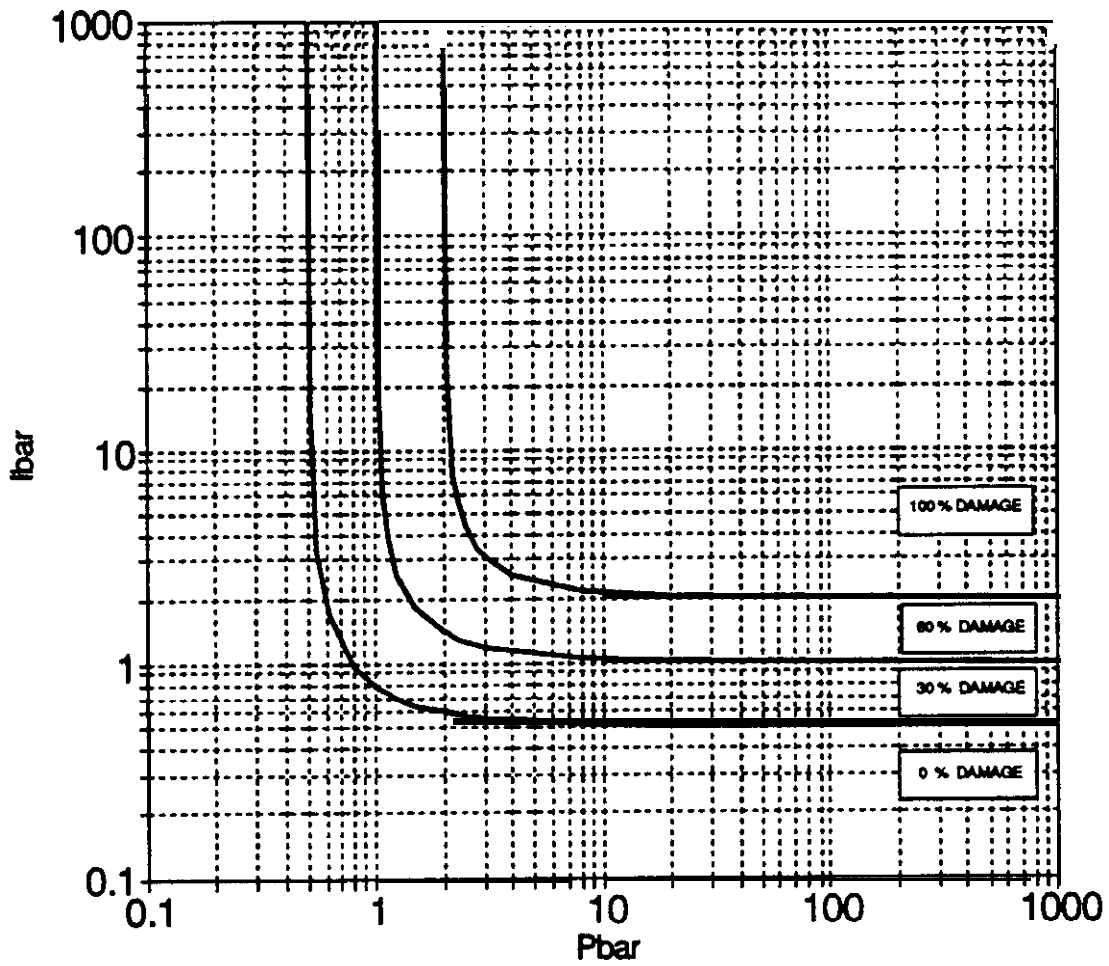


SECTION

$$W = \left[ W' (2 \text{ ft}) + [(5.5 \text{ in}) (1.5 \text{ in}) / 144] (\gamma_w) L \right] (L)$$

$W'$  = meal weight of roof decking and roofing material (lb/ft<sup>2</sup>)  
 $L$  = roof joist span (ft)  
 $\gamma_w$  = density of wood in stud (lb/ft<sup>3</sup>)

# Wood Roofs



$$I_{bar} = \frac{i b_1 h}{\alpha_1 f_y} \sqrt{\frac{E L g}{W I}}$$

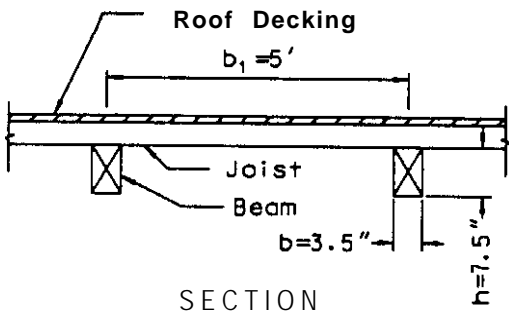
$$P_{bar} = \frac{p b_1 h L^2}{\alpha_y I f_y}$$

Boundary Conditions	$\alpha_1$	4
Simple-Simple	1.4610	8.0
Fixed-Fixed	0.8944	12.0

**P-1 Diagram Input for Wood Beams**

Parameter	Description	Parameter Value for Example Case Below
Peak Pressure (p)	Peak Blast Pressure at Center of Component	
Specific Impulse (i)	Specific Impulse Applied to Center of Component	
Span Length (L)	Span Length Between Supports	
Beam Width (b)	Actual Beam Width (Usually Nominal Width + 0.5")	3.5 in
Beam Depth (h)	Actual Beam Depth (Usually Nominal Depth + 0.5")	1.5 in
Loaded Width (b <sub>1</sub> )	Width of Area Loaded by Blast (Beam Spacing)	5ft
Total Weight(W)	Total Weight of Beam + Weight of Supported Components Within Loaded Width	see equation below figure
Wood Yield Strength (f <sub>y</sub> )	Full Modulus of Rupture Stress of Beam (Approximately 2.5 Times Allowable Design Stress)	
Modulus of Elasticity (E)	Modulus of Elasticity of Beam	1.2E6 psi
Moment of Inertia (I)	Moment of Inertia of Cross Section	123 in <sup>4</sup>
Gravity Constant (g)	Gravity Constant	386.4 in/sec <sup>2</sup>

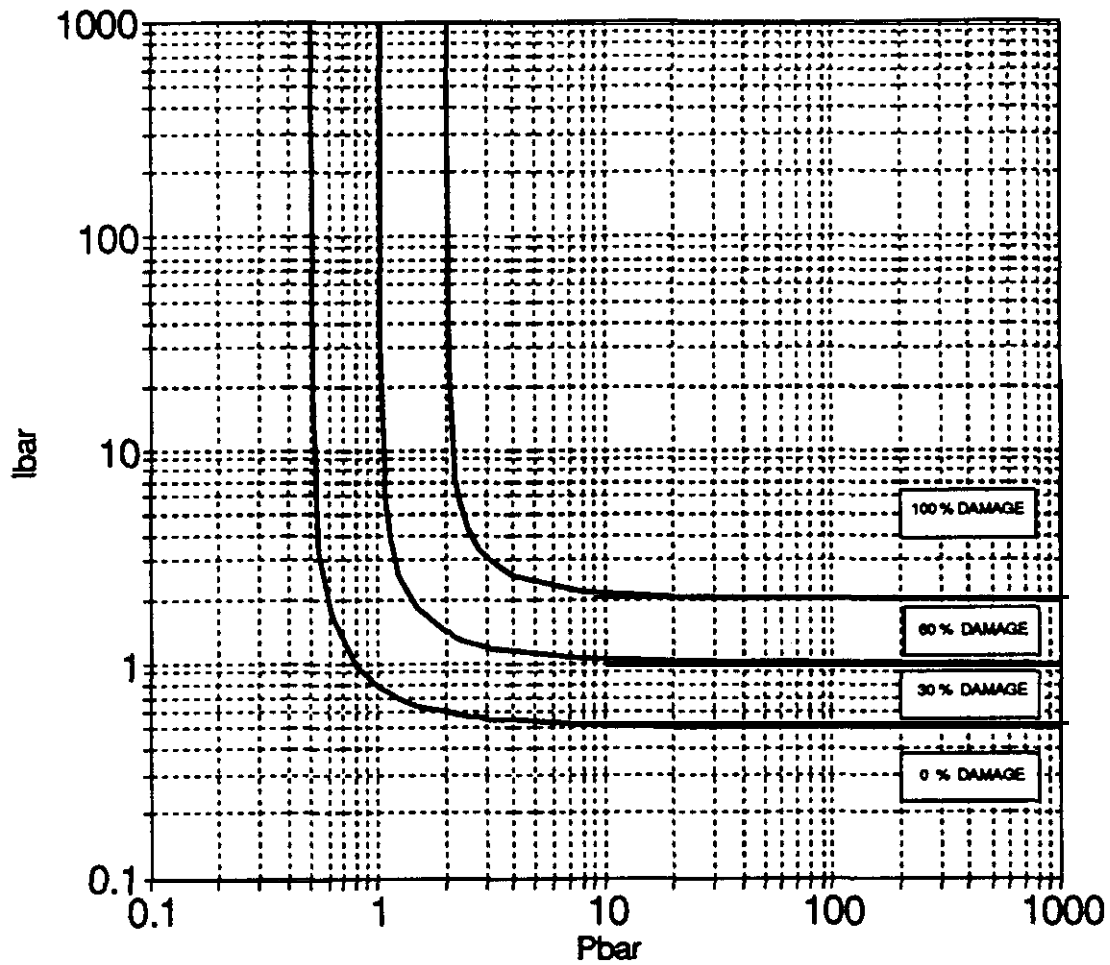
Calculated values  $I = \frac{bh^3}{12}$



$$W = [W^1 (5 \text{ ft}) + [(7.5 \text{ in}) (3.5 \text{ in}) / 144] (\gamma_w) (L)] (L)$$

$W^1 =$  areal weight of roof decking, roofing material, and roof joists (lb/ft<sup>2</sup>)  
 $L =$  span length of beam (ft)  
 $\gamma_w =$  density of wood in beam (lb/ft<sup>3</sup>)

### Wood Beams



$$I_{bar} = \frac{i b_1 h}{\alpha_1 f_y} \sqrt{\frac{E L g}{W I}}$$

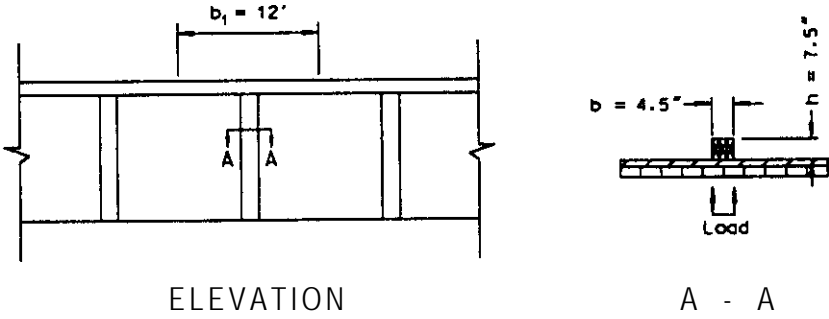
$$P_{bar} = \frac{p b_1 h L^2}{\alpha_2 I f_y}$$

Boundary Conditions	$\alpha_1$	$\alpha_2$
Simple-Simple	1.4610	8.0
Fixed-Fixed	0.8944	12.0

**P-I Diagram Input for Wood Exterior Columns**

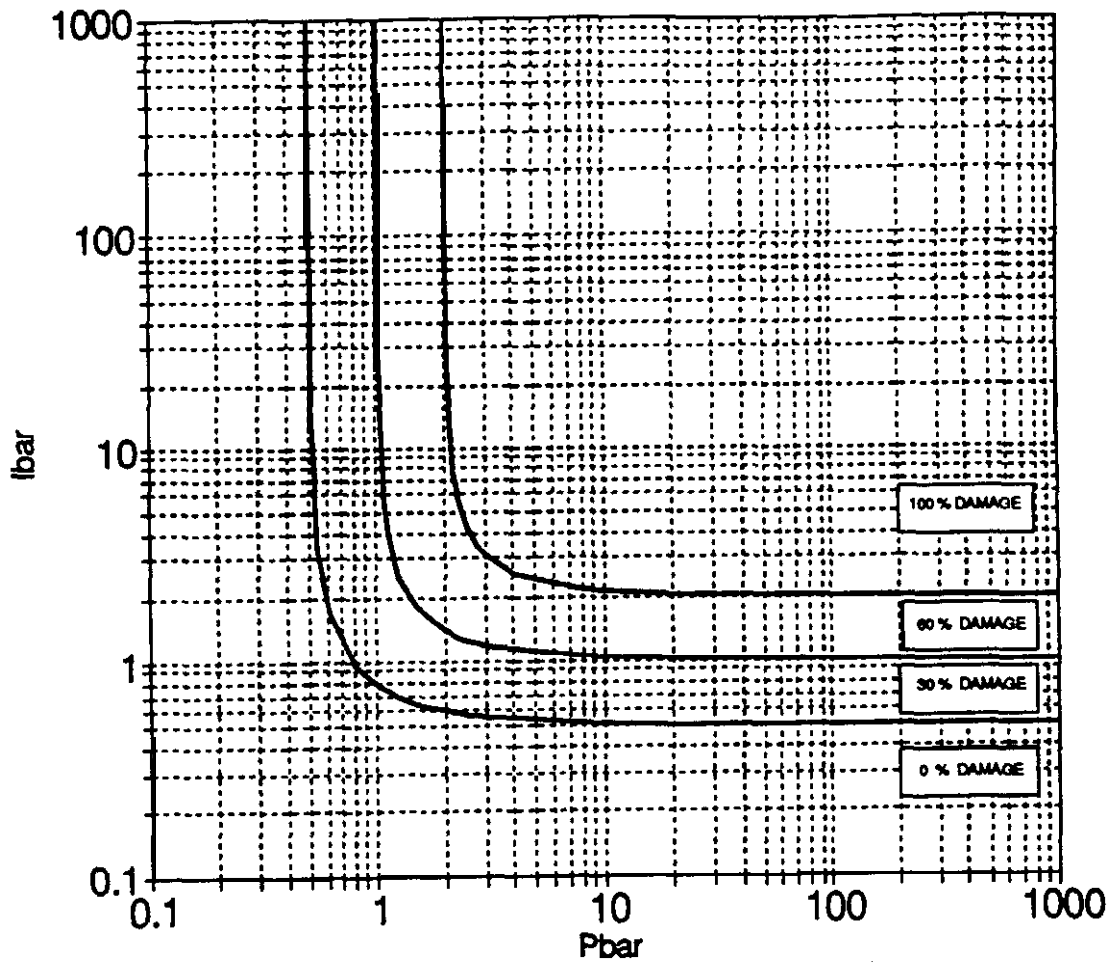
Parameter	Description	Parameter Value for Example Case Below
Peak Pressure (p)	Peak Blast Pressure at Center of Component	
Specific Impulse (i)	Specific Impulse Applied to Center of Component	
Span Length (L)	Span Length Between Supports	
Column Width (b)	Actual Column Width (Usually Nominal Width + 0.5")	4.5 in
Column Thickness (h)	Actual Column Depth (Usually Nominal Depth + 0.5")	7.5 in
Loaded Width (b <sub>l</sub> )	Width of Area Loaded by Blast (Column Spacing)	12ft
Total Weight (W)	Total Weight of Column Plus Attached Components Within Loaded Width	see equation below figure
Wood Yield Strength (f <sub>y</sub> )	Full Modulus of Rupture Strength of Column (Approximately 25 Times Allowable Design Stress)	
Modulus of Elasticity (E)	Modulus of Elasticity of Column	1.2E6 psi
Moment of Inertia (I)	Moment of Inertia of Column Cross Section Resisting Lateral Load	158 in <sup>4</sup>
Gravity Constant (g)	Gravity Constant	386.4 in/sec <sup>2</sup>

Calculated Values  $I = \frac{bh^3}{12}$



$w = \frac{L}{12}$   
 $W' = [W' (12 \text{ ft}) + [(4.5 \text{ in}) (7.5 \text{ in}) / 144] (\gamma_w) L]$   
 $L =$  areal weight of wall, stringers, insulation which are laterally supported by column (lb/ft<sup>2</sup>)  
 $L =$  column height (ft)  
 $\gamma_w =$  density of wood in column (lb/ft<sup>3</sup>)

# Wood Exterior Columns



$$I_{bar} = \frac{i b_1 h}{\alpha_1 f_y} \sqrt{\frac{E L g}{W I}}$$

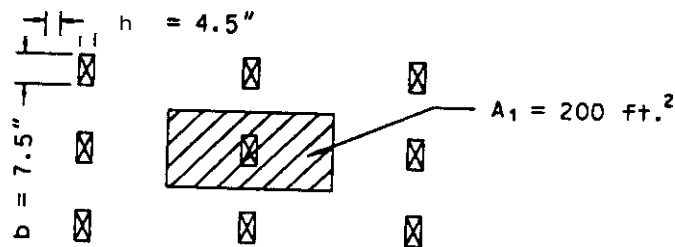
$$P_{bar} = \frac{p b_1 h L^2}{\alpha_p I f_y}$$

Boundary Conditions	$\alpha_1$	$\alpha_p$
Simple-Simple	1.4610	8.0
Fixed-Fixed	0.8944	12.0

### P-I Diagram Input for Wood Interior Columns

Parameter	Description	Parameter Value for Example Cast? Below
Peak Pressure ( <b>p</b> )	Peak Blast <b>Pressure</b> at Center of <b>Component</b>	
<b>Specific Impulse (i)</b>	<b>Specific Impulse</b> Applied to <b>Center</b> of Component	
Smaller Column <b>Dimension (h)</b>	Smaller Column <b>Cross Section Dimension</b>	4.5 in
<b>Larger</b> Column Dimension ( <b>b</b> )	<b>Larger</b> Column <b>Cross Section Dimension</b>	7.5 in
Column Height ( <b>L</b> )	Column Height <b>Between Lateral Supports</b>	
Loaded <b>Area (A<sub>1</sub>)</b>	<b>Loaded Area Supported by Column</b>	<b>200 ft<sup>2</sup></b>
<b>Supported</b> Weight Per Area ( <b>W</b> )	Weight Per Unit <b>Area</b> of <b>Supported Area</b>	-
<b>Wood Yield Strength (f<sub>y</sub>)</b>	Full <b>Compressive Yield Strength (Approximately 2.5 Times Allowable Stress)</b>	-
Modulus of <b>Elasticity (E)</b>	<b>Modulus of Elasticity of Column</b>	<b>1.2E6 psi</b>
<b>Minimum</b> Moment of <b>Inertia (I)</b>	Moment of <b>Inertia</b> of Cross Section About Weak Bending Axis	57 in <sup>4</sup>
<b>Gravity Constant (g)</b>	<b>Gravity</b> Constant	<b>386.4 in/sec<sup>2</sup></b>

*Calculated* values  $I = \frac{bh^3}{12}$

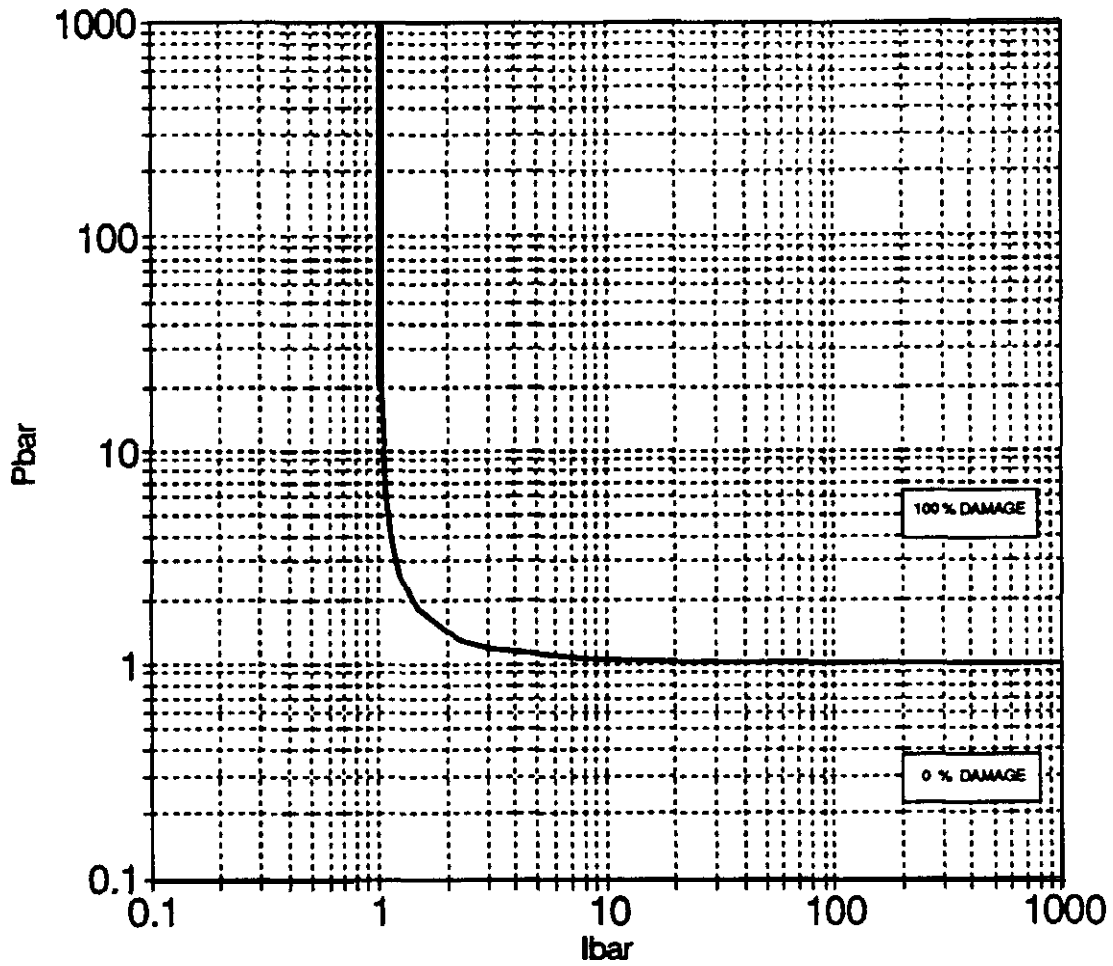


PLAN VIEW

$$W = W^1/A_1$$

$W^1 = \text{total weight of roof supported by column}$

### Wood Interior Columns



$$Pbar = \frac{pA_1 L^2}{\alpha_p EI}$$

$$lbar = \frac{ih}{\alpha_1 f_y} \sqrt{\frac{A_1 E_g}{WL}}$$

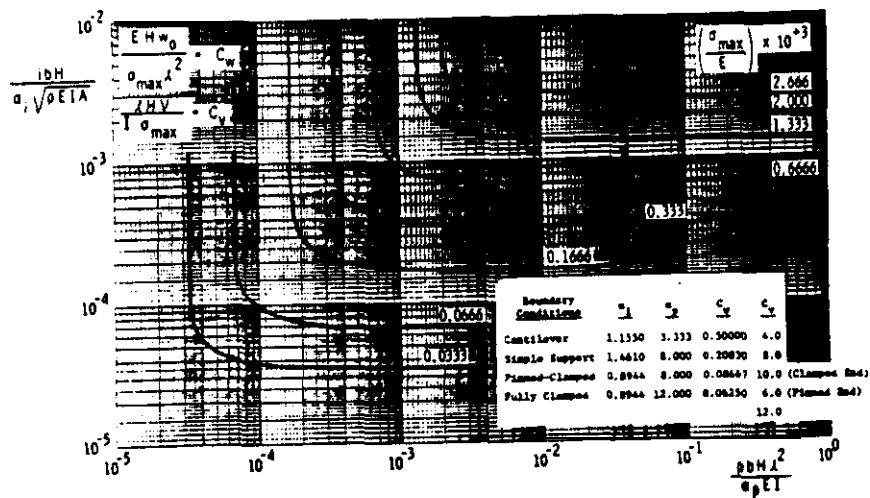
Boundary Conditions	Side Sway	$\alpha_1$	$\alpha_p$
Fixed-Simple	No	0.894	20.99
Fixed-Simple	Yes	1.410	2.41
Fixed-Fixed	No	1.410	39.48
Fixed-Fixed	Yes	1.410	9.87
Simple-Simple	No	1.410	9.87
Simple-Simple	Yes	1.410	2.41

## 4.2 P-i Diagrams

As stated above, P-i diagrams are the basic tool used to formulate the component blast damage prediction method. Figure 5 shows a typical P-i diagram, which, in this particular case, relates the response (**in** terms of maximum dynamic strain) of an elastic **beam** in flexure to the beam properties and the applied dynamic load. The load is assumed to be uniform along the beam length and to have a time history shaped like a **right** triangle (an immediately applied peak pressure which decays linearly to zero). Dynamic response in terms of the maximum strain is calculated as follows, using the P-i diagram in Figure 5. Based on the **known** properties of the component and the blast load, the non-dimensional terms on the vertical and horizontal axes of the P-i diagram are calculated. Then, the point defined by these two terms is plotted on the diagram. Finally, the response (i.e., the maximum strain) is determined based on the **strain** values of the response curves nearest the plotted point. The multi-parameter term on the vertical axis of the diagram is referred to as the "**Ibar**", or **i** term, and the term on the horizontal axis is referred to as the "**Pbar**", or **p** term. This method of **determining** structural response with a P-i diagram is very similar to other graphical methods used in static and dynamic structural design and analysis. The logic in the FACEDAP program essentially follows this same process to determine component damage except that in the code, the response curves, or damage curves, are represented with equations.

Elastic **flexural** response was assumed in the development of the P-i diagram in Figure.5. In general, a P-i diagram can be developed to consider almost any given type of structural response (i.e., elastic and plastic response, **flexural** or buckling response, etc.), any spatial load distribution (although uniform distribution is almost always assumed), and any given load history shape. Two and three degree-of-freedom systems can be considered. Multi-mode response can also be considered. However, the number of variables that must be considered within the P-i diagrams increases with the complexity of the assumed conditions. Since, all the assumptions used to develop the P-i diagrams, such as the mode of response, the load shape, etc., affect the development of the diagram, a P-i diagram cannot generally be used to predict response for conditions or assumptions different from those assumed in the development. For example, a P-i diagram developed to consider **flexural** response cannot, **in** general, be used to consider buckling response. Also, **the** type of response predicted with the P-i diagram, for example component maximum strain or ductility ratio is, in general, **fixed** by the assumptions used in the development of the P-i **diagram**. However, it is usually not **difficult** to develop a "new" P-i diagram which is based on the same assumptions as an existing diagram but expresses the response in terms of a different response parameter.

The P-i diagrams were used as the basis of the component damage prediction method for several reasons. First, the diagrams are a quick, graphical analysis tool for determining structural response or damage from an applied blast load. This was important **in** the initial development of the methodology prior to the BDAM and FACEDAP computer codes. Second, the response curves in the P-i diagram can be easily transformed into a series of damage prediction equations which can be programmed into a computer code. The simple, asymptotic shape. of the curves makes them relatively easy to curve-fit. Finally, P-i diagrams offer a very convenient format for normalizing different groups of component damage data, which have different properties and different applied



- $\rho$  = peak blast pressure
- $i$  = positive phase blast impulse
- $b$  = loaded width
- $l$  = span length
- $H$  = beam depth
- $E$  = Young's Modulus
- $I$  = beam moment of inertia
- $A$  = cross sectional area
- $p$  = mass density

Figure 5. P-i Diagram for **Beam Responding Elastically**

blast loads, so that they **can** be compared with each other and to theoretically predicted response on a simple graph. This type of comparison has been used to validate theoretically developed P-i diagrams for some components and to modify theoretical P-i diagrams for other components.

### 4.3 Theoretical Development of P-i Diagrams

The first step in **the** development of the P-i diagrams is the task of identifying the structural component or group of components which are of interest, and identifying all the factors which affect the dynamic response of the component. These factors include the assumed primary response mode of the component, the stress-strain relationship for the material(s) in the component as they respond in the assumed response mode, the shape of the time history of the applied blast wave, the degrees of freedom of the component, the shape function which expresses **the** movement of each point on the **structure** in terms of the degrees of freedom, etc. In short, **all the** parameters which would be involved in a dynamic analysis of the component must be identified. The second step is the development of the  $\bar{p}, \bar{i}$ , and response terms which are consistent with the assumed dynamic response. The  $\bar{p}$  and  $\bar{i}$  terms must separate out the “impulse sensitive” dynamic response and “pressure sensitive” response and they must, along with the response term, include all **the** variables which affect dynamic response for the given assumed conditions. Impulse sensitive dynamic response occurs when the component response is dependent only on the **impulse** of the applied load and is independent of the pressure magnitude. Pressure sensitive response occurs when the component response is independent of the applied impulse and is only dependent on the peak applied pressure. The manner in which a P-i diagram **separates** out these two response “realms” is **illustrated** in Figure 5. In the region where the response curves are parallel to the vertical axis, the **maximum strain** is independent of the  $\bar{i}$  term. Therefore, whether the impulse is high, or it is very high, the maximum strain in **the** component is unaffected. In **this** region the maximum strain is determined only by the value of the  $\bar{p}$  term, and therefore it is only affected by the peak pressure and not the impulse of the applied loading. In the region where the response curves are parallel to the horizontal axis, the maximum strain is independent of the peak applied pressure and dependent only on the  $\bar{i}$  term. All P-i diagrams, by definition, separate out pressure sensitive and impulse sensitive dynamic response in **this** manner by considering the dynamic load only in terms of its impulse and peak pressure and by forcing these two “load parameters” to appear separately in the vertical axis and horizontal axis terms. This approach is the basis for the simple asymptotic shapes of the response curves.

The most convenient way to derive the  $\bar{i}, \bar{p}$  and response terms is with an energy balance approach. This is a convenient basis to use because the energy balance concept (i.e., energy is neither created nor destroyed) can easily be formulated to consider only impulse sensitive dynamic response or pressure sensitive response. The energy balance equation which applies in the impulsive realm is shown below where the subscript 1 refers to time **zero**, which is taken as the end of the load duration and the subscript 2 refers to the time at which maximum displacement occurs (**Time 2**).

$$KE_1 + SE_1 = KE_2 + SE_2 \quad (4.1)$$

$KE_1$  = **kinetic energy** at Time Zero =  $mv^2/2 = i^2/(2m)$

$KE_2$  = kinetic energy at Time 2 equal to 0, since velocity is zero at time of maximum displacement

$SE_1$  = strain energy at Time Zero equal to 0, since zero displacement is assumed at Time Zero

$SE_2$  = strain energy at Time 2 equal to strain energy at time of maximum displacement

v = component velocity at end of load duration

i = **applied** impulse

m = component mass

In general, the work energy is included in the energy balance equation. However, there is no work energy term in Equation 4.1 because the assumption of impulse sensitive response, or impulsive response, means that the applied load duration is “short enough” so that the load duration is over before the component undergoes any significant displacement. Therefore, it is also true that no resistance develops during the load duration, since no significant component displacement occurs, and **the** applied impulse is related to velocity by the time integral of Newton’s second law over the load duration, as shown above in Equation 4.1 for the KE, **term**. The strain energy term in Equation 4.1 must be consistent with all the assumptions related to all the dynamic **response** of the component mentioned in the first paragraph of this section.

In the third step, Equation 4.1 is algebraically manipulated to solve an  $\bar{i}$  term on one side of the **equation**, which must include the applied impulse, and a response term **on the other** side of the equation. New parameters, such as the component length, can be introduced into both sides of the equation if this ultimately simplifies the  $\bar{i}$  and response terms. The  $\bar{i}$  and response terms account for **all** the parameters which affect the component response to the impulse of the applied blast load because of the manner in which these terms have been developed. For convenience the  $\bar{i}$  (and  $\bar{p}$ ) terms are usually formulated so as to be non-dimensional. The derivation of the  $\bar{i}$ ,  $\bar{p}$ , and response terms in Figure 5 is shown in Reference 12.

The energy balance equation which is applied to the quasistatic response, or pressure sensitive realm, is shown below where the subscript 1 refers to the time when the load duration begins and subscript 2 refers to the time of maximum displacement (**Time 2**). The same response assumptions (i.e., response mode, stress-strain relationship, etc.) used to develop Equation 4.1 must be used to develop the strain energy term in Equation 4.2 so that a consistent set of  $\bar{p}$ ,  $\bar{i}$ , and response terms are formulated for the P-i diagram.

$$WE_1 + SE_1 = WE_2 + SE_2 \quad (4.2)$$

$WE_1$  = the work energy at Time Zero equal to 0, since no displacement is assumed at the initial time

$WE_2$  = the work energy at Time 2, equal to the integral of the blast load multiplied by the displacement over the component area or length

$SE_1$  = strain energy at Time Zero equal to 0, since zero displacement is assumed at Time Zero

$SE_2$  = strain energy at Time 2 equal to strain energy at time of maximum displacement

There is no kinetic energy term in this energy balance because the two times of interest have been chosen to be those when velocity is zero. In general, Equation 4.2 is difficult to solve in a closed form because the time at which maximum displacement occurs is not known and therefore the load magnitude at maximum displacement in the  $WE_2$  term is not known. However, if the basic assumption of the quasistatic realm is considered (i.e., the load duration is assumed long compared to the natural period, or response time, of the component), then the load magnitude can be assumed equal to the peak applied load and the  $WE_2$  term in Equation 4.2 can be formulated in terms of the maximum applied load and the maximum deflection. Equation 4.2 is algebraically manipulated so that the same response term derived from Equation 4.1 is on one side of the equation (the strain energy side). The term on the other side, which will include the constant applied pressure, is the  $\bar{p}$  term. The  $SE_2$  term in Equations 4.1 and 4.2 should be equal because the second time of interest is the same time of maximum response in both equations.

The pair of  $\bar{i}$  and  $\bar{p}$  terms which are asymptotes for a response curve are determined by substituting the response level of interest into Equations 4.1 and 4.2 and solving for the  $\bar{i}$  and  $\bar{p}$  terms. The  $\bar{i}$  is the quasistatic asymptote of the given response curve and  $\bar{p}$  is the impulsive asymptote. For example, the  $\bar{p}$  and  $\bar{i}$  in Figure 5 which correspond to a strain of 0.033 are both equal to 0.033. However, the  $\bar{p}$  and  $\bar{i}$  terms are not generally equal to each other or to the given response level. The exact location of points on the response curve in the "dynamic" region, between the impulsive and quasistatic asymptotes, must be determined using Equation 4.2 without using the simplifying assumption that the load duration is long compared to the response time of the component. Or, in other words, the points in this region of the response curve must be determined with a dynamic analysis which tracks the dynamic response on a time step by time step basis. A spectrum of load histories are assumed, which have the assumed shape and durations ranging from about 3 times the component natural period to about 1/3 of the natural period, and the peak pressure which causes the desired value of the response term is calculated for each load history. The dynamic analyses must be based on the same set of assumptions, such as basic response mode, etc., used to develop the strain energy term that was used in Equations 4.1 and 4.2 to determine the  $\bar{p}$  and  $\bar{i}$  terms. When a dynamic analysis causes the desired value of the response term for a given load history duration,  $\bar{p}$  and  $\bar{i}$  values are calculated based on the peak pressure, the load history, and the structural geometry and material property terms in the analysis. The dynamic analyses can be based on any convenient dynamic system which is compatible with the assumed component type, response mode, stress-strain

relationship, etc. For example, the analyses used to determine the  $\bar{p}$  and  $\bar{i}$  values of the points on the dynamic region of the response curves in Figure 5 can be calculated with a single-degree-of-freedom (**SDOF**) analysis using a wood (or steel, etc.) beam with any given length, cross section, modulus of elasticity, etc. as long as no yielding is allowed in the dynamic analysis and the stiffness and load-mass factor are based on a **flexural** response mode.

This process for determining the dynamic region of the P-i curves can involve some trial and error and it not suited for use in a quick running computer program such as the FACEDAP code. Therefore, an effort has been made to determine a general equation which **fits** the dynamic region of the P-i curves. The following expression has been shown to fit the response curves for **SDOF response** in both the elastic and plastic range, based on limited comparison to response curves developed with dynamic SDOF **analyses**.

$$(\bar{p} - A) (\bar{i} - B) = 0.4 (A/2 + B/2)^{1.5} \quad (4.3)$$

A = the value of the vertical asymptote of the response curve ( $\bar{p}$  asymptote)

B = the value of the horizontal asymptote of the response curve ( $\bar{i}$  asymptote)

A comparison between the curve predicted with Equation 4.3 and points in the dynamic region of response curves for steel beams and open web steel joists generated with a SDOF analysis are shown in Figures 6 and 7. The points generated with the SDOF analyses are shown in the two figures with X's. The equations for "Pbar" and "Ibar" ( $\bar{p}$  and  $\bar{i}$ ) are those shown for these two component types in Section 4.1. The asymptotes for these two components represent near upper bound (in the case of steel beams) and near lower bound (in the case of open web steel joists) values for the asymptotes for the twenty-four component types shown in Section 4.1. If Equation 4.3 is used to generate the dynamic portion of the response curve, then only the values of the asymptotes (A and B in Equation 4.3) need to **be** determined theoretically or with damage data. This equation is used in the FACEDAP code **to** calculate the  $\bar{p}$  and  $\bar{i}$  terms of the response, or damage, curves for each component type.

#### 4.4 Development of the P-i Diagrams for Each Component Type

The discussion above provides a good background for explaining the development of the P-i diagrams for the various components that are included in the FACEDAP program. The P-i diagrams can be developed theoretically for a given component type and for an assumed mode of structural response, stress-strain relationship, blast load history shape, etc. as follows. **First**, a  $\bar{p}$ ,  $\bar{i}$ , and response term are calculated with Equations 4.1 and 4.2 or from a development in the literature based on the desired assumptions. Then, response curves are drawn for those response levels which are upper and lower bounds for given damage levels of interest. These curves partition the P-i diagram into the damage regions. Table 2 shows the relationships between two response terms, the

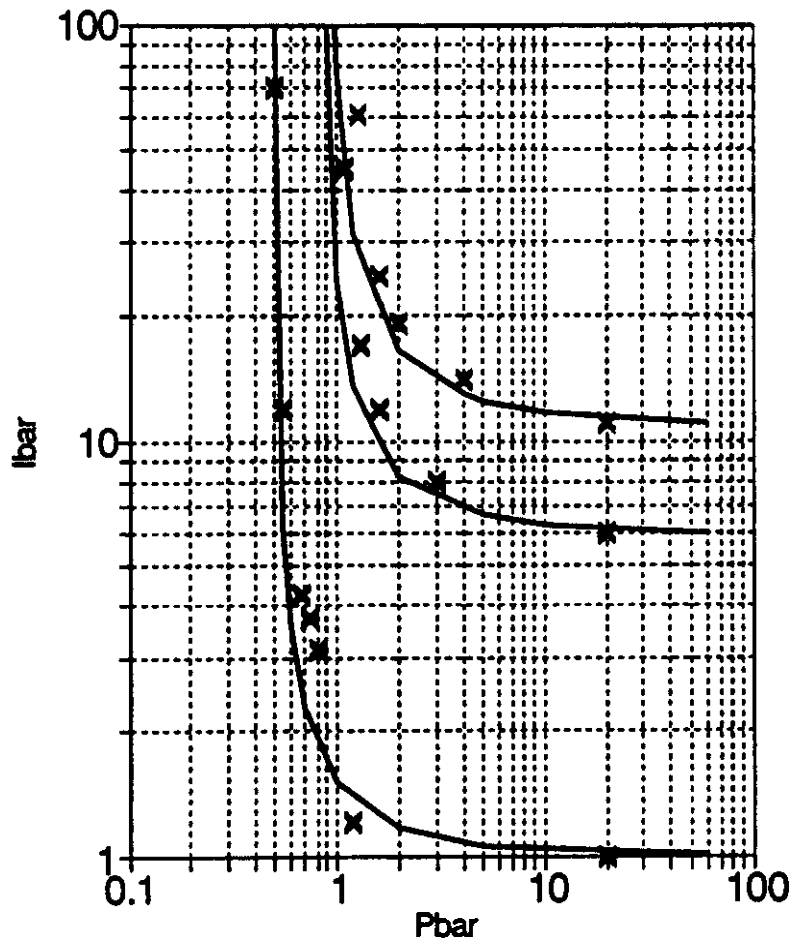


Figure 6. Comparison of Equation 4.3 to  $P_{bar}$  and  $I_{bar}$  Points for Steel Joists Generated with Single-Degree-of-Freedom Analyses

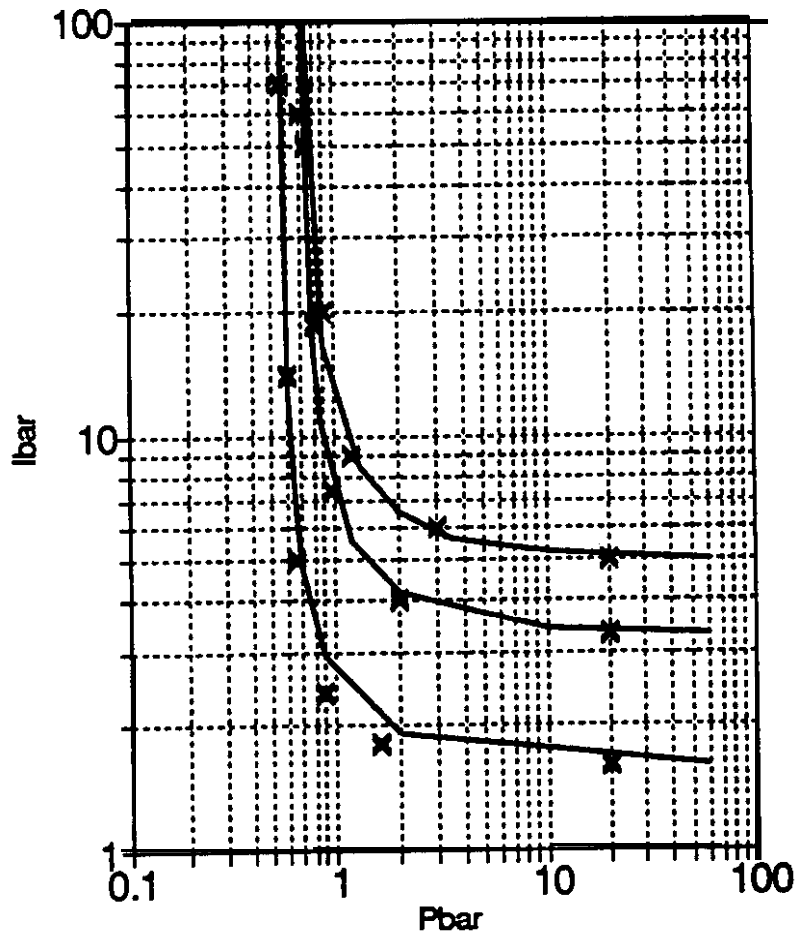


Figure 7. Comparison of Equation 4.3 to  $P_{bar}$  and  $I_{bar}$  Points for Steel Beams Generated with Single-Degree-of-Freedom Analyses

ductility ratio and the deflection to span ratio ( $w/l$ ), and the four damage levels considered in the **FACEDAP** program. This approach can involve some simplification of the actual factors **affecting** the dynamic response of building components to blast loading.

First, it is usually assumed that there is negligible dynamic interaction *between attached building components*. The theoretical P-i diagrams are based on the assumption of single-degree-of-freedom (**SDOF**) component motion. In cases where components are supported by rigid supports, this assumption is valid. However, building components often respond as **two** or three-degree-of-freedom dynamic systems which consist of primary components, such as **beams** and **columns**, and the secondary components they support, such as paneling. The load on the primary component is equal to the dynamic reaction force of the secondary component. The response of the secondary component, and therefore its reaction force, is dependent on support motion and thus on the response of the primary component. None of this interactive effect is considered in the P-i diagrams. Building members which make up a two or three-degree-of-freedom dynamic system can be analyzed accurately as separate systems if the natural periods of the attached components differ by at least a factor of two<sup>[15]</sup> **or if the parameters used in the  $\bar{p}$  and  $\bar{i}$  terms are chosen to account for the effects of dynamic interaction between attached components.**

The simple assumption usually made when using the FACEDAP program is that the blast load on primary members is equal to the blast pressure applied over the full area of the supported members and that the inertial resistance of primary members includes resistance provided by the total mass of all supported components. Secondary components are analyzed assuming negligible support motion. These assumptions **imply** that the secondary components respond very quickly compared to the primary members so that when the **primary member** responds, the full mass of the secondary component provides inertial resistance. It also implies that the secondary component has enough strength to transfer the full applied blast load without yielding. These assumptions do not need to be made, but no better guidance is currently available.

**Secondly, a P-i diagram can only be formulated in terms of one response term.** Traditionally, both ductility ratio and end support rotation have been used to estimate component damage with either one criteria or the other controlling damage (whichever is a worse case). Except where they are modified by the use of data points, the P-i diagrams in the FACEDAP program assume that the ductility ratio controls damage. This approach has been taken because almost all the  $\bar{p}$  and  $\bar{i}$  terms have been taken from Reference 12. where they were developed in a form compatible with a ductility ratio type response term. It would probably be better to reconsider this approach for components like reinforced concrete, which are usually designed in terms of allowable end support rotation””. This problem is also complicated by the fact that the most appropriate response parameter for some component types may be a function of the damage level for some components.

Based on the above list of qualifying assumptions, it is obvious that the theoretical approach has a somewhat **limited** applicability. The simplest way to consider the complicating factors **listed** above is to **first** generate a theoretical P-i diagram which is based on the major response mode (usually flexure) and the other assumptions listed above; plot “damage” points on these theoretical P-i diagrams with the  $\bar{p}$  and  $\bar{i}$  terms calculated from the blast loads and the component properties of the test data; label the damage points based on observed test damage; and **finally** move the theoretical damage regions so that they overlay the measured damage at the plotted “data points”.

In some cases the damage points **fall** within the theoretical damage regions and therefore “validate” the theoretical P-i diagrams. Since the number of data points is limited, the use of theory to get the general shape of the damage regions on the P-i diagram is necessary. The shift of the theoretical damage curves can account for errors in the manner in which two-degree-of-freedom response is simplified, for example, if it is taken from tests on actual buildings rather than tests on components in rigid test frames.

This approach was taken to develop the P-i diagrams of components for which damage data was available. These “shifts” of damage curves on the theoretical P-i diagrams are shown in the following paragraphs, with the data points, for components which have damage prediction equations based **on shifted theoretical curves**. During some of the shifts, some liberties have been taken with the basic theory discussed in the section explaining the theoretical development of P-i diagrams. P-i diagrams which were developed based on the assumption of **flexural** response have been shifted to match data from tests where tension membrane and compression membrane response are known to have occurred. These shifted curves should be treated with caution and used only for building components similar to those in the test data which was used to shift the curves **until** this problem can be corrected in a future project. In many cases, plots of damage data against the **theoretical** curves validate the theoretical curves. Where no damage data was available, the P-i diagrams were developed using the theoretical approach discussed above.

Broadly speaking, the twenty-four different components can be broken into six categories. The development of the P-i diagram for each component is discussed in the following section within these groups.

**Group 1A** ***Ductile one-way members including steel, reinforced concrete, and reinforced masonry one-way members*** - Exterior reinforced concrete and steel columns and reinforced masonry pilasters are included in this group because it is assumed that damage to exterior columns is controlled by **flexural** response rather than buckling. Steel beams and exterior columns which develop tensile membrane response are also included in this group.

**Group 1B** ***Ductile two-way members responding in flexure*** - **This** group includes reinforced concrete **and** reinforced masonry two-way members responding in flexure. Reinforced two-way components which can develop compression membrane response are considered separately in **Group 5**.

**Group 2** ***Brittle one-way members*** - This group includes **all** the **wood** components responding in flexure and one-way unreinforced masonry without arching.

**Group 3** ***Interior columns*** - This group includes **wood**, reinforced concrete, and steel interior **columns**. These components are assumed to be subjected to pure axial load.

**Group 4** *Steel and reinforced concrete frames*-This group includes the two frame components considered in the FACEDAP program. Damage **to all interior** and exterior columns and roof beams that make up the frames is controlled by the lateral sway of the frame.

**Group 5** *One-way and two-way masonry and reinforced concrete components with both arching, or compression membrane response, and flexural response.*

These six groups are discussed below. In this discussion, damage data points from tests where components were loaded with blast pressures are generally plotted by calculating the appropriate  $\bar{p}$  and  $\bar{i}$  values from the component properties and geometry reported in test data and reported blast load parameters. In some cases, the qualitative damage levels were directly reported by the experimenters. However, in most cases the **maximum** observed deflection was reported. In these cases, damage levels were determined by calculating the ductility ratio using the reported deflection and the component geometry and the criteria relating ductility ratio and damage level in Table 2 for the applicable component type.

The equations for  $\bar{P}$  and  $\bar{I}$  ( $\bar{p}$  and  $\bar{i}$ ) on the following figures are the same as those shown for the given component type in Chapter 4.1. The equations are not repeated **here since the** primary purpose of these figures is simply to compare the P-i diagram damage curves used in the FACEDAP program to damage data. Each component type is discussed regardless of whether damage data has been used to shift or validate the damage curves or whether no such data has been available. Some damage curves have been moved **from** their previous positions during this project as discussed below. In general, the location of the damage curves for each component type is an evolving process which considers new damage data when it becomes available and, in some cases, reconsideration of previous damage data

### **Group 1A - Ductile One-Way Members Responding in Flexure**

**Steel Beams** Separate P-i diagrams are given for steel beams responding in tension membrane response and responding solely in **flexural** response. Figure 8a shows the P-i diagram for steel beams responding in tension membrane response plotted against data which is almost solely from cold formed metal girts and **purlins** (from 4" to 9" in depth) on Butler-type prefabricated metal buildings subjected to relatively long duration blast loads (between 25 and 70 ms)<sup>[16]</sup>. The P-i diagram shown in this figure is basically the same diagram used in Reference 4. Figure 8b shows the P-i diagram for steel beams responding in flexure plotted against data which is **from** laboratory tests on determinate beams with roller **supports**<sup>[17]</sup>.

In Reference 16, where this data is reported, the authors **analyzed** one of the metal girts taking into account both **flexural** and tension membrane or **catenary** action of the girt and of the aluminum siding spanning between the foundation and the eave **strut**. The girts spanned horizontally between heavy moment resisting frames and the siding spanned vertically from floor (the sill angle) to the roof **frame** (the **eave strut**) since it was observed that the movement of the **girts** did not allow

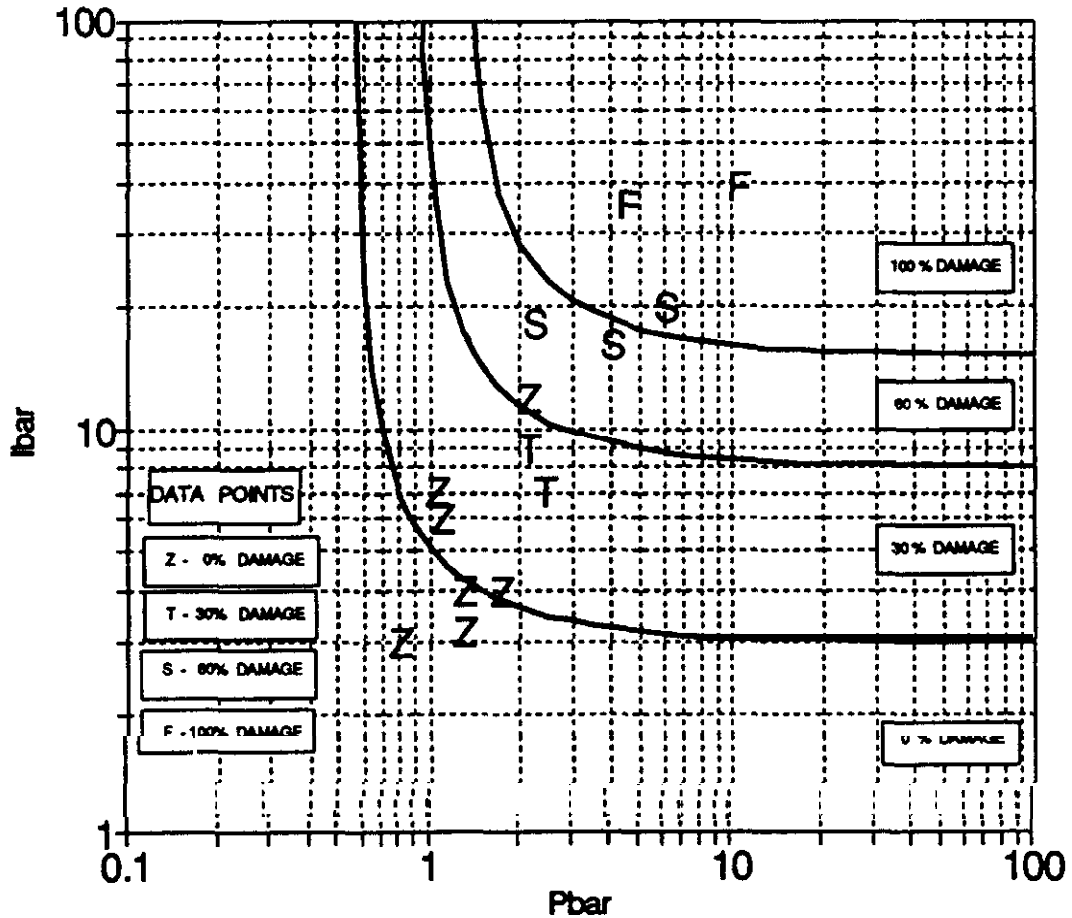


Figure 8a. Comparison of Damage Data from Steel Beams Responding in Tension Membrane with Damage Curves on P-i Diagram

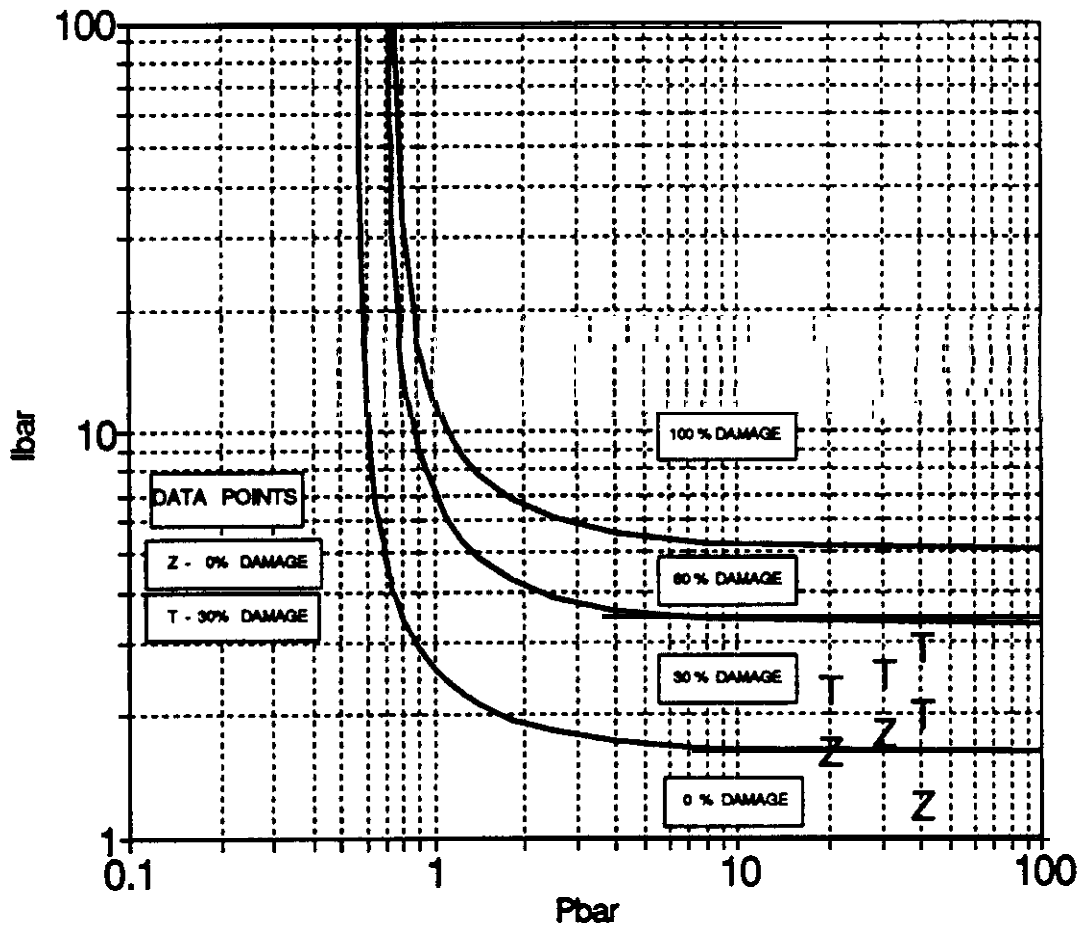
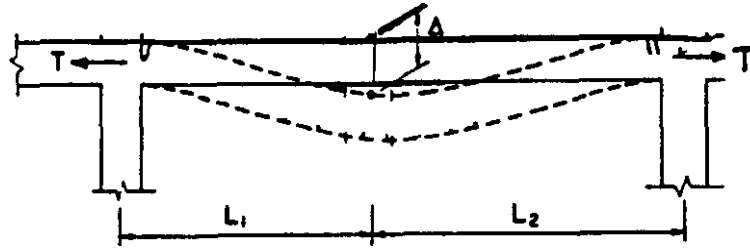


Figure 8b. Comparison of Damage Data from Steel Beams Responding in **Flexure** with Damage **Curves** on P-i Dim

them to act as supports for the siding. Figure 9 illustrates the concept of tensile membrane, or catenary response. Figure 10 shows the resistance-deflection curve for the girt calculated in Reference 16. This curve shows the response of the wall system in terms of each of its three major response modes. The **midspan** yield deflection of the girt in flexure is 2". Some allowance for connection slip, which affects tension membrane response, was made in the analysis. It is obvious that even at a ductility ratio of two (the lower bound criteria for 30% damage in Table 2), which corresponds to 4" of **midspan** deflection, considerable tension membrane response is occurring in addition to **flexural** response. The damage curves in Figure 8 were originally fit through some of the data shown in the figure. In this project more data points have been plotted which **confirm** the applicability of these curves for predicting blast damage to light, flexible steel beams which can develop tensile membrane response. Unfortunately, it is not clear whether these **curves** will predict combined **flexural/tension** membrane response well for heavy steel frame members within the range of ductility ratios that correspond to the steel beam damage categories in Table 2. A given ductility ratio corresponds to much less deflection in these stiffer types of members and therefore, in all likelihood, less tensile membrane response.

Tension membrane response requires the in-plane lateral support forces shown in Figure 9. In most buildings the symmetry of the blast load provides the necessary in-plane restraint to girts and **purlins** in all but the end bays. However, in some cases, particularly in cases where heavy steel framing components are considered, this restraint may not be available. Data which is applicable for these cases, where **only flexural** response occurs, is also available. Damage data from tests of small scale steel and aluminum beams where tensile membrane was precluded by the use of roller **supports** is plotted on Figure 8b<sup>(17)</sup>. The explosive loading was applied with sheet explosive and, since the experimenters assumed this would cause impulsive loading on the beams, no peak applied blast pressure was measured. Therefore, the data is plotted in terms of its  $\bar{i}$  value and it is assumed to have a large  $\bar{p}$  value. The data is plotted in terms of damage level, which is based on the reported **midspan** deflection, and the criteria relating ductility ratio to damage level for steel beams in Table 2. As Figure 8b shows, this data matches the theoretically predicted damage curves for a beam responding in flexure.

In summary, two sets of data are presented **with data points** from beams in tension membrane response and in **only flexural** response. The curves shown in Figures 8a and 8b are those incorporated into the FACEDAP code for steel beams with and without tension membrane response. The P-i diagrams for steel beams are relatively well validated for the case of light, flexible steel beams. It is not known if the P-i diagram which includes tension membrane response is applicable for steel members which differ significantly from this type of beam. The  $\bar{p}$  and  $\bar{i}$  terms on the P-i diagram are not formulated to take into account strain energy absorbed during tensile membrane response and, therefore, the implicit manner in which this strain energy is accounted for by shifting the theoretical damage curves may not apply to other types of steel beams in tensile membrane response. This factor, and the fact that it is less likely that larger steel framing components would have adequate lateral support restraint necessary to develop significant tensile membrane response, suggest that major steel framing components should probably be considered to have no tensile membrane response in this methodology. A recommended improvement of this methodology is to derive the  $\bar{p}$  and  $\bar{i}$  terms to explicitly consider tensile membrane response occurring during beam response to blast load and **replot** the data using the new terms. It is quite possible that the damage data will



$$T \cdot \Delta = \frac{W(L_1 + L_2)^2}{8}$$

$$T = \frac{W(L_1 + L_2)^2}{8\Delta}$$

- T = tensile restraint provided by **stiffness** of supports or symmetry of load
- w = applied load supported by tensile membrane **response**
- A = maximum deflection

Figure 9. Tension Membrane **Response**

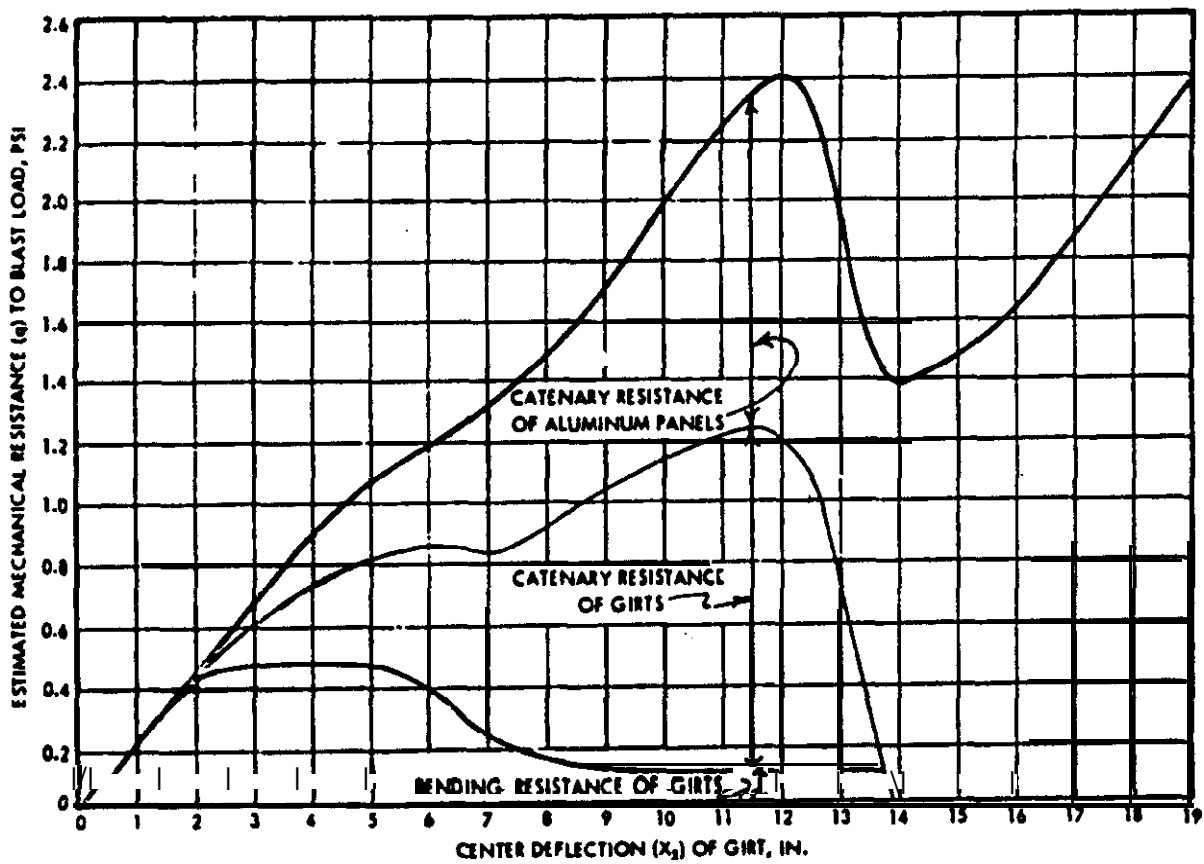


Figure 10. Deflection-Resistance Curve from Reference 16 for Steel Girt in Butler Building Subjected to Blast Load

validate the theoretical damage curves for this case and then these curves could be used with some confidence to predict damage to larger steel beams during tension membrane response due to their theoretical development.

**Steel Exterior Columns** - Exterior columns are assumed to be damaged primarily during **flexural** response to lateral blast load applied over the wall area supported by this component.. The columns also support some roof area so that they are also loaded axially. Unfortunately, the consideration of beam-column response is outside the scope of the current blast damage assessment methodology in the **FACEDAP** program. Therefore, damage must either be based on lateral loading or axial loading acting alone. Lateral loading is assumed to cause the greater damage for **two** reasons. First, lateral blast pressure on the wall area supported by the column is a reflected pressure in many cases whereas blast pressure on the roof is always less intense side-on pressure. Secondly, exterior columns are **typically** not sized to resist axial load or to resist lateral load only as part of a moment resisting frame. Therefore, they are not usually sized to resist significant lateral load as a vertical beam. When exterior columns are part of moment resisting frames, damage due to frame sway is calculated separately using the steel frame component type as discussed below.

Since this component is essentially a vertical beam, it is considered similar to **steel** beams. The parameters in the  $\bar{p}$  and  $\bar{i}$  terms in the P-i diagram for steel beams are equally applicable to a laterally loaded exterior steel column. Therefore, the same damage curves as those discussed above for steel beams are incorporated into the **FACEDAP** program for **this** component. It is recommended for now that tension membrane response should be assumed with caution for exterior steel columns since these components are **typically** large framing components. The reasons for this are discussed in the previous section on steel beams.

**Corrugated Steel Decking** - This component is presented next because, like the steel beams, there are a relatively large number of available damage data points. The data was generated from testing described in Reference 18. Three span continuous corrugated metal panels were attached to steel support beams spaced at 5 ft with puddle welds. The steel beams were attached to large, box-like test structures. Panels ranging from 16 gage to 20 gage, with rib heights from 4" to 1", and with both open and closed hat type cross sections were subjected to peak blast pressures between 0.3 psi to 15 psi. Damage data from the tests described in Reference 18 is plotted in Figure 11 along with theoretical damage curves based on elastic, perfectly-plastic **flexural** beam and the correlation between limit ductility ratios and damage levels for corrugated metal decking in Table 2. The plotted data points in Figure 11 show that the measured blast damage of corrugated metal panels is **well** predicted by the theoretical damage curves. Therefore, these damage curves have been incorporated into the **FACEDAP** code. This represents a significant change from the previous damage curves for corrugated steel deck, which were the same as those in Figure 8a.

The form of the  $\bar{p}$  and  $\bar{i}$  terms has also been changed slightly for this component type. The section modulus used in the  $\bar{p}$  and  $\bar{i}$  terms has been changed from the plastic section modulus to the elastic section modulus. This change was made partially for practical reasons, since the plastic section modulus of corrugated metal decking is rarely reported, and also because local buckling in the compression flange typically precludes substantial plasticity all the way through the **thickness**<sup>[10]</sup>. Such through-thickness plasticity is implied in the use of a plastic section modulus.

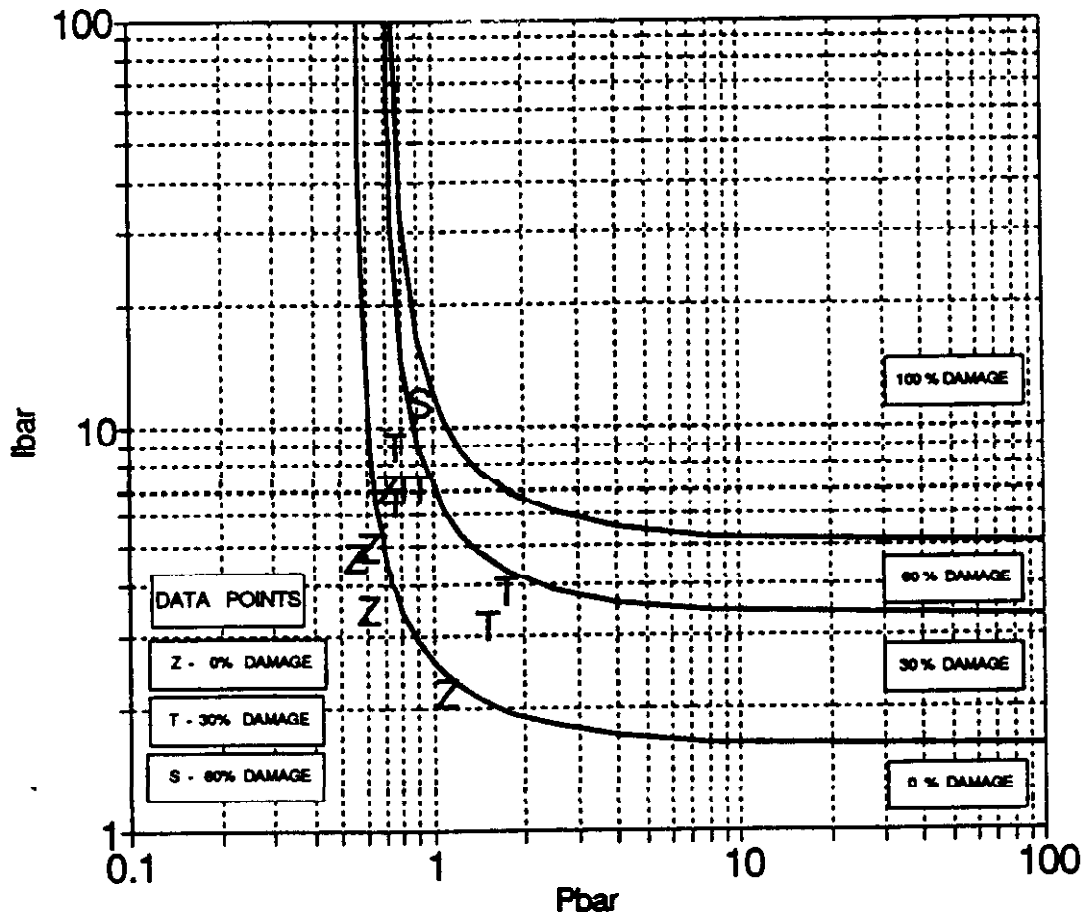


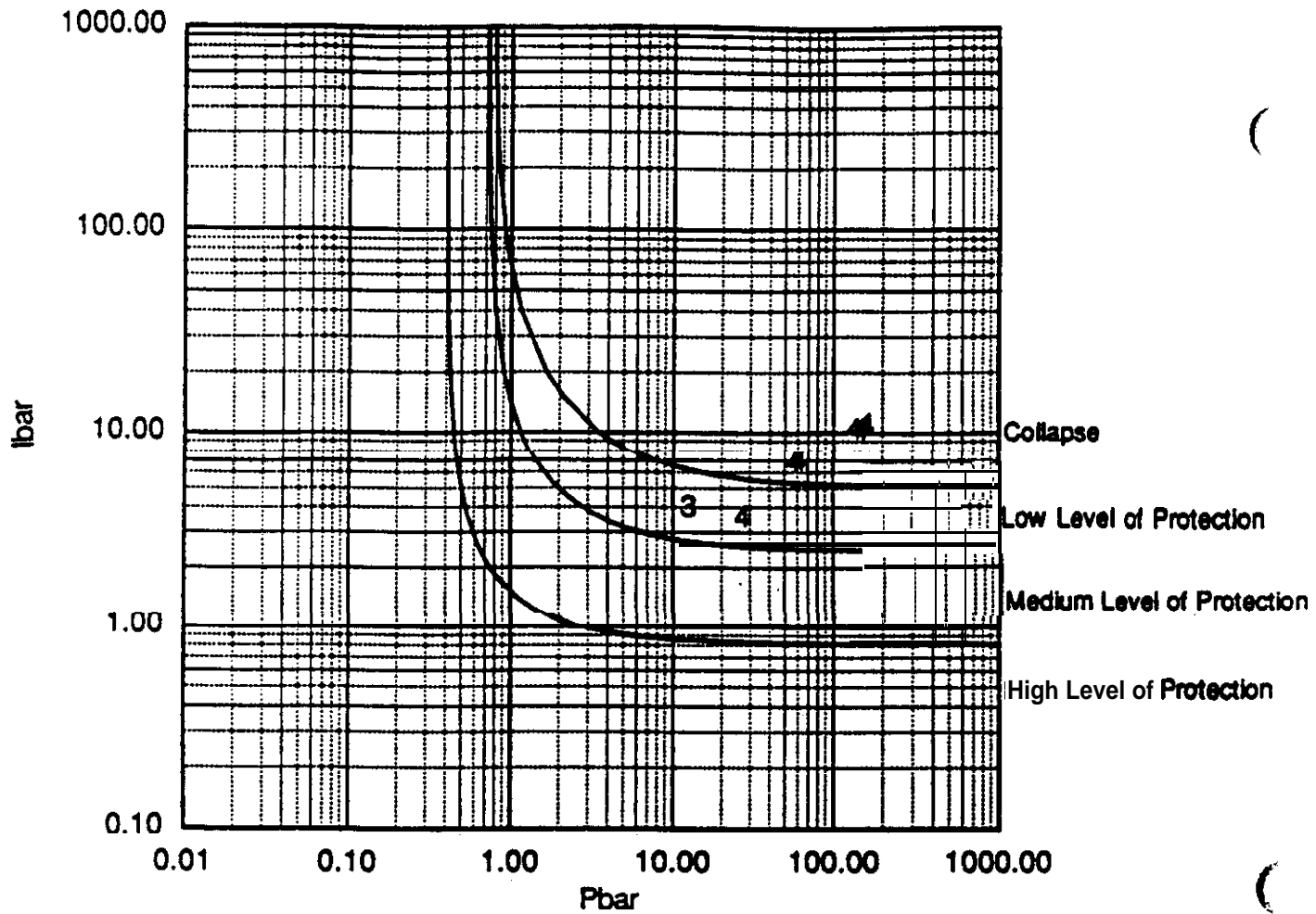
Figure 11. Comparison of Data from Blast Loaded Corrugated Metal Panels to Theoretical P-i Curve for Elastic Plastic Beams Responding in Flexure

**Metal Stud Walls** - The preexisting P-i diagram for this component type predicted damage based the damage curves shown in Figure 8a for steels beams responding in tensile membrane. Since studs are usually attached to **runners** which are **only** intermittently nailed and screwed **into** floor slabs and overhead beam, it is assumed that the typical supports for metal stud walls cannot provide the in-plane lateral restraint necessary for significant tensile membrane response to develop. The theoretical damage curves corresponding to pure **flexural** response are judged to be better predictors of blast damage than the previous curves which are based on data that included tensile membrane response **until** more blast damage data becomes available. The data discussed above for steel beams and corrugated metal deck indicates that the theoretical damage curves are reasonable for one-way steel members responding in flexure. Therefore, the new P-i diagram curves incorporated into the FACEDAP program are similar to those shown in Figure 11. The plastic section modulus in both the  $\bar{p}$  and  $\bar{i}$  terms has also **been** replaced with the elastic section modulus for reasons similar to those discussed above for corrugated metal deck.

**Open Web Steel Joists** - The preexisting P-i diagrams for *open* web steel joists required that the user calculate blast damage caused by both **flexural** response and buckling of the critical web member near the support. The P-i diagram for **flexural** response had pressure and impulse asymptotes which were between five and ten times greater than those of the theoretical damage curves. This was due to two assumptions used in the development of the previous curves. **First**, it was assumed that available data on blast damage to steel beams, which included tensile membrane response, was applicable to open web joists. Secondly, it was assumed that corrugated paneling over joists would sustain more blast damage from a given explosive threat than the joists. The latter assumption led to the especially large increase in the damage curve asymptotes compared to theoretical values since such an increase was necessary to cause calculated panel damage to exceed that calculated for joists in typical buildings. Both these assumptions are now considered nonconservative, especially considering the fact that there is no data to support them. This is reinforced by recent observations of blast damaged structures made by **SwRI** engineers, where it was not uncommon for joists to sustain more blast damage than the overlying panels. The joists are designed to resist the expected roof loads whereas the paneling is often sized according to a conservative minimum **thickness** and rib height requirements. The theoretical damage curves for open web steel joists responding in flexure with an elastic, perfectly-plastic yield criteria have now been incorporated into the FACEDAP program. Also, the second damage mode which was previously considered, web buckling, is no longer considered because open web joists are almost always sized for static design so that their capacity is controlled by **flexural** response.

**Reinforced Concrete One-Way Slabs** - Data is shown in Figure 12 from tests performed by the U.S. Navy on one-way reinforced concrete slabs. Six inch **thick** reinforced concrete slabs were loaded with peak blast pressures between 1 psi and 7 psi. In general, severe damage was observed. This data is plotted **in** Figure 12 with  $\bar{p}$  and  $\bar{i}$  values calculated **from** the slab properties and geometry and the measured blast load parameters. The data is described qualitatively as shown on the figure.

The data is plotted against theoretical damage curves for teams with an elastic, perfectly-plastic yield criteria responding in flexure at the limit ductility ratios for this component shown in Table 2 for the four damage levels. The high, medium, low, and “collapse” levels of protection shown in Figure 12 are roughly equivalent to the **0%, 30%, 60%** and 100% damage



Observed Damage Levels

3 - Severe Damage (large deformations. just prior to collapse)

4 - Failure (**structural collapse**)

Figure 12. **Comparison of Damage Data from Blast Loaded Reinforced Concrete Slabs to Theoretical P-i Diagram for Elastic Plastic Slabs Responding in Flexure**

levels. These damage curves are those **of the existing P-i** diagram for reinforced **concrete** one-way slabs. Figure 12 shows that the 100% damage level corresponds with the test data described as collapsed, or near collapse, and the 60% damage level corresponds with the **limited** test data described as severe. Since, the limited data seems to correspond well **with** the theoretical damage curves shown in Figure 12, these curves are used for reinforced concrete one-way slabs, and for other similar components described below, in the FACEDAP program. Since these are the preexisting damage curves developed during previous work for the Corp of Engineers, this does not represent any change.

**One-Way Reinforced Masonry Walls** - This component is considered identical to a one-way reinforced *concrete* slab since it resists applied load **in** the same manner. The parameters in the  $\bar{p}$  and  $\bar{i}$  terms in the P-i diagram for a one-way reinforced concrete slab are equally applicable to reinforced masonry walls except that **masonry** compressive strength is considered rather than concrete compressive strength. Therefore, the theoretical damage curves shown in Figure 12 for one-way reinforced concrete slabs are incorporated into the FACEDAP program for this component. This does not represent any change in the P-i diagram for this component.

**Reinforced** - This component is considered similar to one-way reinforced concrete slabs since it resists load in essentially the same way. **The** parameters in the  $\bar{p}$  and  $\bar{i}$  terms in the P-i diagram for one-way reinforced concrete slabs are equally applicable to reinforced concrete beams. Therefore, the theoretical damage curves for one-way reinforced concrete slabs are incorporated into the FACEDAP program for this component **This** does not represent any change in the P-i diagram for this component No dynamic interaction between slabs **supported** by reinforced concrete beams, such as that which would occur in a two-degree-of-freedom system, is explicitly considered in the P-i diagram. The usual assumption is to assume that the slab transfers the full blast load over the supported area into the beam and the mass of the slab over the full supported area adds to the inertial resistance of the **beam**.

**Reinforced Concrete Prestressed Beams** - The existing P-i diagram for this component was developed during the work described in Reference 4. **Prestressed** beams resist load in a similar manner as reinforced concrete beams and one-way reinforced concrete. beams, especially when the steel stress is near yield, or has yielded. No data for the response of prestressed beams or slabs to blast loading was located at the time the P-i diagrams were developed. However, based on the good comparison between theoretically developed damage curves and limited blast response data plotted in Figure 12 for conventionally reinforced concrete members, it is probable that the theoretical damage curves for prestressed concrete beams are also realistic. The parameters in the  $\bar{p}$  and  $\bar{i}$  terms in the P-i diagram for one-way reinforced concrete. slabs are applicable to prestressed concrete beams except that some of these parameters are calculated using the equations **for prestressed** beams in Reference 10. These formulas are shown in Section 4.1 in the P-i diagram for **prestressed** beams. With these modifications, the same theoretical damage curves discussed above for one-way reinforced concrete slabs are incorporated into the FACEDAP program for this component. This does not represent any change in the P-i diagram for this component.

**Reinforced Concrete Exterior Columns** - As discussed above for exterior steel columns, exterior columns are assumed to be damaged primarily during **flexural** response to lateral blast load applied over the wall area supported by **this** component. Since this component is **essentially** a vertical beam, it is considered similar to one-way reinforced concrete slabs and reinforced concrete beams. The parameters in the  $\bar{p}$  and  $\bar{i}$  terms in the P-i diagram for a one-way reinforced concrete slab and a reinforced concrete beam are equally applicable to a laterally loaded exterior reinforced concrete column. Therefore, the same theoretical damage curves discussed above for one-way reinforced concrete slabs and reinforced concrete beams are incorporated into the FACEDAP program for this component. This does not represent any change in the P-i diagram for this component.

**Masonry Pilasters** - Masonry pilasters are assumed to be reinforced in the same manner as reinforced concrete columns with the exception that the reinforcement is surrounded by grout and masonry brick or block rather than concrete. Pilasters are also assumed to be exterior building components. Therefore, they are assumed to be damaged **primarily** during **flexural** response to lateral blast loads applied over **the** supported wall area based on the same reasoning discussed above for exterior reinforced concrete columns. The parameters in **the**  $\bar{p}$  and  $\bar{i}$  terms in the P-i diagram for exterior reinforced concrete columns are also applicable to reinforced masonry pilasters except that masonry compressive strength is considered rather than concrete compressive strength. Therefore, the same theoretical damage curves as those discussed above for both exterior reinforced concrete columns and one-way reinforced concrete slabs are incorporated into the **FACEDAP** program for **this** component. This does not represent any change in the P-i diagram for this component. If a masonry pilaster is not located in a building wall, and only provides support to **the** roof, then it should be considered an interior reinforced concrete column **and the** P-i diagram for an interior reinforced concrete column should be used to calculate blast damage with masonry compressive strength substituted into the  $\bar{p}$  and  $\bar{i}$  terms for concrete compressive strength.

### **Group 1B - Ductile Two-Way Members Responding in Flexure**

**Reinforced Concrete Two-Way Slabs without Arching** - The P-i diagram for **this** component was developed during **the** project described in Reference 4. The  $\bar{p}$  and  $\bar{i}$  terms of the P-i diagram are taken from Reference 12. As shown in this reference, these terms are equal to **the** maximum shearing strain **in** the corner of a plate divided by the von Mises yield **strain** for **quasistatic and** impulsive loading, **respectively**. The  $\bar{p}$  and  $\bar{i}$  terms were calculated in **this** form because it is assumed in Reference 12 that a **full** plastic mechanism forms in a plate when the shearing strain in the corner equals the von Mises yield strain. This is somewhat different than **the more** typical assumption that a fully plastic mechanism forms in a ductile plate when bending strains have exceeded yield along all assumed yield lines in the plate<sup>[10,15]</sup>. No work has been done to look into what effects these different assumptions have on the P-i diagram for this component. The damage curves for this component are theoretical curves calculated for the limit **ductility** ratios in Table 2 for each damage category. The strain energy was calculated using an **ultimate** resistance calculated with yield line theory rather than **with** the approach used in Reference 12. Damage data from explosive **testing** was only available from tests where arching is assumed to have occurred when the P-i diagram for this component was developed. **These** data points are shown later in this section in Figure 19. A

comparison between the damage curves for reinforced concrete two-way slabs. with and without arching in **Section 4.1** shows that there is not much difference between them. No change has been made to the preexisting P-i diagram for this component.

**Reinforced Masonry Two Way Walls** - It is assumed that reinforced masonry and reinforced concrete resist lateral load in essentially the same manner. Also, the parameters in the  $\bar{p}$  and  $\bar{i}$  terms in the P-i diagram for two-way reinforced concrete slabs are equally applicable to reinforced masonry walls except that masonry compressive strength is considered rather than concrete compressive **strength**. Therefore, the same theoretical damage curves as those discussed above for two-way reinforced concrete slabs are incorporated into the FACEDAP program for this component This does not represent any change in the P-i diagram for this component.

## **Group 2 - Brittle Components Responding in Flexure**

**Wood Walls and Wood Roofs** - Figure 13 shows damage data from wood roofs and wood walls loaded with an applied blast load<sup>[19]</sup>. These tests, which applied long duration blast loads to simulate nuclear blast effects, were conducted on standard construction and “strengthened” two-story wood frame houses at the Nevada Test Site. The component type “wood **walls**” in the **FACEDAP program** refers to the composite section of the **wall stud** and exterior or interior sheathing which acts with the stud to resist lateral load. This requires that the sheathing is **well** nailed to the stud and that is continuous in along the **length** of the stud. One half the conventional 16” spacing between studs is considered as the effectivewidth of the sheathing for calculating sectional properties for the composite section. This is an approximate value based on the fact that this width is typically close to four **times** the stud width. The component type “wood roofs” includes both a typical roof joist and the effective width (usually **assumed** equal to one halfthejoist spacing) of plywood decking attached to the roof. In **the** tests shown in Figure 13, the inner plaster and lathe wallboard nailed to the wall stud were considered in the composite wall section. The walls also had tongue-in-groove type exterior sheathing which added to the mass of the walls, but was not included **in** the section properties because it was not continuous. The wood roofs included both the roof joist and the **3/8** inch plywood deck nailed to the joists.

The blast damage was reported in Reference 19 in terms of percent damage to each major component of the houses. This information was used to assign the damage categories shown in Figure 13. The full yield strength (modulus of rupture) of the wood was assumed to be 10,000 psi and Young’s modulus was assumed to be **1.4E6** psi per values reported in ASTM **D143** for small (**2"x2"**) fir and pine specimens at 12% moisture. Tests on small specimens generally overestimate the strength of a larger specimen, but high quality lumber was used and it is conservative to overestimate the wood yield strength when plotting damage data which will be used to fit the P-i diagram damage curves. The member sizes are assumed to be **1/4** inch less than the nominal sixes called out in the drawings in Reference 19 based on standard **sizing** used at the **time** of the tests.

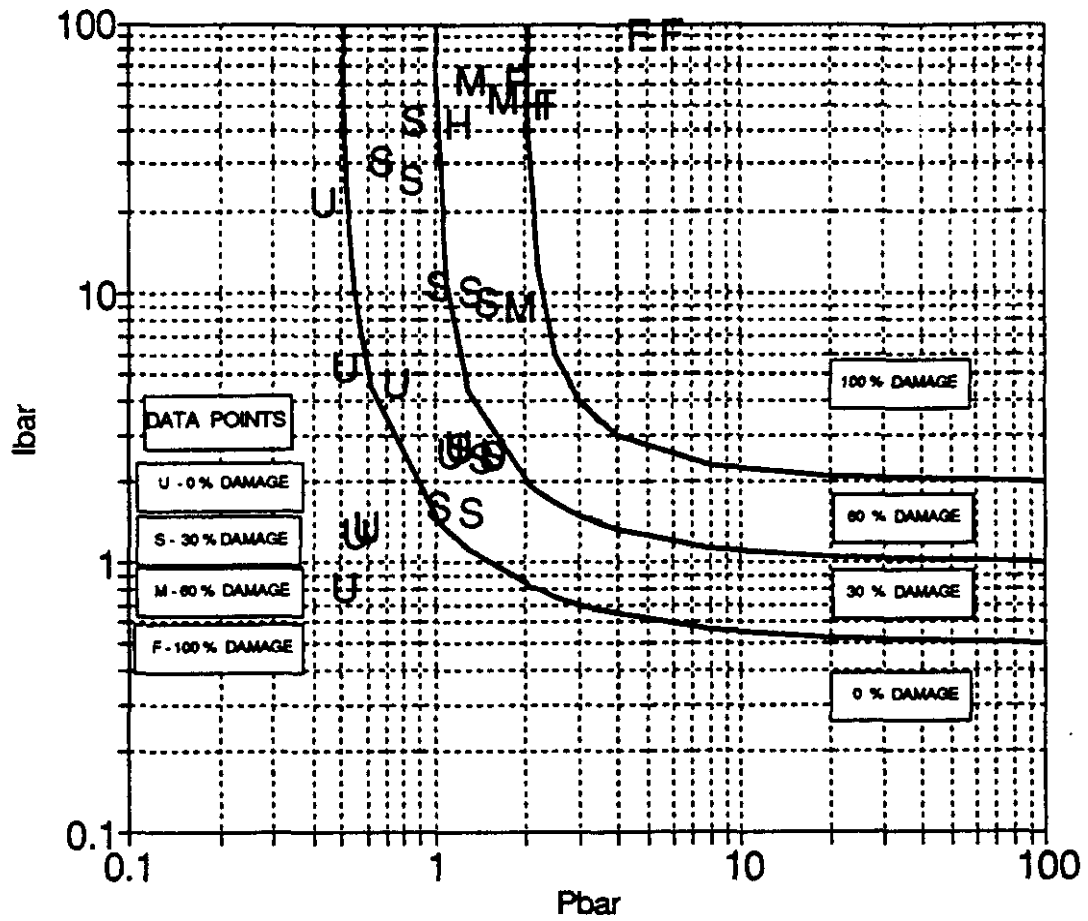


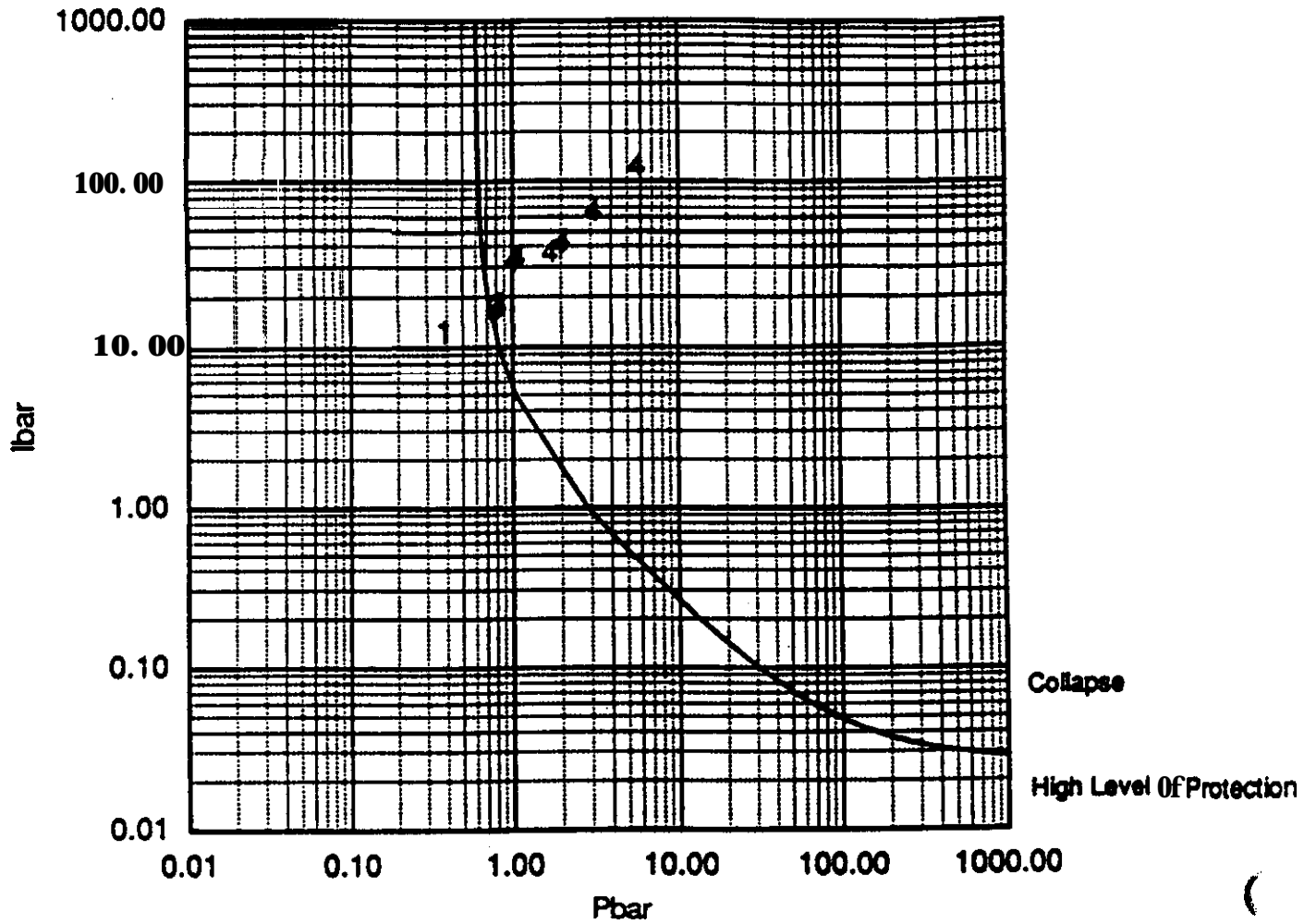
Figure 13. Comparison of **Damage** Data from Blast Loaded Wood Houses to P-i Diagrams for Wood Components Responding in **Flexure**

Damage categories are fit based on the data and based on the fact that **theoretically** the  $\bar{p}$  and  $\bar{i}$  terms for a given ductility ratio are equal. The latter fact is based on the development of the  $\bar{p}$  and  $\bar{i}$  terms. The preexisting  $\bar{p}$  and  $\bar{i}$  terms for all wood components responding in **flexure** were equal to those shown in Figure 5. These have been divided by the static yield strain to get the current  $\bar{p}$  and  $\bar{i}$  terms. This change was made in order to normalize the data used to generate the P-i diagrams so that it will be representative for wood with different yield strains. A  $\bar{p}$  and  $\bar{i}$  value of 1.0 represents dynamic strain equal to the static yield strain. The plotted data indicate that the dynamic strain at 100% damage is approximately twice the static yield strain. This may be reflecting a dynamic increase factor in the yield strain and more support restraint than that provided by the simple support conditions which were assumed. The damage curves shown in Figure 13, and the new  $\bar{p}$  and  $\bar{i}$  terms, **are** incorporated into the FACEDAP program. These damage curves are significantly different from the previous curves in that: 1) they predict more damage based on a more conservative interpretation of the test data from Reference 19; 2) they have new  $\bar{p}$  and  $\bar{i}$  terms as discussed above; and 3) wood walls and wood roofs have identical damage curves. Previously this was not the case.

**Wood Beams** - This component is considered to be similar to wood walls and wood roofs since it is constructed in a similar manner and it resists load in essentially the same manner. The parameters in the  $\bar{p}$  and  $\bar{i}$  terms in the P-i diagram for wood walls and roofs are also applicable to wood beams. Usually the component type wood beams is used for a framing member which supports joists. Therefore, the sectional properties for wood beams that are used in the  $\bar{p}$  and  $\bar{i}$  terms do not usually include the area of any attached sheathing or decking. The same damage curves discussed above for wood walls and roofs are incorporated into the FACEDAP program for this component. This is a change in the P-i diagram for this component because, previously, damage was predicted with a simple fail/no fail criteria based on the preexisting 100% damage curves for wood walls and wood roofs.

**Exterior Wood Columns** - As explained above for exterior steel columns, exterior columns in this blast damage assessment procedure are assumed to be damaged primarily during **flexural** response to blast pressure acting on the **wall** area supported laterally by the column. Based on this assumption, this component is similar to wood walls and wood roofs since it is essentially a vertical beam. The parameters in the  $\bar{p}$  and  $\bar{i}$  terms in the P-i diagram for wood walls and roofs are also applicable to exterior wood columns. Usually any composite action with attached wall sheathing is ignored because, unlike a wall stud or roof joist, the larger column cross sectional properties are not significantly increased by the effects of attached sheathing. **The** same damage curves discussed above for wood walls and roofs are incorporated into the **FACEDAP** program for this component. This is a change in the P-i diagram for this component because, previously, damage was predicted with a simple fail/no fail criteria based on the preexisting 100% damage curves for wood walls and wood roofs.

**One-Way Unreinforced Masonry (No Arching)** - The previous P-i diagram for this component was developed during work summarized in Reference 4. This diagram, which assumes one-way **flexural** response, has only a fail/no fail damage curve as would be expected for a brittle component with very little strength. It would be expected that this damage curve should correspond to a ductility ratio of 1.0 which occurs when the peak dynamic **flexural** stress is equal to the tensile



**Observed Damage Levels**

- 1 • Minimal Damage (little or no cracking)
- 2 • Moderate Damage (major cracking)
- 3 • Severe Damage (large deformations, just prior to collapse)
- 4 • Failure (structural collapse)

**Figure 14. Comparison of Damage Data from Blast Loaded One-Way Unreinforced Masonry Walls Responding in Flexure to Previous P-i Diagram for Component**

strength of the bond between the mortar **and masonry** block. The pressure asymptote in the preexisting P-i diagram is consistent with this expectation but the impulse asymptote was only one-fourth the expected value. Figure 14 shows data collected from blast loaded masonry **walls**. Since there are no data to support the low value of the impulse asymptote, this asymptote has been increased to the theoretical value corresponding to a ductility ratio of 1.0 in the FACEDAP program. The previous pressure asymptote has not been changed since the data in Figure 14 indicate that it predicts measured blast damage well.

### Group 3 - Interior Columns

**Wood, Steel, and Reinforced Concrete Interior Columns** - The P-i diagrams used for calculating blast damage to these components in the FACEDAP program are unchanged from those originally developed in the initial work for NCEL<sup>(3)</sup>. The P-i diagrams for these three component types, which are essentially identical, were taken from Reference 12. A single fail/no fail damage curve (0% **damage/100%** damage ) is shown for these components. In Reference 12, the derivation of the  $\bar{p}$  and  $\bar{i}$  terms is presented. It shows that the  $\bar{p}$  term at the pressure asymptote is **equal** to the classic Euler buckling formula for unstable buckling. Therefore, the dynamic failure load predicted by the damage curve for a long duration blast wave is equal to that which would be predicted with a static analysis based on the peak applied blast pressure applied over the full area supported by the column. The  $\bar{i}$  term is a stable buckling term. It is calculated using Equation 4.1 where kinetic energy which occurs during axial shortening is set equal to strain energy absorbed in flexure. Axial shortening is assumed to cause corresponding lateral deflection of the column, in a sine wave shape between inflection points, because of some slight eccentricity in the applied axial load. **The** impulse asymptote of the fail/no fail curve **in** the P-i diagram corresponds to yield of the outer **fiber** of the column in the maximum moment region. Thus, the impulsive asymptote is conservative for ductile members such as reinforced concrete and steel columns.

### Group 4 - **Frames**

**Steel and Reinforced Concrete Frames** - **The** P-i diagrams used for calculating blast damage to frame components in the FACEDAP program are also unchanged from those originally developed in the initial work for **NCEL**. The P-i diagrams for these two component types, which are essentially identical, were developed in Reference 3. This development, which is heavily based on design criteria for steel frames in Reference 10, is shown **in** the Appendix of Reference 3. The  $\bar{p}$  and  $\bar{i}$  terms were determined by setting up the energy balance described in Equations 4.1 and 4.2 and algebraically manipulating the terms until one side of the equation was only a function of the ductility ratio. The stiffness and **ultimate** resistance **required** in the strain energy term in the energy balance equations are generally complex terms. In order to simplify these terms, and therefore simplify the  $\bar{p}$  and  $\bar{i}$  terms, the following assumptions were made: 1) the columns in the **frame** were weaker than the beams and, therefore, yield of the columns controls the frame ultimate resistance; 2) the base of each frame column is a pinned connection; 3) the span to height ratio in each story of the frame is **approximately 1.0**; 4) elastic **strain** energy **absorbed** by the **frame** prior to yield is negligible compared to the strain energy absorbed after yield; and, 5) the incident pressure acting on the back side of the frame (away from the charge) could be conservatively ignored. Theoretical damage curves were initially calculated based on the ductility ratios shown for frames in Table 2. Based on limited data for steel frames in light Butler buildings subjected to blast loading, the theoretical

curves were shifted upwards, so as to predict less damage for a given value of  $\bar{p}$  and  $\bar{i}$ , by about 40%. This shift may not have been necessary if assumption No. 5 listed *above was not made since* the incident pressure acting on the far side of the frame, away from **the** explosive charge, reduces the response and blast damage compared to that which would otherwise be calculated.

Figure 15 shows additional data points plotted for steel frames in light Butler buildings subjected to peak blast pressures between 20 psi and 2 psi. These data are **reported** in References 16, 20, and 21. The damage is plotted in terms of the reported frame sway deflection, which is converted to a ductility ratio and assigned a damage level based on the criteria for frames in Table 2. The data points marked F and Z are approximate since it is not known how much reflected blast pressure the asbestos siding on the buildings transmitted into the **frame** prior to its failure. Based on the observations reported in the references, the siding failed very quickly (within 6-10 milliseconds).

The plotted data in Figure 15 assume that no reflected **blast** pressure was transmitted into the frames, as is hypothesized in References 20 and 21, and only the dynamic blast pressure **acting** over the presented area of the frame is used as the load when calculating the  $\bar{p}$  and  $\bar{i}$  values for these two data points. It is quite possible that the **actual  $\bar{p}$  and  $\bar{i}$**  values for these two points are larger than those shown in Figure 15 but it is nearly impossible to estimate the applied load with any certainty. In any event, the plotted points generally support the previous damage curves and, therefore, they have not been changed in the FACEDAP program.

There is one **modification** to the approach used previously to calculate total damage to frame components. **Previously**, damage to beams and **columns** in **frames** was equal to the sum of the damage levels, expressed as a fraction rather than as a percentage, calculated for the components responding in flexure or in pure axial response between their supports and the frame as a whole. This has been **modified** during this project so that both types of damage are still considered for each frame component, but they are considered separately. The building damage is calculated first, assuming all components in the **frame** respond as individual **beams**, exterior **columns**, etc. and then it is recalculated without considering any of the frame components individually and considering the entire frame as a single component. The more severe calculated building damage controls. This change was based on the reasoning that **frame** damage and **flexural** response damage to individual frame members do not typically add. This assumption is based on the following reasoning. First, it is assumed that frame damage occurs primarily to frame columns and, therefore, any addition of the two response modes would **occur** in the columns. However, for the exterior columns, frame sway implies that the top of the frame moves significantly compared to the base and, therefore, the top is not acting as the rigid support necessary to develop **significant flexural** response. For interior **columns**, **frame** sway may increase the tendency for column buckling, depending on when the **frame** sway occurs in time relative to the peak axial force in the column. Beam-column response, though, is not considered in the component damage calculation procedure in the FACEDAP program. Therefore, damage is assumed to be caused by the worse case of frame damage and **flexural/buckling** damage to frame components responding as individual members.

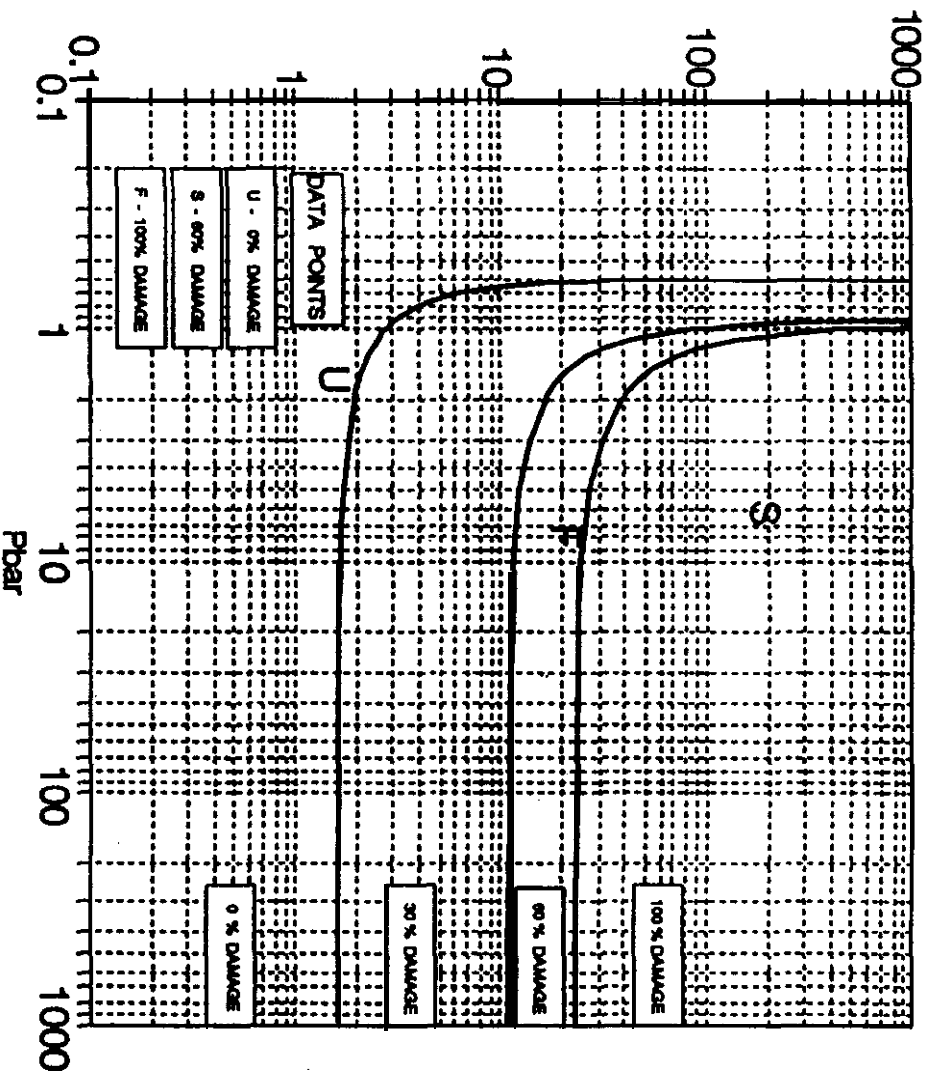


Figure 15. Comparison of Damage Data from Blast Loaded Steel Steel Frames to P-i Diagram for Steel Frames

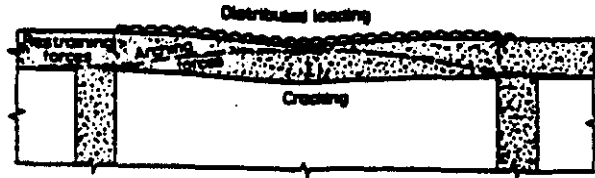
## Group 5 - Masonry and Concrete Components with Arching

The components in this group are: 1) Two-Way Unreinforced Masonry Walls, 2) One-Way Unreinforced Masonry Walls with Arching, and 3) Two-Way Reinforced Concrete Walls with Arching. The existing P-i diagrams for these three component types were developed during the project described in Reference 4. **The** damage curves on the P-i diagrams for these components are intended to account for the effects of compressive membrane response, which is known to increase the strength and therefore reduce the damage of reinforced concrete and masonry components. Compressive membrane response, which is illustrated in Figure 16 and discussed in **detail** in Reference 22, will occur if all outward lateral movement is prevented at the supports of concrete and masonry components.

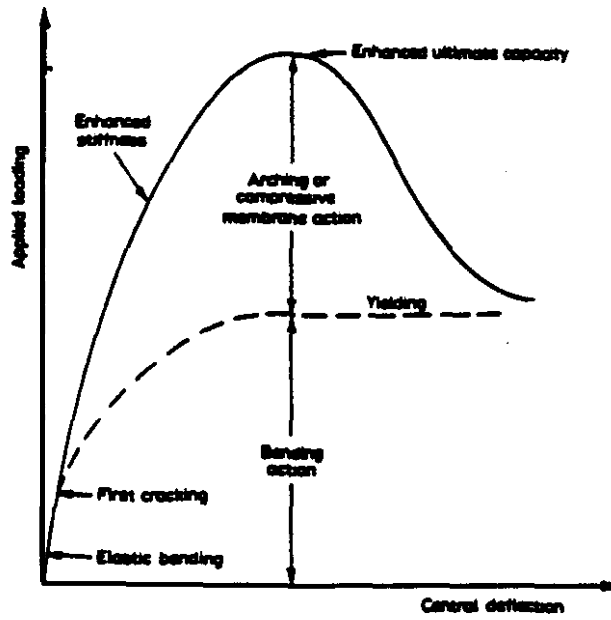
The  $\bar{i}$  and  $\bar{p}$  terms in the P-i diagrams of the components in this group are taken from Reference 12, where they were developed **using** strain energy expressions which only considered flexural response. Therefore, the P-i diagrams do not inherently account for **compression** membrane response. The approach taken was to try to place damage curves on the P-i **diagrams** at a location **where** these curves will represent the damage occurring during compression membrane response, the methodology explained next.

Equations 4.1 and 4.2 were used to set up energy balances in the quasistatic and **impulsive** loading realms **which** included strain energy absorbed **during compression membrane response**. This strain energy was calculated for reinforced concrete components using criteria in **Reference** 22. It was calculated for unreinforced masonry components assuming a roughly hiangular shaped **resistance function which peaks at a very small deflection (approximately 0.001 times the thickness)**. Then, these equations were solved so that an input peak pressure and impulse **would cause** dynamic **response** which had a **ductility** ratio equal to limit values at the four damage levels shown in Table 2 for the components. A typical set of component **properties** and component **geometry** terms were used in the equations. Next,  $\bar{p}$  and  $\bar{i}$  values were calculated for each limit ductility ratio using the component properties and **geometry** and blast load parameters used in each equation to cause the given ductility ratio. These  $\bar{p}$  and  $\bar{i}$  values were then plotted as the asymptotes for the damage levels.

The general problem **in this** approach **is** that the strain energy term used in the above approach is relevant for compressive membrane response whereas **the**  $\bar{p}$  and  $\bar{i}$  terms, which are calculated based on the two equations which include the compression membrane strain energy term, only include terms related to **flexural** response. **There** is considerable overlap between the material and **geometrical properties** which affect compression **membrane** response and **flexural** response, but they are not identical. This leads to the problem, for example, where the  $\bar{i}$  value used as a new asymptote for the damage curves which account for compression membrane response is influenced by the bending stiffness (**EI**), whereas the **strain energy** absorbed in compression membrane response is not directly affected by bending stiffness. If a set of component **properties** with a high bending stiffness is assumed in the above approach, the impulse asymptote may be much less than it would be if a set of component properties with a low bending **stiffness** was assumed even though the ability of both sets of component properties to resist impulsive loading in compression membrane response may be nearly equal. The solution to **this** potential problem, which is thought to be worse for the impulsive asymptotes, is to use the energy balance expression which includes the compressive



*Compressive membrane action in laterally restrained slab*



*Qualitative illustration of enhanced behaviour of a laterally restrained slab*

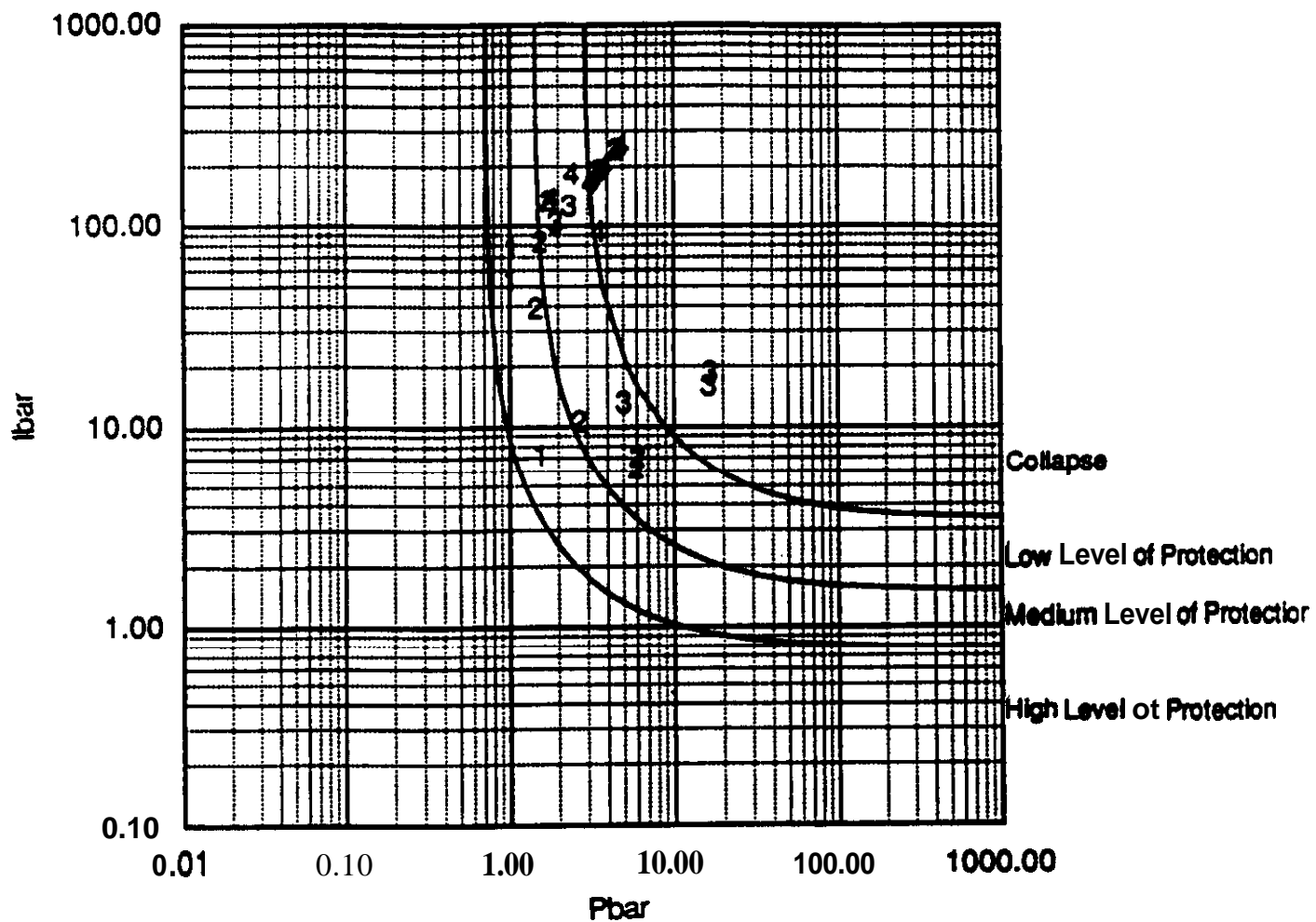
**Figure 16. Compression Membrane Response**

membrane strain energy term to generate  $\bar{n}$  and  $\bar{p}$  terms. When this approach is taken, the  $\bar{n}$  and  $\bar{p}$  terms will include terms properly accounting for the influence of compression membrane on component response. Situations where the tensile strength of unreinforced masonry, which affects its flexural response, is an input into a P-i diagram which determines blast damage when the masonry is responding in compression membrane response will also be avoided.

One-Way Unreinforced Masonry Components with Arching - Figure 17 shows the existing P-i diagram for this component plotted with data points from blast tests on unreinforced one-way masonry walls in rigid test frames<sup>[23,24]</sup>. The frame rigidity is assumed to have allowed compression membrane response to occur. The testing was performed on 10 inch thick walls loaded with short duration blast loads with peak pressures between 15 psi and 120 psi. Damage was qualitatively described as shown on the figure. The measured maximum deflections ranged between 0.5 inch and 4 inches. The damage curves on the diagram are those obtained using the procedure described above. The high, medium, low, and "collapse" levels of protection shown in Figure 17 are roughly equivalent to the 0%, 30%, 60% and 100% damage levels. Figure 17 shows that the data fits relatively well in the pressure sensitive region, near the top of the graph, assuming that the four qualitative damage descriptions are roughly equivalent to the four damage levels. The fit is not quite as good in the dynamic region. The damage curves shown in Figure 17 are those included in the FACEDAP program.

Two-Way Unreinforced Masonry Components - Figure 18 shows the existing P-i diagram for this component plotted with data points from blast tests on unreinforced two-way masonry walls in rigid test frames<sup>[23]</sup>. The testing was performed on 8 inch thick walls loaded with relatively long duration blast loads with peak pressures between 3 psi and 15 psi. Damage was Qualitatively described as shown on the figure. The damage curves on the diagram are those obtained using the procedure described above. It is important to note that although the component type name does not specifically mention arching, arching is always assumed for this component in the FACEDAP program based on the high likelihood that a typical two-way unreinforced masonry wall will be framed by an overhead beam and columns either side which provide the necessary lateral confinement. The high, medium, low, and "collapse" levels of protection shown in Figure 18 are roughly equivalent to the 0%, 30%, 60% and 100% damage levels. Figure 18 shows that the data fit relatively well in the pressure sensitive region, near the top of the graph, assuming that the four qualitative damage descriptions are roughly equivalent to the four damage levels. No data were available for the dynamic or impulsive regions of the diagram. The damage curves shown in Figure 18 are those included in the FACEDAP program.

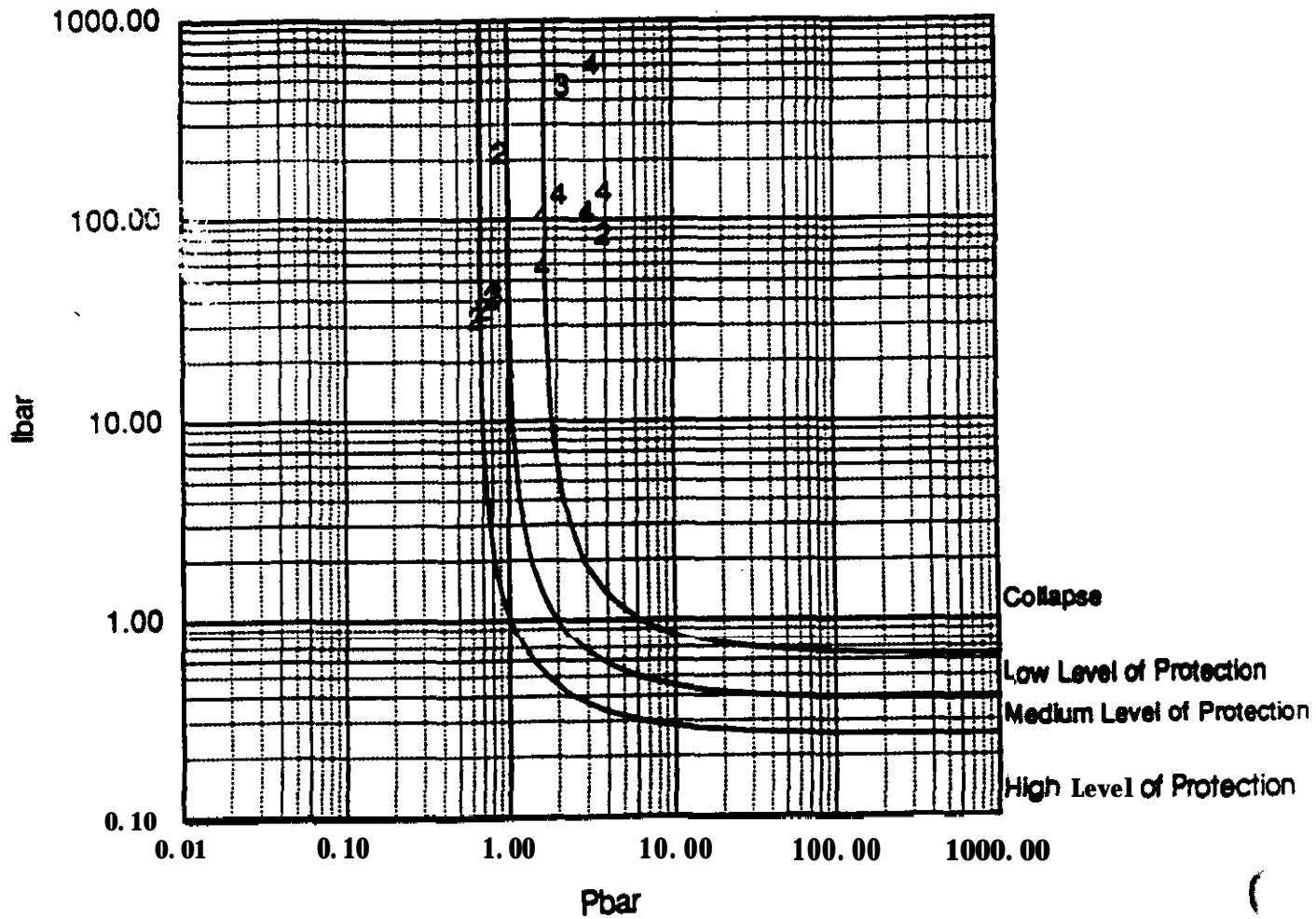
Two-Way Reinforced Concrete Components - Figure 19 shows the existing P-i diagram for this component plotted with data points from blast tests on reinforced concrete two-way walls in rigid test frames<sup>[25]</sup>. The testing was performed on 3 to 6 inch thick walls loaded with relatively long duration blast loads with peak pressures between 3 psi and 100 psi. Damage was qualitatively described as shown on the figure. The damage curves on the diagram are those obtained using the procedure described above. The high, medium, low, and "collapse" levels of protection on Figure 19 are roughly equivalent to the 0%, 30%, 60% and 100% damage levels. This figure shows that the data fit the damage curves well assuming that the four qualitative damage descriptions are roughly equivalent to the four damage levels. The damage curves shown in Figure 19 are those



Observed Damage Levels

- 1 • Minimal Damage (little or no cracking)
- 2 • Moderate Damage (major cracking)
- 3 • Severe Damage (large deformations, just prior to collapse)
- 4 • Failure (**structural** collapse)

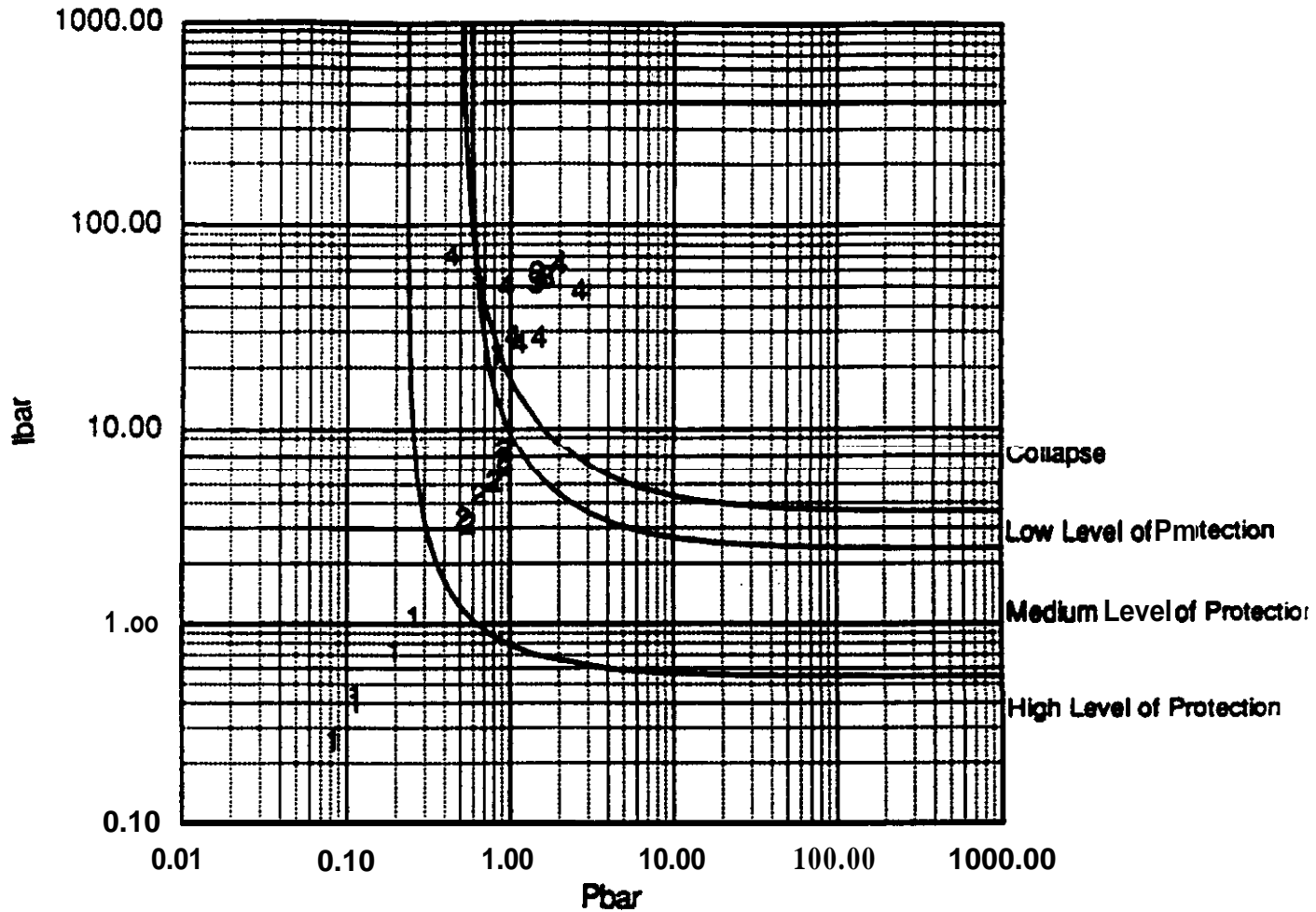
Figure 17. Comparison of Damage Data from Blast Loaded Unreinforced One-Way Masonry Walls with Arching to the P-i Diagram for **This** Component



Observed Damage Levels

- 1 - Minimal Damage (little or no cracking)
- 2 - Moderate Damage (major cracking)
- 3 - **Severe** Damage (large **deformations**, just prior to collapse)
- 4 - Failure (structural collapse)

Figure 18. Comparison of Damage Data from Blast Loaded Unreinforced **Two-Way** Masonry Walls with Arching to the P-i Diagram for **This Component**



**Observed Damage Levels**

- 1 - **Minimal** Damage (little or no cracking)
- 2 - **Moderate** Damage (major cracking)
- 3 - **Severe** Damage (large deformations, just prior to collapse)
- 4 - **Failure** (**structural** collapse)

Figure 19. 'Comparison of Damage Data from **Blast Loaded** Reinforced Concrete Two-Way Masonry Slabs **with** Arching to the P-i Diagram for This Component

included in the FACEDAP program. It is interesting that this P-i diagram is almost identical to the P-i diagram in Section 4.1 for two-way reinforced concrete without arching.

## 5.0 COMPONENT DEPENDENCIES

After all component damage has been determined on a component-by-component basis using the P-i diagrams described previously, secondary component damage is considered based on component “dependencies”. The “dependencies” of each component are the list of other components which support the given component. Some components are only supporting components, and therefore have no dependencies. The dependencies are **used** in the blast damage assessment procedure in the **FACEDAP program** only **if one** of the supporting components sustains 100% blast damage and the calculated damage of the supported component is less than 100% damage. In this case, **the** procedure increases the damage level of **the** supported component to **100%** damage. This is based on the reasoning that 100% damage of the supporting component precludes it from providing the assumed support and this causes the supported component damage to also sustain 100% damage. This type of secondary failure is also referred to as “cascading” failure. Since, the supporting components are typically designed to be at least as strong (compared to their loaded area and span) as the supported components, the dependencies are usually never used. A notable exception to **this** general rule is the case of corrugated metal decking over closely spaced open web steel joists. The decking is often **strong** for its short span compared to the open web steel joists.

### 5.1 Non-Frame Component Dependencies

Tables 3 and 4 describe the rules used by the Preprocessor to generate dependencies. In **these** tables, the supported component is called the Dependent Component and the supporting components are called the Independent Components. These tables show how the twenty-four components are divided into five groups, called “dependency types”. A dependency is calculated if one out of eight different dependency rules called out in the tables is satisfied. These rules allow dependencies based on: 1) the dependency type of **the** dependent component, 2) the dependency type of the independent component, 3) the location of the dependent and independent components (in a building wall or roof), and 4) matching endpoints, or midpoints, of the independent and dependent components. “Matching” means that **the** points are not more than 1 ft from each other. This tolerance distance was chosen since it would be very unusual for the input endpoints of any components in a typical building which do not **connect** with each other to be within 1 ft. In some cases there are two candidate independent components which satisfy one of the eight rules. In this case, priority is given to the Dependency Type 3 component

In addition to the “**primary**” dependencies described in the preceding tables, “secondary” component dependencies are also calculated. An example of a secondary dependency is a case where Component A is dependent, or supported by Component B and Component B is dependent on Component C, A secondary dependency exists between Component A and Component C which is calculated automatically by the FACEDAP program. A potential problem with the automatic procedure in the FACEDAP program is that a wall component (Component A) can be laterally supported against blast loading by a roof component (Component B) which is supported vertically on a component in the opposite wall (Component **C**). The secondary dependency for this case is

Table 3. Rules Used in FACEDAP Program to Calculate Component Dependencies\*

Dependent Component Type	Maximum Possible Number of Independent Components	Independent Component Type	Location of Dependent and Independent Components				
			Location Case 1	Location Case 2	Location Case 3	Location Case 4	Location Case 5
1	2	1	n/a	n/a	n/a	<b>1</b>	n/a
		2	n/a	n/a	n/a	<b>4</b>	n/a
		3	<b>9</b>	n/a	<b>9</b>	<b>9</b>	<b>9</b>
		4	<b>9</b>	<b>9</b>	n/a	n/a	n/a
		5	n/a	n/a	n/a	n/a	n/a
2	4	1	n/a	n/a	n/a	<b>4</b>	n/a
		2	n/a	n/a	n/a	<b>3</b>	n/a
		3	<b>5</b>	n/a	<b>5</b>	<b>5</b>	<b>5</b>
		4	<b>5</b>	<b>5</b>	n/a	n/a	n/a
		5	<b>7</b>	n/a	n/a	n/a	n/a
3	2	1	n/a	n/a	n/a	<b>1</b>	n/a
		2	n/a	n/a	n/a	<b>2</b>	n/a
		3	<b>8</b>	n/a	n/a	<b>8</b>	<b>8</b>
		4	<b>9</b>	<b>9</b>	n/a	<b>1</b>	n/a
		5	<b>6</b>	n/a	n/a	n/a	<b>6</b>

\*Bolded numbers in table represent different rules explained on next page.

**Location Case**

**Description**

- 1 Both dependent and independent components in same wall a roof area.
- 2 Dependent and independent components in adjacent wall areas.
- 3 Dependent component in a wall area and independent component in an adjacent roof area.
- 4 Dependent component in a roof area and independent component in an adjacent wall area.
- 5 Dependent and independent components in adjacent roof areas.

Table 4. List Showing the "Dependency Type" of Each Component

Component	Dependency Type
Concrete Reinforced Beam	3
One-Way Reinforced Concrete Slab	1
Two-Way Reinforced Concrete Slab	2
Exterior Reinforced <b>Concrete</b> Column	4
Interior Reinforced Concrete Column	5
<b>Prestressed Concrete Beam</b>	3
<b>Steel Beam</b>	
Metal Stud Wall	1
<b>Open Web Steel Joists</b>	3
<b>Steel Corrugated Decking</b>	1
Exterior Steel Column	4
Interior Steel Column	5
One-Way Unreinforced Masonry Wall	1
Two-Way Unreinforced Masonry Wall	2
One-Way Reinforced Masonry Wall	1
Two-Way Reinforced Masonry Wall	2
Masonry Pilasters	4
Wood Wall	1
Wood Roof	1
Wood Beam	3
Exterior Wood Column	4
Interior Wood Column	5

Role Number	Description
1	An endpoint of dependent component must match an endpoint of independent component.
2	An endpoint of dependent component must lie along one side of a Type 2 independent component but not within the tolerance distance of a corner.
3	A midpoint along a side of dependent component must match a midpoint along a side of independent component.
4	An endpoint of a Type 1 component must match a midpoint along a side of a Type 2 component
5	A midpoint along a side of dependent Type 2 component must match a midpoint along a Type 3 or 4 independent component.
6	An endpoint of the dependent Type 3 component must match the (roof) point of the independent Type 5 component.
7	A corner point of the dependent Type 2 component must match the (roof) point of the independent Type 5 component. This applies only to the case of a flat slab. The FACEDAP code first looks for two way roof slabs to be dependent on beams or walls and, if the maximum four dependencies are not satisfied, goes back to consider the case discussed here.
8	An endpoint of Type 3 dependent component must lie along a Type 3 independent component, but not within a tolerance distance of either endpoint.
9	An endpoint of Type 1 or 3 dependent component must lie along a Type 3 or Type 4 independent component anywhere between the endpoints of independent component.

that a component in one wall (Component A) is dependent on, or supported by, a component in an opposite **wall** (Component C), which makes no sense. The logic in the preceding tables is designed to preclude the calculation of “primary” dependencies which will lead to this situation. As a consequence, roof components providing lateral support to the top of the wall components are not included as independent components except for some special cases where it is known that this potential problem will not occur.

## 5.2 Frame Dependencies

Frame dependencies are calculated based on the assumption that the column and beam members of the frame provide either primary or secondary support to all components within the loaded width of the frame. For frames with 100% damage, the FACEDAP program changes the damage of all components within the loaded width to 100% damage if a lesser damage level was calculated for these components due to **direct** blast loading. The loaded width is the same value input into the P-i diagram for the frame component.

## 6.0 BUILDING DAMAGE CALCULATIONS

In **building vulnerability analyses, four building damage terms are calculated with summation** procedures that take into account the damage calculated for each building component. These **four parameters** are: 1) the percentage of building damage, 2) the replacement factor, 3) the percentage of reusable building floor without repair, and 4) the building level of protection. They are **discussed** in the next four subsections. **They** are approximate because they are based on component damage that is calculated with approximate procedures and because the criteria used to relate component damage to the various building damage parameters is, in large part, subjective.

### 6.1 Percentage of Building Damage

The percentage of building damage is a weighted percentage of building component damage. After the damage to each component is calculated using the P-i diagrams and the methodology discussed above, the percentage of building damage is calculated as follows. In the first step of this **process, the damage level of each component in decimal form (e.g., the 30% damage level is considered** as 0.3) is multiplied by the user defined component weighting factor. This product is the weighted component damage level. A weighting factor is assigned to each building component by the user in order to cause blast damage **occurring** in major building components to influence the calculated building damage parameters more than an equal level of damage to minor components. Any scheme of assigning positive, non-zero weighting factors to building components which correctly influences the calculated overall building damage in the user’s judgement is valid. A scheme which is commonly used is to **assign** a weighting factor of 1.0 to cladding components, a factor of 2.0 to stringer, girts and other secondary beams which support cladding components, a factor of 3.0 to primary beams and girders, and a factor of 4.0 to **columns**. Frames should have a weighting factor equal to the sum of the weighting factors assigned to **all** the columns and beams in the frame. This is necessary so that comparable building damage **values will** be calculated in the two **required** analyses which consider frame components responding to blast load as separate, laterally loaded beam and column components and as a frame component. For example, a single bay **frame** comprised of two columns (with weighting factors of 4) and a beam (with a weighting factor of 3) would have a weighting factor of **11**.

In the second step of the procedure used to calculate the percentage of building **damage**, the weighted damage levels of all components **in** the building are summed. Then, in the **final** step, the percentage of building damage is calculated from the ratio of this sum divided by the **corresponding** sum for the case of **100%** damage to all building components.

## 6.2 Building Replacement Factor

The blast damage to components can also be described in terms of the amount of required component replacement **in** the building. This is done in the FACEDAP program with a replacement factor which is assigned to each component based on the damage level calculated for the component. If the damage level is greater than a given level, the component is considered unrepairable and a replacement factor of 1.0 is assigned to the component. **Otherwise** the component is considered repairable and a replacement factor of 0 is assigned. The building replacement factor is the weighted average of the replacement factors of all the components in the building. This factor is determined in an analogous manner as the percentage of **building** damage except that the **repair/replace** factor of each component (equal to 0 or 1) is considered in the weighted averaging scheme rather than the damage level of the component. A **high** replacement factor (near 100%) indicates that almost all building components **require** replacement

Table 5 lists **the** correlation between replacement and damage level which is used by **the** FACEDAP program to determine the replacement factor for the 24 component types. Note that the R's indicate a repairable component (with a **replacement** factor of 0), while the U's indicate a component requiring replacement (with a replacement factor of 1). The break points between repair and replace for each component were based on economics concerns as well as the amount of damage associated with each damage category<sup>[3]</sup>. Higher damage levels were generally chosen as **the** break points for load bearing components because such components are more expensive to **replace**, and are therefore more likely to **be** repaired at the higher damage levels. Similarly, components such as steel beams were designated as requiring **replacement** at the 30% damage level even though they might **typically** be repairable because they are considered relatively easy to replace. The subjective criteria used to correlate component **repair/replacement** with **component** damage level were not based on or **influenced** by the level of protection associated with each damage level in Section 4.1.

## 6.3 Percentage of Reusable Floor Space

In the original development of the methodology used **in** the **FACEDAP** program to calculate component and building blast damage, the percentage of building floor space reusable without repair was calculated with a graphical procedure which summed the floor space not affected by components with a calculated 100% damage level and then divided this floor space by the total floor space. This ratio is the percentage of reusable floor space. A simplified approximation of this procedure is

**Table 5. Correlation Between Component Damage and Assumed Replacement**

<b>Component Type</b>	<b>Component Damage Level'</b>			
	<b>0%</b>	<b>30%</b>	<b>60%</b>	<b>100%</b>
<b>R/C Beams</b>	R	R	R	U
R/C One-Way Slabs	R	R	U	U
R/C Two-Way Slabs	R	R	U	U
<b>R/C Exterior Columns (bending)</b>	R	R	R	U
<b>R/C Interior Columns (buckling)</b>	R	<b>N/A</b>	<b>N/A</b>	U
<b>R/C Frames</b>	R	R	R	U
<b>Prestressed Beams</b>	R	U	U	U
Steel Beams	R	U	I-u	u
Metal Stud Walls	R	U	U	U
Open <b>Web Steel</b> Joists (chord bending failure)	(chord	R	U	U
<b>Corrugated Metal Deck</b>	R	U	U	U
Steel Exterior <b>Columns</b> (bending)	R	R	U	U
Steel Interior Columns ( <b>buckling</b> )	R	<b>N/A</b>	<b>N/A</b>	U
Steel Frames	R	R	R	U
<b>One-Way Unreinforced Masonry</b>	R	R	U	U
Two-Way Unreinforced <b>Masonry</b>	R	R	U	U
One-Way Reinforced <b>Masonry</b>	R	R	U	U
Two-Way Reinforced <b>Masonry</b>	R	R	U	U
<b>Masonry Pilasters</b>	R	R	U	U
wood stud <b>Walls</b>	R	R	U	U
Wood Roofs	R	R	U	U
Wood Beams	R	R	U	U
<b>Wood Exterior Columns (bending)</b>	R	R	U	U
Wood <b>Interior</b> Columns ( <b>buckling</b> )	R	<b>N/A</b>	<b>N/A</b>	U

Note: R = repairable, U = replace

programmed in the FACEDAP program. **The** total number of components with 100% damage is counted and divided by the total number of building components. This is subtracted **from** 100% to determine the percentage of reusable floor space. The weighting factor is not considered in calculating **this building** damage parameter. This definition of building reusability is meant to apply to wartime situations when **only** very severe component damage is assumed to affect reusability. This is considered the most approximate of the building damage parameters, and it really should be determined using the original graphical procedure for accurate results.

#### 6.4 **Building Level of Protection**

The building level of **protection** is **calculated** equal to the lowest level of protection provided by any of the building components. This is a conservative approach which assumes that the personnel or assets requiring protection are located right beside or near the building component with the largest amount of blast damage. The component levels of **protection** are determined directly from the calculated component damage levels as discussed in Section 4.1. **The** levels of protection used by the U.S. Army Corps of Engineers to **characterize** the level of protection provided to personnel and equipment by a structural component subjected to blast loading are **defined** in Reference 13 as follows.

***Low Level of Protection*** - unreparable structural components, a high level of damage without collapse

***Medium Level of Protection*** - repairable structural components, a significant degree of damage

***High Level of Protection*** - superficially damaged

A fourth level is also considered as follows.

***Collapse*** - collapse, or near collapse of the structure

This building level of protection should only **be** considered as one indicator of the amount of personnel injury and equipment damage **in** a building which can be caused by the input explosive threat. Among other factors, these protection levels do not consider the injury/damage caused by failed windows or doors and by building component accelerations during response to the blast loading.

## 7.0 LIMITATIONS OF THE BLAST DAMAGE ASSESSMENT METHODOLOGY IN THE FACEDAP PROGRAM

Most of the limitations of the BDAM code have been discussed in the preceding chapters. However, they are summarized in this chapter for quick reference.

- 1) **Only** component blast damage caused by **flexural** bending and buckling of components is explicitly considered in the P-i diagrams used to predict component blast damage. Damage caused by **flexural** shear response, torsional response, and by localized breaching or spalling is not predicted by the FACEDAP program. The recommended minimum scaled standoff of 3.0  $\text{ft/lb}^{1/3}$  between the explosive charge and the closest building component is intended to prevent the use of the program in situations where localized damage and highly nonuniform blast pressure distributions can occur on the building components. The reduced damage which **will** occur when a component responds in tension membrane or compression membrane response, rather than only **flexural** response, is accounted for in several P-i diagrams. The theoretical curves for damage occurring during **flexural** response have been shifted to match blast damage data from components responding in tension or compression membrane. The fact these curves have been "**shifted**", rather than theoretically developed, means that they may not **be** applicable for components with sectional properties significantly different than those of the components in the test data which are used to construct these P-i diagrams.
- 2) The simplified method used to calculate blast load on building components may be nonconservative in two respects. First, component blast damage due to the negative phase being "in-phase" with component response is not predicted. This is only a possible concern for components with strengths (ultimate resistances) less than 2 psi. The inclusion of damage from this type of loading is outside the scope of the "simple" component damage prediction methods currently included in the FACEDAP program. Secondly, blast load on building components facing the explosive charge and oriented at angles of incidence (see Figure 2) between 45° and 75° with respect to the blast wave is calculated assuming a fully side-on blast pressure. This can underpredict the blast load by factors between 2 and 5.
- 3) No component beam-column response is considered in the FACEDAP methodology. Neither the case of "short" columns (columns not affected by stability considerations), where bending and axial stresses superimpose, nor the case of long columns, where **flexural** deflections cause eccentricity in the axial load and therefore additional bending moment, are considered. Consideration of the interaction between axial and bending stresses in short steel and reinforced concrete columns during dynamic response is addressed as it pertains to design in Reference 10. This reference also advises that the dynamic response of "long" beam columns, where stability is a criterion, can be considered for design purposes in the same manner it is considered

for static design. The static analysis of long **beam-columns** is described in Reference 26. The design of long steel and reinforced concrete beam-columns for static loading is described in References 27 and 28.

- 4) The P-i diagrams in the FACEDAP procedure analyze each component as a separate, independent single-degree-of-freedom dynamic (**SDOF**) system. Therefore, the dynamic interaction which can occur between primary structural members and the secondary members they support is not explicitly accounted for.
- 5) The building damage assessment procedure in the FACEDAP program has not been compared against blast damage to buildings except for one case” where very **little** information was available about the buildings damaged by blast. Therefore, the cascading failure procedure and building damage summation procedures have not been well validated against data. Also, the P-i diagrams which predict component blast damage for a number of component types have not been compared against measured blast damage.

## 8.0 RECOMMENDATIONS FOR **FUTURE WORK**

Recommendations for future improvements to the FACRDAP procedure for calculating approximate blast damage to buildings are itemized below. In general, the basic procedure is considered to be well suited for quickly calculating blast damage to buildings. This is particularly true because of the manner **in** which the FACEDAP preprocessor and postprocessor facilitate the rather large task of inputting the material properties, geometry, and dependencies of all building components loaded by the blast. However, the procedures used to determine the component and **building** blast damage are limited by **the** factors discussed in Chapter 7. Therefore, **the** following improvements to the FACRDAP program, and to the blast damage assessment procedure used by the program, are proposed.

**Validation of calculated building damage** - The cascading failure procedure and summation procedures in the assessment method should be validated against data. Since these procedures depend on rules to assign dependencies and weighting factors, this “validation” process is actually envisioned as a process where dependency rules and weighting factors are determined which cause the calculated building damage to match measured damage. The need for validation also includes conducting a new literature search to find recent blast damage data, and any previously overlooked data, to validate component P-i diagrams

**Provide better guidance on input properties for components affected by the dynamic response of attached components** - Often secondary and primary building components form a two or three degree-of-freedom dynamic system, where the dynamic response of the components is affected by response of **the** attached components. However, the P-i diagrams in the FACRDAP blast damage assessment procedure analyze each component as a separate, independent single-degree-of-freedom dynamic (**SDOF**) system. A parameter study is needed which calculates blast damage of typical primary and secondary building components which respond as a two or three-degree-of-freedom dynamic system with an approach which considers this interdependence and then also calculates the damage of the

same components separately using the SDOF approach in the FACEDAP program. This approach **can** be used to provide guidance on program inputs for properties of components which are affected by the dynamic response of **attached components, particularly the loaded** width and weight (or inertial resistance), so that the interactive nature of dynamic component response can be accounted for better with the SDOF approach in the FACEDAP program.

**Development of P-i diagrams which explicitly consider modes of structural response other than flexure and buckling** - P-i diagrams which explicitly consider the strain energy absorbed in tension membrane and compression membrane response need to be formulated so that component damage data from these types of response can be used to validate, or modify, theoretical damage curves which consider this type of response. Also, P-i diagrams must **be** formulated to consider shear and spalling type component damage **before** the building damage assessment procedure in the FACEDAP program can be extended to include component damage occurring at close-in scaled standoffs (less than 3.0 Mb”).

**Implementation of a blast load prediction method which considers the effect of the angle of incidence in more detail than the existing method** - Existing algorithms for calculating blast load based on the magnitude of the angle of incidence of the component with respect to the blast wave should be included in the FACEDAP program in place of the existing method which only considers whether the angle of incidence is greater than or less than 45°. The simple existing criteria is a holdover from the original version of the blast damage assessment procedure which was performed with hand calculations.

**Better definition of component damage categories and limit criteria defining damage categories** - Users of the FACEDAP program must be provided with a means of interpreting or understanding the damage levels which are predicted by the program. This can be done best with a combined approach of a qualitative description of the component damage categories and approximate quantitative criteria defining each damage criteria based on component type. The initial damage descriptions in the blast damage assessment procedure were primarily qualitative. More recently, some effort, which is shown in Table 2, has been spent to provide approximate quantitative criteria defining the damage levels for each component type. However, more work is required to **define** the component damage categories so that the qualitative and quantitative descriptions of component damage are more compatible for all component types.

**Implementation of graphics into the FACEDAP program** - This would allow the user to see the input building and component geometry and correct mistakes much more easily than they can **with** the existing program, which relies on error messages. The calculated damage could also be displayed graphically in the postprocessor by displaying the building with its components colored in a manner which represents blast damage to each component

**Improvement of several other features of the FACEDAP preprocessor** - These include: 1) the use of highlighted input cells on the preprocessor component property input screens to show when default property calculation formulas have or have not been used to **calculate** the existing input, 2) a flag to warn users when they have changed a “master” component

but have not regenerated the components which are **defined** based on the master component, 3) a single key to generate component dependencies in all **wall/roof** areas at one time, 4) a flag to warn users when they have changed the component geometry but have not regenerated the component dependencies, 5) an option which will allow the calculation of the blast damage to a single **structural** component without requiring the need to **define** building wall/roof areas.

> - T h e U . S . A r m y C o r p o f E n g i n e e r s , as well as other governmental agencies, are moving towards metrification. Currently, all input into the FACEDAP code must be in specific English units as shown in Section 4.1. It is recommended that the code should **be** modified to allow input in metric units and to display output in metric units.

## REFERENCES

1. Oswald, C.J. and Skerhuf D., "FACEDAP User's Manual," Contract No. DACA 45-91-D-0019, U.S. **Army** Corps of Engineers, **Omaha** District, April 1993.
2. **Skerhut**, D. and Oswald, C.J., "FACEDAP Programmer's Manual," Contract No. DACA 45-91-D-0019, U.S. Army Corps of Engineers, Omaha District, April 1993.
3. **Oswald, C.J., Polcyn, M.A., Ketchum, D.E., Marchand, K.A., Cox, P.A.**, and Whitney, M.G., "Blast Damage Assessment Procedures for Common Construction Categories," Final Report prepared for the Naval Civil Engineering Laboratory, October 1987.
4. Marchand, K.A., Cox, P.A., and Peterson, J.P., "Blast Analysis Manual Part I • Level of Protection Assessment Guide • Key Asset Protection Program Construction **Option (KAPPCO)**," Contract No. DACW 45-89-D-0139, Final Report prepared for the U.S. Army Corps of Engineers, **Omaha** District, PD-MCX and U.S. Forces Command Engineer, Fort McPherson, GA, July **19, 1991**.
5. Polcyn, M., Bowles, P., Quioco-Smith, M., and Peterson, J. "Users **Manual** for Blast Damage Assessment Model, BDAM Volume 2. **Procedures** and Supporting Data for BDAMA Module," Contract No. **N47408-91-D-1127**, Naval Civil Engineering Laboratory, December 1991.
6. **Ferritto, J.M.**, NCEL UG, "User's Manual for Blast Damage Assessment **Model**, BDAM, Volume **1**, Program Usage," Naval Civil Engineering Laboratory, Port Hueneme, CA, 1992.
7. Bowles, P., Peterson, J., Quioco-Smith, M., **Domel, M.**, and Polcyn, M., "Validation of Blast Damage Assessment Model, BDAM," Contract No. **N47408-91-D-1127**, Naval **Civil** Engineering Laboratory, December 1991.
8. Polcyn, M.A., **Ketchum, D.E.**, and Whimey. M.G., "Procedures to Assess **Internal** Blast Damage to Common Construction Categories," Contract No. **N00123-86-D-0299**, Final Report for Tecolote Research, Inc., Santa Barbara, CA, May 1988.
9. Kingery, C.N. **and Bulmash, G.**, "Airblast Parameters From TNT Spherical Air Burst and Hemispherical Surface Burst," BRL Technical Report ARBRL-TR-02555, April 1984.
10. **Design Manual Army TM5-1300, NAVFAC P-397, and AFM-88-22: Structures to Resist the Effects of Accidental Explosions,** Department of the Army, Navy, and Air Force, Washington, DC, 1990.
11. **Fundamentals of Protective Design for Conventional Weapons,** Technical Manual No. 5-855-1. Headquarters Department of the Army, Washington, D.C., 3 November 1986.
12. Baker, W.E., Cox, P.A., **Westine, P.S., Kulesz, J.J., and Strehlow, R.A., Explosion Hazards and Evaluation,** Elsevier Scientific Publishing Company, Amsterdam, 1983.

13. **Security Engineering Manual**, U.S. Army Corps of Engineers Missouri River Division-Omaha District Protective Design Center, January 1990.
14. Healey, J., Ammar, A., Vellozzi, J., Pecone, G., Weissman, S., Dobbs, N., and Price, P., "Design of Steel Structures to Resist the Effects of HE Explosives," **Technical Report 4837**, Picatinny Arsenal, Dover, NJ, 1975.
15. Biggs, J.M., **Introduction to Structural Dynamics**, McGraw-Hill Book Company, 1964.
16. "Operation TEAPOT Nevada Test Site," **DTIC AD-A995 309**, ABC Company: Health and Safety, February - May 1955.
17. Florence, A.L. and Firth, R.D., "Rigid Plastic **Beams Under** Uniformly Distributed **Impulses**," **Journal of Applied Mechanics**, **32**, Series E, **1**, pp 7-10, March 1965.
18. Stea, W., Sock, F., and Caltagirone, J., "Blast-Resistant Capacities of Cold-Formed Steel Panels," Contract No. **DAAK10-77-C-0134**, ARRADCGM, LCWSL, Dover, NJ, May 1981.
19. Wilton, C. and Gabrielsen, B.L., "Summary Report, House Damage Assessment," Contract No. **DASA 01-70-C-001 1**, Defense Nuclear Agency, Washington, D.C., June 1972.
20. Watt, Jr., J.M., "**Mill Race Event**, 16 September 1981, **Experiments 2601 and 2602; Industrial Structures Test**," Technical Report **SL-84-4**, U.S. Army Engineer Waterways Experiment Station Structures Laboratory, Vicksburg, MS, **April** 1984.
21. Falls, T.C. and Watt, J.M., "**Industrial Structures Test**, Direct Course Event, 26 October 1983," **Technical Report SL-85-2**, U.S. Army Engineer Waterways Experiment Station Structures Laboratory, Vicksburg, MS, June 1985.
22. Park, R. and Gamble, W.L., **Reinforced Concrete Slabs**, Wiley Interscience, New York, 1980.
23. Forsén, R., "**Airblast Loading of Wall Panels**," FOA Report C **20586-D6**, Försvarets Forskningsanstalt, Huvudavdelning 2. Stockholm, October 1985.
24. Wilton, C. and Gabrielsen, B.L., "**Shock Tunnel Tests of Wall Panels**," **URS 7030-7**, Technical Report, URS Research Company, San Mateo, CA, January 1972.
25. Keenan, W.A., "Strength and Behavior of Restrained Reinforced Concrete Slabs Under Static and Dynamic Loadings," Technical Report R621, Naval Civil Engineering Laboratory, Port Hueneme, CA, April 1969.
26. Timoshenko, S.P., **Theory of Elastic Stability**, McGraw-Hill Book Company, 1961.
27. **Manual of Steel Construction**, Ninth Edition, American Institute of Steel Construction, New York, NY, 1989.
28. **American Concrete Institute Standard Building Code Requirements for Reinforced Concrete**, **ACI Committee 318-89**, American Concrete Institute, Detroit, **MI**, November 1989.